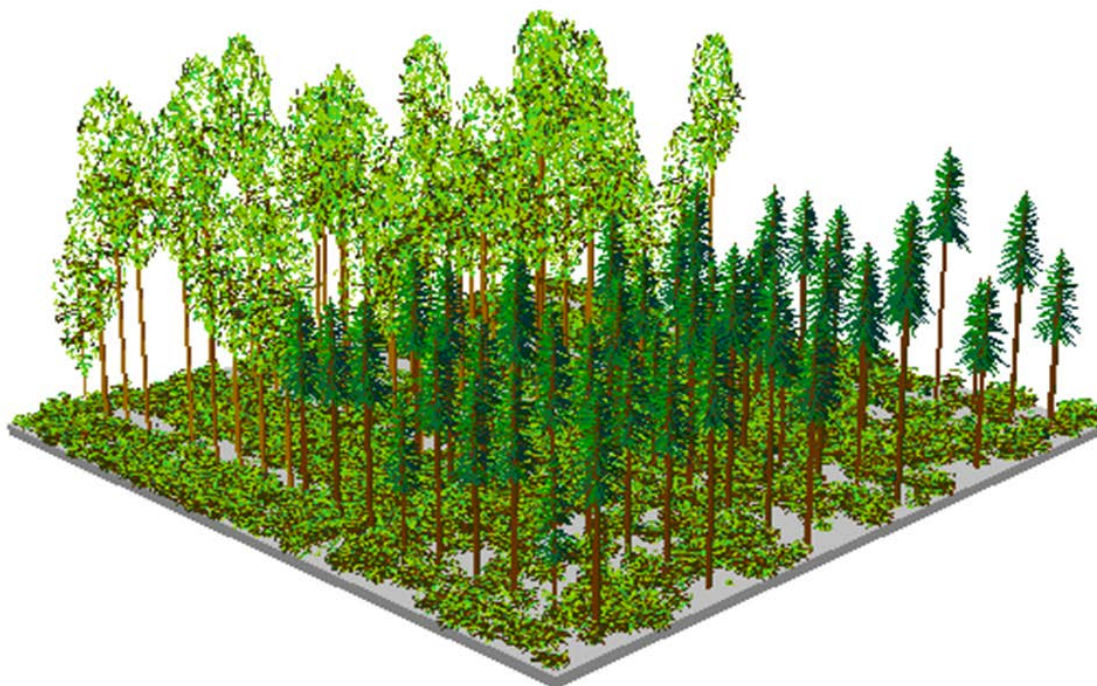**Model assessment of impacts of climate change, forest management and transfer of forest reproductive material**

Deliverable nr. 3.4

Towards the Sustainable Management of Forest Genetic Resources   FORGER FP7- 289119

Document Properties

Document number	FP7-FORGER 289119 / D3.4
Document title	Model assessment of impacts of climate change, forest management and transfer of forest reproductive material
Work document number	D 3.4
Working package nr.	WP 3
Working package title	Use and management of forest genetic resources
Related Milestone nr.	-
Related Milestone title	-
Responsible	Koen Kramer
Due time (month)	42
Dissemination level	RE
Dependencies	
Author(s)	Koen Kramer, Mart-Jan Schelhaas, Bert van der Werf, Geerten Hengeveld
Version	
Date of last revision	16-12-2015
Status	final

Abstract

The model ForGEM was parametrized, validated and initialized throughout the distribution range of Fagus sylvatica, Quercus robur, Picea abies and Pinus sylvestris. The model was used to assess the effect of environmental drivers on the performance of these species, the role of forest management on adaptation of functional traits and the species' genetic diversity throughout the distribution range, and extensive provenance trials were performed *in silico*. Due to heavy computational demands of the model, not all analyses could be performed on all species in due time.

Keywords (up to 5):

Executive Summary

The model ForGEM on forest genetics, ecophysiology and management was parametrized and validated for Fagus sylvatica, Quercus robur, Picea abies and Pinus sylvestris. An initialisation system was designed such that the model can be initialised and run in the entire geographic distribution of these tree species. The model was tested for species performance with respect to changes in temperature, precipitation and ambient CO2 concentration, and the effect of adaptation to local climatic conditions. Tree populations were allowed in the model to adapt to local environmental conditions throughout the species' distribution. With the locally adapted tree populations, the effect of forest management systems on traits related to water use and the onset of the growing season and their genetic diversity were tested, also throughout the distribution range of the species. Furthermore, provenance trials were performed in silico in which populations were planted throughout the distribution range and its performance compared relative to that of the locally adapted populations.

The model results indicated that the deciduous tree species and coniferous tree species differed in their response to precipitation, temperature and, to a lesser extent ambient CO_2 concentration. Within these plant functional groups the responses to these environmental drivers was similar.

Overall, on a time horizon of 100 years, there were minor differences between the management systems in their effect on the rate of adaptive response of the traits, and thereby on the loss of genetic diversity by selection. However, between sites, distributed throughout the species range, there were clear differences on the importance of the role of management on the adaptive response and genetic diversity of these adaptive traits.

The *in silico* provenance trials showed the general pattern that provenances obtained from the north of Europe, and tested throughout the distribution range, performed worse compared to the locally adapted populations for most of the test sites. Whereas provenances obtained from the south of Europe, generally performed better compared to the provenances adapted to the conditions of the test site.

Overall we conclude that the ForGEM model is a suitable tool to make future assessments on impact of climate change, the effect of management on genetic diversity and rate of adaptation, and to evaluate a large number of provenance trials at many environmental conditions.

The genetic model analyses proved to be very expensive in terms of computing power required to make the abovementioned assessments. In total we spend around 1.3. million computing processor unit (CPU) hours, which was not enough to calculate adaptation to local environmental conditions of all 4 tree species. Currently, the model and all necessary auxiliary data and database structures are uploaded at the national academic supercomputing centre in the Netherlands, and is available for use by others.

Towards the Sustainable Management of Forest Genetic Resources   FORGER FP7- 289119

1. Introduction

1.1. Background and aims

This Deliverable contributes to *Objective 3: To analyse historic, current and future management and use of forest genetic resources. This objective is addressed in Work Package 3: Use and management of forest genetic resources*. One of the approaches to meet this objective is by model prediction of the impacts of (i) environmental change, (ii) management practices and (iii) transfer of FRM on both GD (additive variance) and rate of adaptive response of functional traits.

1.2. Description of Task 3.4 [1]

At the pan-European scale, predictive modelling was used to study impacts of climate change and forest management on growth and genetic diversity of *Fagus sylvatica, Quercus spp., Pinus sylvestris* and *Picea abies*. This task will be performed by testing, improving and applying the process-based model ForGEM (Kramer et al. 2008, Kramer et al 2010; Kramer & Van der Werf 2010). Using the model, we will analyse the effects of forest management, climate change (temperature, precipitation) and transfer of FRM, on genetic diversity and rates of adaptive response of functional traits.

The outputs of this activity will be pan-European maps with simulated genetic diversity and adaptive responses of key-phenotypic traits (phenology and water use) and impacts of transfer of FRM on genetic diversity and the rate of adaptation of functional traits. The final deliverable of Task 3.4 will indicate the consequences of the simulated future assessment for the *Guidelines and Recommendations*, as input to Task 5.3. Activities distinguished for Task 3.4 are:

---

[1] The numbering of tasks and subtasks follows that of the Description of Work

- 3.4.1. Selection of sites and scenarios
- 3.4.2. Process-model parametrization
- 3.4.3. Process-model initialization
- 3.4.4. Process-model validation
- 3.4.5. Process-model analyses

The results of these tasks are described below.

2. Selection of sites and scenarios

2.1. Species and sites

Species distribution data is available through the European tree species maps constructed by Brus et al.(2012). For the 20 species groups they used a combined approach of compositional kriging, multinomial logistic regression and scaling to incorporate high precision distribution data from National forest inventories where available, the coarser resolution ICP network and several European-wide environmental data to predict European species occurrence on a 1 x 1 km grid and relying on nationally reported species densities to incorporate national traditions.

For each of the 1 km^2 pixels a vector of the area covered by the 20 species in the map is given. Coupled to the map is a database of representative plots, derived from national forest inventory data, describing local forest state. The area covered by each species is the basis for a Representative Forest Stand (RFS). This RFS is then characterised by a regional plot from the database in which the species occurs. Regional is defined in a hierarchical way as the sampling region of the NFI, the biogeographical region and the whole of Europe. The RFS can consist of several different species that are each represented by their basal area, height, volume, DBH and stem number.
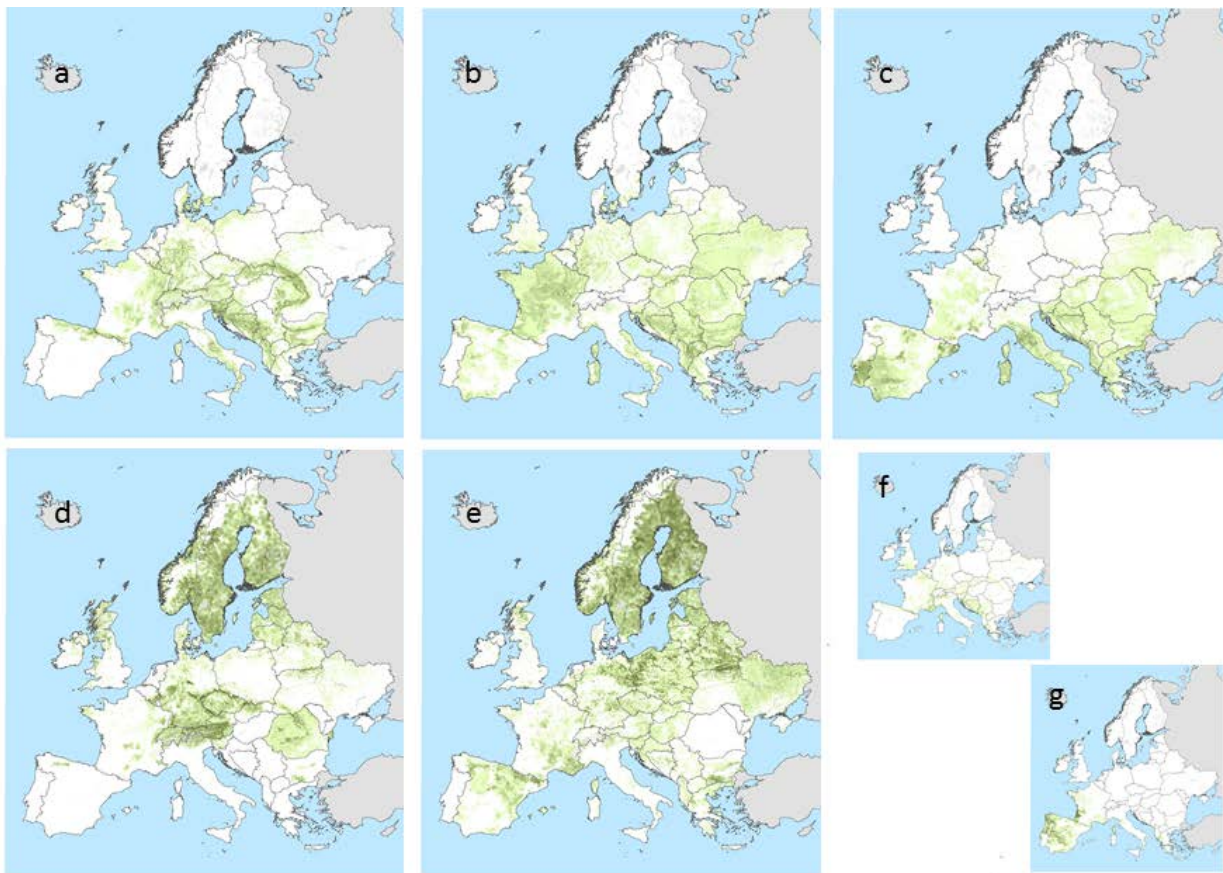
Figure 2.1. Species distribution and density from Brus et al.(2012). For a) Fagus spp, b) Quercus robur & Q. petraea, c) other Quercus species, d) Picea spp, e) Pinus sylvestris f) Fraxinus spp. and g) Pinus pinaster

Site and species data are available and ready for use in the European Forest Database at Alterra. Site data are available for the following species and species-groups:

species name
Abies spp
Alnus spp
Betula spp
Carpinus betulus

Castanea sativa
Eucalyptus spp
Fagus sylvatica
Fraxinus spp
Larix spp
other broadleaved
other conifers
other Pinus spp
other Quercus spp
Picea spp
Pinus pinaster
Pinus sylvestris
Populus spp
Pseudotsuga menziesii
Quercus robur + petraea
Robinia pseudoacacia

2.1.1. Representative Forest Stand - data

RFS data are presented per grid cell in a 1x1 km grid :

example:

x	y	spec ID	spec Name	Area ha	plot ID	Basa Area	DBH	height	volume per ha	nr. per ha
2712500	1937500	12	other Pinus spp	1.935482	1000	62.40033	29.8	0.06	457.663	893

x	y	spec ID	spec Name	Area ha	plot ID	Basa Area	DBH	height	volume per ha	nr. per ha
2707500	1751500	12	other Pinus spp	5.408228	1000	62.40033	29.8	0.06	457.663	893
2721500	1835500	12	other Pinus spp	7.162835	1000	62.40033	29.8	0.06	457.663	893
2700500	1915500	12	other Pinus spp	10.39521	1000	62.40033	29.8	0.06	457.663	893
2674500	1814500	12	other Pinus spp	2.500675	1000	62.40033	29.8	0.06	457.663	893

2.1.2. Input data

Formats of the raw primary data as described above.

tables:

unip_var	
AVGRADIA	INTEGER
AVGRAIN	DOUBLE PRECISION
AVGTEMP	DOUBLE PRECISION
BIOGEO4	INTEGER
SOILCLUS	INTEGER
ELEVATION	INTEGER
SLOPE	INTEGER
FOREST	DOUBLE PRECISION
BROADL	DOUBLE PRECISION
CONIFER	DOUBLE PRECISION
AREAREGID	INTEGER
VOLREGID	INTEGER
COUNTRYID	INTEGER
POINT_X	DOUBLE PRECISION
POINT_Y	DOUBLE PRECISION
NATION	CHARACTER VARYING(3)
CNTRYNAME	CHARACTER VARYING(25)
UNIGRD_ID	DOUBLE PRECISION

Plots_Filled_Complete_1010	
SpeciesGroup	BIGINT
LocRecID2	BIGINT
Location_ID	BIGINT
RecordingNr	INTEGER
StandardOrCoppice	BIGINT
BA_d	DOUBLE PRECISION
DBH_d	DOUBLE PRECISION
H_d	DOUBLE PRECISION
V_d	DOUBLE PRECISION
N_d	DOUBLE PRECISION

AreaMapPlots_120308	
Cell	DOUBLE PRECISION
Species	DOUBLE PRECISION
Area_ha	DOUBLE PRECISION
AML_Pls	DOUBLE PRECISION

SI_SpeciesGroup_Names	
SpeciesGroupMap_Name	CHARACTER VARYING(255)
SpeciesGroupMap_ID	BIGINT
TreeType	BIGINT
decidious	BIGINT

2.1.3. Intermediate datasets

Queries to convert primary data to a more developer-friendly format.

vwGrid	
cell_ID	DOUBLE PRECISION
x	DOUBLE PRECISION
y	DOUBLE PRECISION
COUNTRYID	INTEGER
ELEVATION	INTEGER
SLOPE	INTEGER
region_ID	INTEGER

vwPlots	
location_ID	BIGINT
BasalArea	DOUBLE PRECISION
DBH	DOUBLE PRECISION
H_d	DOUBLE PRECISION
V_d	DOUBLE PRECISION
N_d	DOUBLE PRECISION

vwMapPlots	
cell_ID	DOUBLE PRECISION
species_ID	DOUBLE PRECISION
Area_ha	DOUBLE PRECISION
plot_ID	DOUBLE PRECISION

vwPlotSpecies	
species_ID	BIGINT
species_Name	CHARACTER VARYING(255)

Powered by yFiles

2.2. Forest management

For forest management, we follow the classification of Forest Management Approach (Table 2.1, (Duncker et al. 2012)), projected to the European scale (Figure 2.2 (Hengeveld et al. 2012)). As simulations at the European scale for each km^2 grid cell is too calculation intensive, a stratified sampling scheme is used based on the Global Environmental Stratification (Figure 2.3 (Metzger et al. 2005, Metzger in press)). Details how the Forest Management Approaches are characterised in the ForGEM model is presented at Chapter 4 (Process-model initialization) and at:

http://vle-models.wur.nl/wiki/index.php/Forest_management

Table 2.1. Characterisation of Forest Management Approaches (FMAs) (Duncker et al., 2012).

FMA	title	management intensity	objective
1	unmanaged forest / nature reserve	passive	to allow natural processes and natural disturbance regimes to develop without management intervention
2	close-to-nature forestry	low	to manage a stand with the emulation of natural processes as a guiding principle; any management intervention in the forest has to enhance or conserve the ecological functions of the forest
3	combined objective forestry	medium	a mix of different objectives, additional objectives to timber production can be water and soil protection, mushroom production, habitat protection, avalanche prevention, game management and nature protection, fire prevention and/or recreation, and are adapted to the local situation
4	intensive even-aged forestry	high	to produce timber
5	short rotation forestry	intensive	to produce the highest amount of merchantable timber or wood biomass
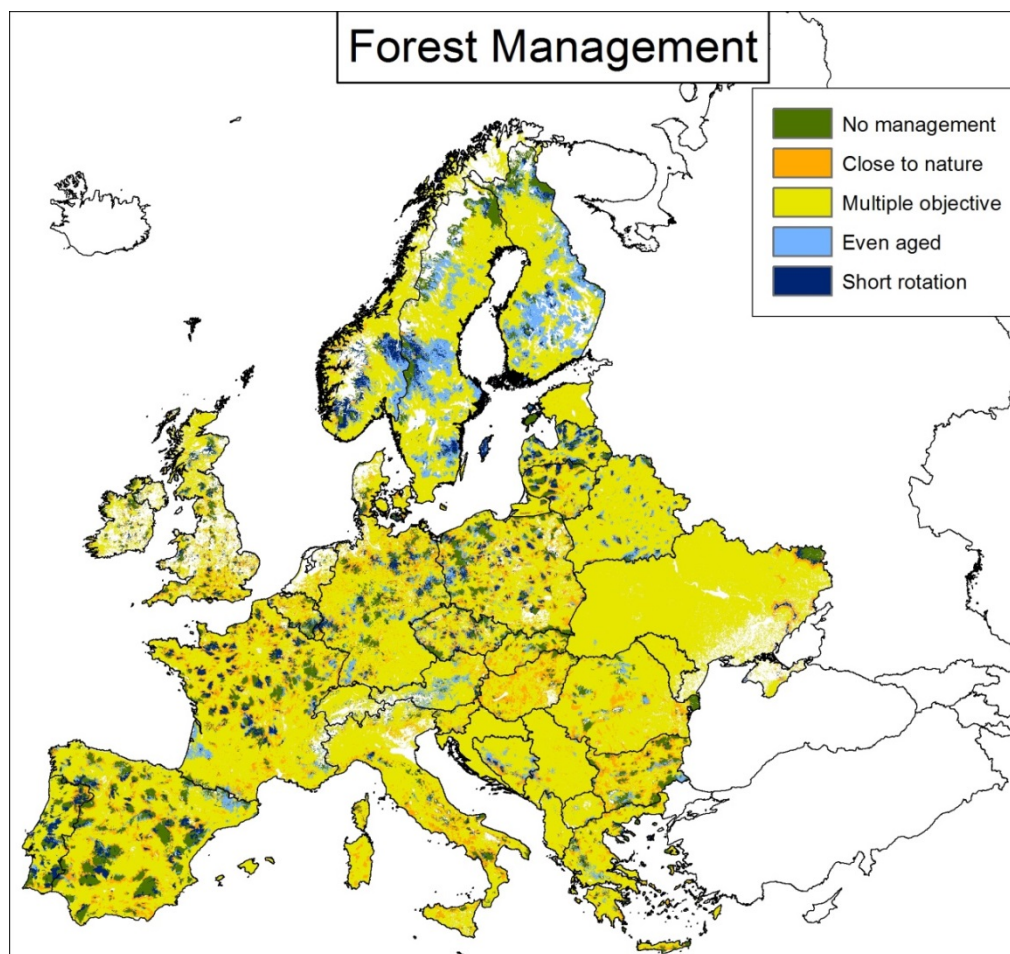
Figure 2.1. Distribution of Forest Management Approaches over Europe (Hengeveld et al., 2012).

Towards the Sustainable Management of Forest Genetic Resources   FORGER FP7- 289119
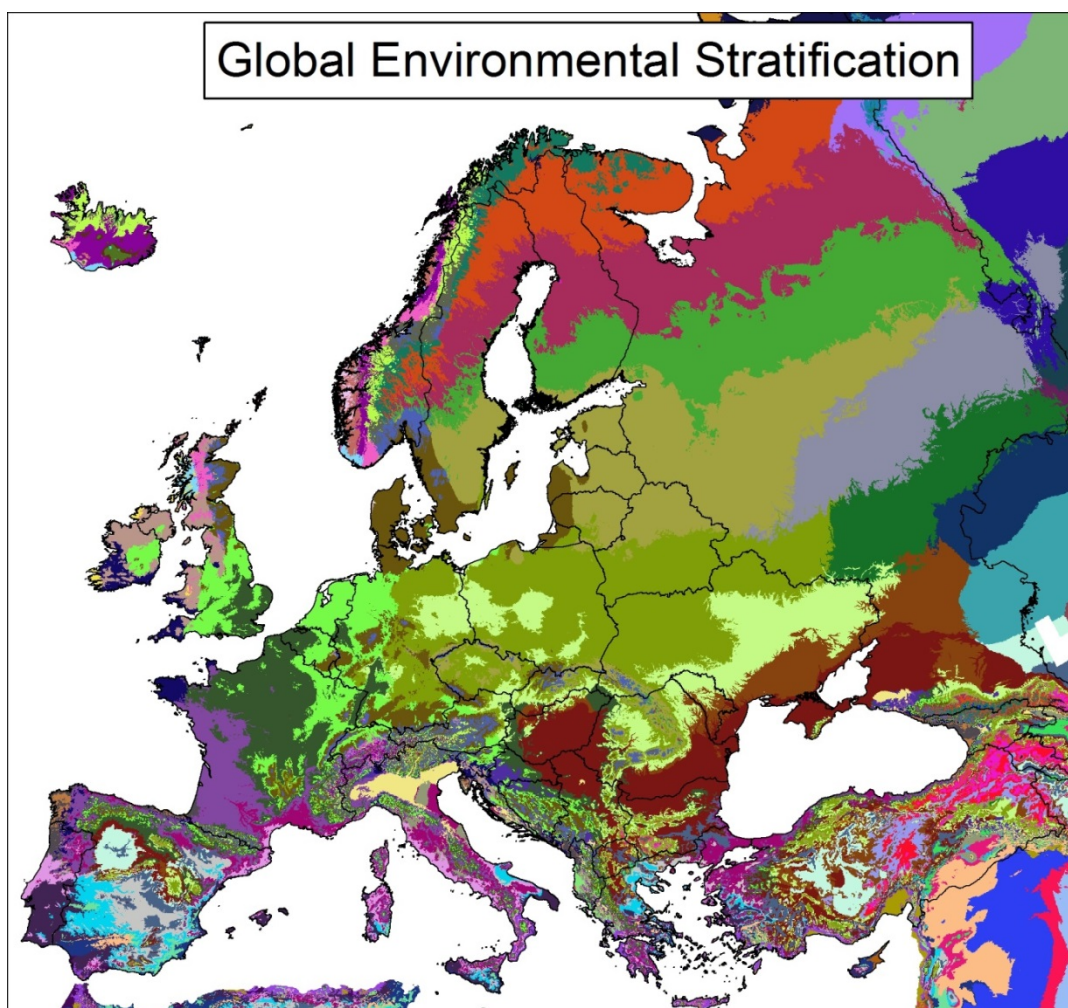
Figure 2.2. Global Environmental Stratification (Metzger et al. 2013).

2.3. Weather and Climate change scenarios

2.3.1. MARS grid - weather

Input data are coming from JRC's CGMS containing the interpolated daily grid weather. The values interpolated onto the 50*50 km grid are the following:

Variable	Description
MAXIMUM_TEMPERATURE	maximum temperature (□C)
MINIMUM_TEMPERATURE	minimum temperature (□C)
VAPOUR_PRESSURE	mean daily vapour pressure (hPa)
WINDSPEED	mean daily windspeed at 10m (m/s)
RAINFALL	mean daily rainfall (mm)
E0	Penman potential evaporation from a free water surface (mm/day)
ES0	Penman potential evaporation from a moist bare soil surface (mm/day)
ET0	Penman potential transpiration from a crop canopy (mm/day)
CALCULATED_RADIATION	daily global radiation in KJ/m2/day
SNOW_DEPTH	daily mean snow depth in cm

These values describe the 'average' conditions prevalent in the grid cell for this day. They do not necessarily represent the meteorological conditions that could be measured at the grid cell centre. The altitude value used to describe the grid cell is a value that describes the mean altitude of agricultural activity in the grid cell.

In order to carry out the interpolation of the above-mentioned variables, they need to be available at the weather station level. Unfortunately, the global radiation and the potential evaporation values are not widely measured or distributed on a regular basis. These values are therefore estimated at the station level, using the available measured meteorological parameters.

The "*Technical description of interpolation and processing of meteorological data in CGMS*" by Erik van der Goot & Stefania Orlandi (2003) describes these procedures in detail (link: http://mars.jrc.ec.europa.eu/mars/About-us/AGRI4CAST/Data-distribution/Data-Distribution-Grid-Weather-Doc).

The global radiation calculation is performed using one of three formulae, depending on the availability of the meteorological parameters for a station. The calculation is based on work by Supit as described in 'Global Radiation, EUR 15745 EN' and Supit and Van Kappel, 'A simple method to estimate global radiation' (in prep.).

The potential evapotranspiration is calculated with the well-known Penman formula. The three values E0, ES0 and ET0 represent the evapotranspiration from a water surface, a wet bare soil surface and a crop canopy respectively.

The interpolation has been implemented following the recommendations of a study carried out by SC-DLO by van der Voet et. al. (1994).

The basis of the interpolation is the selection of the suitable meteorological stations for the determination of the representative meteorological conditions for a grid cell. The actual interpolation, once this selection has been made, is in fact a simple average for most of the meteorological parameters, corrected for an altitude difference in the case of temperature and vapour pressure. The exception is the rainfall data, which is taken directly from the most suitable station.

2.3.2. European Climate Assessment Dataset

The ECA dataset contains 33305 series of observations for 12 elements at 7512 meteorological stations throughout Europe. Both blended and non-blended ECA series are available. Blended series are series that are near-complete by infilling from nearby stations. They are also updated using synoptical messages. Meteorological observations are taken at many stations across Europe, each day. To minimize the effects of changes over time in the way the measurements were made, rigorous quality control is applied before the data is used to analyse extremes. The list of available variables is given below. The selection of variables may differ per station. The global radiation, essential for the model, is not present and must be added.

Element	Ele ID	Description
MAXIMUM TEMPERATURE (TX)		
TX1	Maximum temperature unknown interval	0.1 °C
TX2	Maximum temperature 18-18 UT	0.1 °C
TX3	Maximum temperature 0-0 UT	0.1 °C
TX5	Maximum temperature morning previous day 06,07,08 until morning today (shifted	0.1 °C

Element	Ele ID	Description
	1 day back by ECA staff)	
TX6	Maximum temperature morning today 06,07,08 until morning next day	0.1 °C
TX7	Maximum temperature between 06 and 18 UT today	0.1 °C
TX8	Maximum temperature 21-21 CET	0.1 °C
TX9	Maximum temperature morning previous day 09 h GMT until morning today (shifted 1 day back by ECA staff)	0.1 °C
TX10	Maximum temperature from 21:30 previous day until 21:30 CET	0.1 °C
TX11	Maximum temperature morning today 9 UTC until morning next day	0.1 °C
TX12	Maximum temperature 19-19 UTC	0.1 °C
MINIMUM TEMPERATURE (TN)		
TN1	Minimum temperature unknown interval	0.1 °C
TN2	Minimum temperature 18-18 UT	0.1 °C
TN3	Minimum temperature 0-0 UT	0.1 °C
TN5	Minimum temperature morning previous day 06,07,08 until morning day	0.1 °C
TN6	Minimum temperature between 18 UT previous day and 06 UT today	0.1 °C
TN8	Minimum temperature 21-21 CET	0.1 °C
TN9	Minimum temperature morning previous day 09 h GMT until morning today	0.1 °C
TN10	Minimum temperature from 21:30 previous day until 21:30 CET	0.1 °C
TN11	Minimum temperature 19-19 UTC	0.1 °C
MEAN TEMPERATURE (TG)		
TG1	Mean temperature unknown interval	0.1 °C
TG3	Mean temperature 0-0 UT	0.1 °C
TG5	Mean temperature calculated as average of TN and TX	0.1 °C
TG6	Mean temperature calculated as weighted average of TN, TX and observations at 06, 12 and 18 UT (5 values)	0.1 °C
TG7	Mean temperature calculated as average of 3 or more observations each day	0.1 °C
TG8	Mean temperature calculated as weighted average of 06, 13 and 20 (twice) UTC	0.1 °C
TG9	Mean temperature 06-06 UTC	0.1 °C
TG10	Mean temperature calculated as weighted average of 07:30, 14:30 and 21:30 (twice) CET	0.1 °C
TG11	Mean temperature 18-18 UT	0.1 °C
TG12	Mean temperature calculated as average of 00, 06, 12, 18 UTC	0.1 °C
TG13	Mean temperature calculated as average of 01, 07, 13 and 19 UT	0.1 °C

Element	Ele ID	Description
TG14	Mean temperature calculated as average of 07, 14, 21, 21 UTC	0.1 °C
TG15	Mean temperature calculated as average of 8 observations	0.1 °C
SUNSHINE (SS)		
SS1	Daily sunshine	0.1 Hours
SS2	Daily sunshine, unknown interval	0.1 Hours
SS3	Daily sunshine, 0-0 UT	0.1 Hours
SS4	Daily sunshine 18-18 UT	0.1 Hours
SS5	Daily sunshine 21-21 CET	0.1 Hours
SNOW DEPTH (SD)		
SD1	Mean daily snow depth, 0-0 UT	1 cm
SD2	Mean daily snow depth, unknown interval	1 cm
SD3	Snow depth at 6,7,8 am (local time)	1 cm
SD4	Snow depth at 07:30 CET	1 cm
SD5	Snow depth at 6 or 9 UTC	1 cm
PRECIPITATION AMOUNT (RR)		
RR1	Precipitation amount unknown interval	0.1 mm
RR2	Precipitation amount morning previous day 06,07,08,09 until morning today (shifted 1 day back by ECA staff)	0.1 mm
RR3	Precipitation amount morning today 06,07,08 until morning next day	0.1 mm
RR4	Sum of 12-hourly precipitation of observations at 06 and 18 UT (2 values). Date of 18 UT	0.1 mm
RR5	Precipitation amount morning today 07:30 CET until morning next day	0.1 mm
RR6	Precipitation amount 18-18 UT (sum of 4 values)	0.1 mm
RR7	Precipitation amount 0 - 0 UT	0.1 mm
RR8	Sum of 12-hourly precipitation of observations at 18 UT today and 6 UT tomorrow (2 values)	0.1 mm
RR9	Precipitation amount morning today 06:00 UTC until morning next day	0.1 mm
SEA LEVEL PRESSURE (PP)		
PP1	Sea level pressure at 12 UT	0.1 hPa
PP2	Mean sea level pressure, 0-0 UT	0.1 hPa
PP3	Mean sea level pressure calculated as weighted average of observations at 00, 06, 12 and 18 UT (4 values)	0.1 hPa
PP4	Sea level pressure at 06 UT	0.1 hPa

Element	Ele ID	Description
PP5	Sea level pressure, mean of 13, 20 UT previous day and 7 UT current day (shifted 1 day back by ECA staff)	0.1 hPa
PP7	Mean sea level pressure calculated as weighted average of observations at 00, 07, 13 and 18 UT (4 values)	0.1 hPa
PP8	Mean sea level pressure unknown interval	0.1 hPa
PP9	Sea level pressure, mean of 06, 13 and 20 UTC of the current day	0.1 hPa
PP10	Sea level pressure, mean of 7:30, 14:30 and 21:30 CET	0.1 hPa
PP11	Sea level pressure, mean 18-18 UT	0.1 hPa
PP12	Sea level pressure, mean of 8:00 and 13:00 local time	0.1 hPa
PP13	Mean sea level pressure, 21-21 UTC (8 values)	0.1 hPa
PP14	Mean sea level pressure, 23-23 UTC (24 values)	0.1 hPa
PP15	Mean sea level pressure, mean of 7, 13, 20 UT current day	0.1 hPa
PP16	Mean sea level pressure, mean of daily minimum and maximum pressure	0.1 hPa
PP17	Mean sea level pressure, average of 7, 14 and 19 UT	0.1 hPa
PP18	Mean sea level pressure, average of 6, 12 and 18 UT	0.1 hPa
PP19	Mean sea level pressure calculated as average of 8 observations	0.1 hPa
HUMIDITY (HU)		
HU1	Relative humidity, mean of 0,7,13 18 UT current day	0.01
HU2	Relative humidity, unknown interval	0.01
HU3	Mean relative humidity, 0-0 UT	0.01
HU4	Relative humidity, average of 07:30, 14:30 and 21:30 CET	0.01
HU5	Relative humidity, mean of 7, 14 and 21 UTC	0.01
HU6	Relative humidity, mean 18-18 UT	0.01
HU7	Relative humidity, mean of 7, 14 and 21 CET	0.01
HU8	Relative humidity, 23-23 UTC (24 values)	0.01

Element	Ele ID	Description
HU9	Relative humidity, mean of 7, 14 and 19 UT	0.01
WIND GUST (FX)		
FX1	Maximum 3 second wind gust, 0-0 UT	0.1 m/s
FX2	Maximum 2 second wind gust, 0-0 UT	0.1 m/s
FX3	Maximum 10 second wind gust, 18-18 UT	0.1 m/s
FX4	Maximum value of wind gust speeds 18 - 18 UT	0.1 m/s
FX5	Maximum 3 second wind gust, 18-18 UT	0.1 m/s
FX6	Average wind gust from 23 UT previous day - 22 UT today (24 values)	0.1 m/s
WIND SPEED (FG)		
FG1	Average wind speed of 24 hourly measurements of 10-min average (0-0 UT)	0.1 m/s
FG2	Average wind speed of measurements at 06, 12, 18, (00) UTC	0.1 m/s
FG3	Average wind speed of 3 measurements at 06.30, 13.30 and 20.30 UTC	0.1 m/s
FG4	Average wind speed, mean of 7, 14 and 21 CET	0.1 m/s
FG5	Average wind speed 18 - 18 UT, 8 3-hourly observations	0.1 m/s
FG6	Average wind speed, mean of 4 10-min averages of 00, 07, 13 and 18 UT	0.1 m/s
FG7	Average wind speed of 24 hourly measurements (6 10-min average per hour) 0-0 UT	0.1 m/s
FG8	Average 10-minute wind speed from 23 UT previous day - 22 UT today (24 values)	0.1 m/s
WIND DIRECTION (DD)		
DD1	Average vectorial wind direction calculated from 3 measurements at 06, 12 and 18 UTC.	degrees
DD2	Wind direction at time of maximum gust	degrees
DD3	Average vectorial wind-speed-weighted wind direction calculated from 3 measurements at 06.30, 13.30 and 20.30 UTC	degrees
DD4	Wind direction at 12 UTC	degrees
DD5	Average wind direction, mean of 00, 07, 13 and 18UT	degrees
DD6	Average vectorial 10-minutes wind direction, 0 - 0 UTC	degrees
DD7	Average vectorial 2-minute wind direction from 23 UT previous day - 22 UT today (24 values)	degrees
CLOUD COVER (CC)		
CC1	Mean daily cloud cover, 0-0 UT	oktas
CC2	Mean daily cloud cover, mean of 7, 13, 18 UT current day	oktas
CC3	Mean daily cloud cover, unknown interval	oktas

Element	Ele ID	Description
CC4	Mean daily cloud cover, mean of 7, 13, 20 UT current day	oktas
CC5	Mean daily cloud cover, average of 07:30, 14:30 and 21:30 CET	oktas
CC6	Mean daily cloud cover, mean of 7, 14 and 21 UTC	oktas
CC7	Mean daily cloud cover, 18-18 UT	oktas
CC8	Mean daily cloud cover, average of 00, 13 and 18 UT	oktas
CC9	Mean daily cloud cover, average of 0, 6, 12 and 18 UTC	oktas
CC10	Mean daily cloud cover, 23-23 UTC (24 values)	oktas
CC11	Mean daily cloud cover, average of 3-hourly values, 0-0 UTC	oktas
CC12	Mean daily cloud cover, average of 7, 14 and 19 UT	oktas
CC13	Mean daily cloud cover, average of 6, 12 and 18 UTC	oktas

2.4. Soil

European covering soil data are available at Alterra which can be used in the context of the FORGER project. This includes high resolution data of soil texture and position as indicated as follows:

A brief example of this database looks as follows:

x	y	Altitude	Slope	sand	silt	clay
4925500.0	5357500.0	450	8	0.33	0.33	0.33
4926500.0	5357500.0	450	8	0.33	0.33	0.33
4927500.0	5357500.0	370	10	0.33	0.33	0.33
4928500.0	5357500.0	310	11	0.33	0.33	0.33
4929500.0	5357500.0	270	10	0.33	0.33	0.33

2.4.1. Input data

The species-plot data grid links to the soil cluster from which the soil parameters (sand, silt, clay, C/N, C/P) can be derived. Soil water availability for tree growth can be deferred using Van Genuchten's pedotransfer functions. The parameters of the pedotransfer functions are available throughout Europe (Wösten et al. 1999, Wösten et al. 2001).

unip_var	
AVGRADIA	INTEGER
AVGRAIN	DOUBLE PRECISION
AVGTEMP	DOUBLE PRECISION
BIOGEO4	INTEGER
SOILCLUS	INTEGER
ELEVATION	INTEGER
SLOPE	INTEGER
FOREST	DOUBLE PRECISION
BROADL	DOUBLE PRECISION
CONIFER	DOUBLE PRECISION
AREAREGID	INTEGER
VOLREGID	INTEGER
COUNTRYID	INTEGER
POINT_X	DOUBLE PRECISION
POINT_Y	DOUBLE PRECISION
NATION	CHARACTER VARYING(3)
CNTRYNAME	CHARACTER VARYING(25)
UNIGRD_ID	DOUBLE PRECISION

2.5. Conclusion

For the species addressed in FORGER, data is available on species, site, soil, climate and climate change data which covers the entire EU so that the model can be initialized on a 1x1 km based throughout the EU (see Chapter 4 on Process-model initialization).

3. Process-model parametrization

3.1. Introduction

Below the documentation of the ForGEM model is presented, including the parameter values as they are used for the main species of the FORGER project, *i.e. Fagus sylvatica, Picea abies, Pinus sylvestris* and *Quercus robur.* For the latter species, parameter values are valid for both *Q. robur* and *Q . petraea*. Therefore in the tables below both species are referred to as *Quercus spec.* Parameter values of other tree species are also available in the parameter database, but not presented in this document.

The structure of this chapter is that we first describe the general features of the trees and the key parameters, subsequently the processes related to the life cycle and the annual cycle are presented. Then, the processes operating at the daily scale are presented, i.e. allocation of net primary production to plant components resulting in growth, and the increment of trees structural features such as height and stem and crown diameter. This is then followed by a description of the processes operating at sub-daily scale, i.e. photosynthesis, transpiration and conductance. The integration to the daily scale of these processes is only outlined as we take a well-established approach here that is described in detail in the literature. The description of whole-ecosystem processes is closed by a description of the water balance of the soil.

The genetic processes that drives the evolutionary response to environmental changes is subsequently described. For completeness of the features of the ForGEM model, also the genetic statistics related to diversity and differentiation of populations is described. These statistics are based on post-processing of the model output.

The key-publications in which the modelling principles and parts of the model descriptions with applications are presented include: (Kramer et al. 2015, Kramer et al. 2008a, Kramer K.; van der Werf 2010, Kramer 2007, Schelhaas 2008, Schelhaas et al. 2007).

3.2. Model description

The ForGEM model is a spatially explicit, individual tree model on genetics, ecology and management of forests. ForGEM is developed to assess impacts of environmental change and forest management on forest growth and dynamics, the rate of adaptive response of functional traits and the adaptive potential of tree populations (Kramer et al 2008, 2010). The model is based on the ecophysiological functioning of whole trees with a mechanistic coupling between genetic and eco-physiological processes. The biophysical- and biochemical environment that drive the eco-physiological processes are described in detail by the model. The genetics module describes the quantitative genetics of functional traits of trees, by potentially assigning a genetic system to each of the model's parameters. Gene flow is described through the production and dispersal of pollen and seed and thus the spatial exchange of genetic information. This genetic system makes that seedlings differ in their genetic makeup from their parents and thereby in the parameter values that determine the ecophysiological processes. The model allows to calculate a large number of genetic statistics that characterize the genetic make-up of an individual tree, the genetic diversity of a population and differentiation between populations. Individual tree statistics include the genotype of the individual, and methods for its spatial distribution. The population statistics, within and among populations, include diversity measures, differentiation measures between populations, heterozygozity and F-statistics. The user of the ForGEM model can define forest management, i.e. silvicultural operations, to realistically simulate species composition and demographic dynamics driven by forest management.

Earlier versions and parts of the model description below are presented in the literature or reports. These descriptions and updates thereof are repeated in this document to have a full and consistent description in one place including the parameter values that are used in the latest version of the ForGEM model. The content of this document is the base of the model documentation at the ForGEM wiki (http://vle-models.wur.nl/wiki/index.php/ForGEM_-_Forest_Genetics,_Ecology_and_Management) which allows dynamic updating of the model documentation and parameterisation. The

numbering of the tables and figures follows that for the model wiki and therefore deviates from the style of numbering of the other chapters of this deliverable.
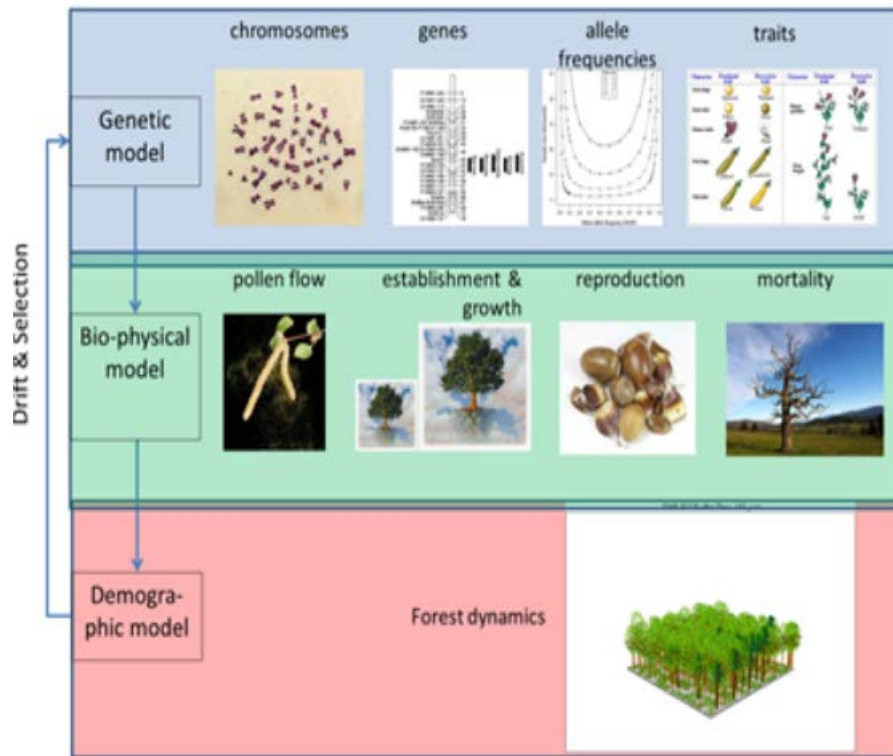
Figure ForGEM 1. Schematic overview of the processes described by the ForGEM model

The demographic dynamics of the tree population is simulated by the number of seeds arriving and germinating at a patch, and subsequent mortality of seedlings, saplings and adult trees. Furthermore, the dynamics of both structural features and weight of different tree components of individual trees are simulated. The principal state equations used in the ForGEM model are thus those describing the stand dynamics, the structural features of trees, and the weight of the different tree components.

$$\frac{dN_x}{dt} = NNew_x - NMrt_x$$ *Eqn ForGEM 1*

$$\frac{dS_y}{dt} = RS_y$$ *Eqn ForGEM 2*

$$\frac{dW_z}{dt} = f_z \cdot NPP - T_z$$ *Eqn ForGEM 3*

Table ForGEM 1. General variables of the ForGEM model.

Symbol	Description
N_x	Number of trees per unit area
New_x	New individual seed, seedling or tree in the population
Mrt_x	Mortality of individual or cohort in case of seeds and seedlings
x	seeds, seedlings, trees
S_y	Structural feature y
R	Rate of change
y	Tree height, stem volume, diameter at breast height, crown volume, crown diameter
W_z	Weight of tree component z
NPP	Net Primary Production
f_z	Fraction of NPP allocated to tree component
T_z	Turnover rate of tree component z
z	foliage, branches, heartwood, sapwood, coarse roots, fine roots, reserves

Detailed descriptions of the processes and empirical relationships determining the rate of change of the these principal state variables are presented below.

3.2.1. Life cycle

The model ForGEM describes the life- and annual cycle of individual trees. The life cycle is characterized by the production, dispersal and germination of seeds, growth of seedlings, saplings, juvenile and adult trees that produce and disperse seeds. The annual cycle is characterised by bud burst leading to new leaves or needles thus initiating the growing season. The end of the growing season is determined by leaf fall for deciduous trees, and the

hardening of needles and thereby the loss of photosynthetic capacity of coniferous trees, thus leading to the dormant period of trees in the boreal and temperate zones.
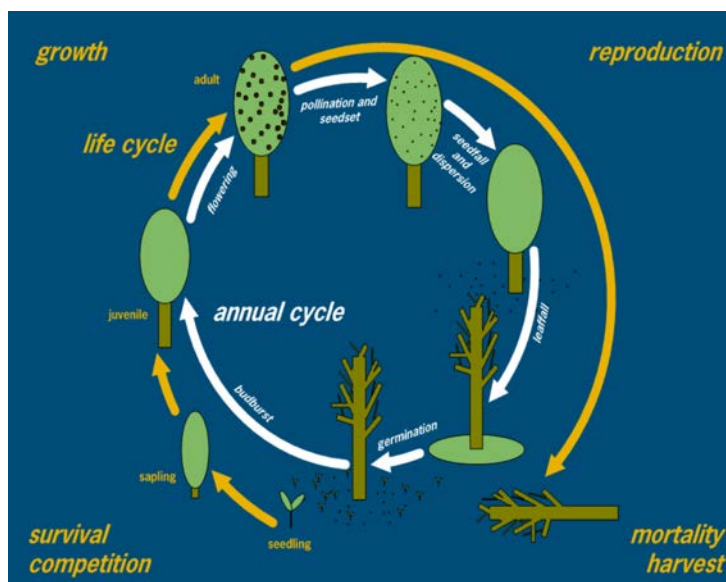
Figure LifeCycle 1. Scheme of the coupled life and annual cycle of trees as applied in the ForGEM model

3.2.1.1. Germination and establishment

Germination is a simple process in ForGEM entailing the germination of available seeds and establishment of seedlings. Only a fraction of the seeds in the seed bank are considered viable, and are considered to germinate on average at the same date. Germination further depends on the fraction of light that reaches the forest floor. After germination, a cohort of seedlings of a tree species is established on a grid by the model. The population size of the cohort depends on the number of viable seeds in the seed bank. The initial height and crown radius of the seedlings is determined based on an initial reference height and crown diameter some variation based on a coefficient of variation of these parameters. This is done to avoid that all cohorts are exactly the same initially so that competitive mortality is very slow.

The co-ordinates of the seedlings are at the moment of establishment unknown. Only the seedlings of cohorts that reach 2m in height get co-ordinates in the grid and thereby become individual trees. This approach is taken because computational demands to simulate every germinated seed are too high. For each cohort it is stored who the father and the mother trees are. This is necessary to assign individual parameter values to saplings, i.e. individual trees, based on the genetic make-up of the parents (see Genetics section for details). A cohort is thus defined as the number of seedlings per father – mother combination per year.

Based on the initial crown radius and height of the seedling, the initial states of the plant component are determined. The crown length is set at the same value of the seedling heights. Thus the crown volume can be determined and based on the optimal foliage density both the initial foliage weight and initial weight of the reserve pool ((Kramer 2001), see Allocation section).

To determine the initial weights of the other tree components, first the shoot weight is determined from the initial height based on an allometric relationship. The weights of the branches and stem are then calculated based on the empirical relationships described in the Allocation section (see also: (Kramer 2001). Initial total root weight is a fixed fraction of total plant weight. Also the distribution of total root weight to fine and coarse roots is based on a fixed optimal partitioning.

$$W_{sh} = c_1 \cdot H^{c_2}$$ *Eqn Germ 1*

Table Germ 1. Variables of the germination and establishment sub-model.

Symbol	Description	Unit
W_{sh}	Shoot weight	kg individual^{-1}
H	Tree height	m

Table Germ 2. Parameter values of the germination sub model.

Symbol	Parameter name	ParameterDescription	Unit
c_1	C1HghWsh	Coefficient allometric height – shoot relationship	kg

c_2	C2HghWsh	Coefficient allometric height – shoot relationship	-
	CFGrmSd	Fraction of viable seeds	[0,1]
	CGerminationDay	Mean date of germination	day of year
	CIniHgh	Initial height of seedling after germination	m
	CIniRds	Initial crown radius of seedling germination	m
	CMnFRdnGrm	Minimal fraction of radiation on soil to allow germination	[0,1]
	CTrnNsd	Turnover fraction of seeds	yr^{-1}
	CVariationCoeficient-CrownRadius	Variation coefficient initial crown radius	m
	CVariationCoeficient-Height	Variation coefficient initial seedling height	m
	cOptWrt2WtotRatio	optimal root to total plant weight ratio	kg root kg plant^{-1}
	cOptWfr2WrtRatio	optimal fine root to total root weight ratio	kg fine root kg total roots^{-1}

Table Germ 3. Parameter values of the germination sub model. Default indicates parameter values applied to all tree species.

Parameter name	Default	*Fagus sylvatica*	*Picea abies*	*Pinus sylvestris*	*Quercus spec.*
C1HghWsh[1]		0.086282	0.041405	0.060895	0.085703
C2HghWsh[1]	3				
CFGrmSd[1]		0.8	0.61	0.85	0.81
CGerminationDay	120				
CIniHgh	0.25				
CIniRds	0.1				
CMnFRdnGrm[2]		0.015	0.02	0.10	0.05
CVariationCoeficientCrownRadius	0.1				
CVariationCoeficientHeight	0.1				
cOptWrt2WtotRatio	0.175				
cOptWfr2WrtRatio	0.8				

References: [1] (Kramer 2001), [2] (Kramer et al. 2006b)

3.2.1.2.   Mortality

Mortality is implemented as the probability that a tree will die during the time step under consideration. For any time step, the combined mortality chance is compared to a random sample from a uniform distribution. If the sample is smaller than the probability of mortality, the tree is considered to die and removed from the tree list. Mortality is the combined probability of mortality due to the following causes: reserves are completely depleted; the tree is outcompeted by others; self-thinning; age; storm; frost; (optionally random mortality to reduce number of saplings).

The overall probability of mortality, *P*, is calculated according to:

$$P = 1 - \prod_i (1 - P_i)$$ *Eqn. Mort 1*

With P_i the probability mortality due to cause *i*. The different causes of mortality, P_i , are determined as follows:

- if the reserves of a tree are depleted, it receives a 100% mortality probability
- if the ambient temperature exceeds the level of frost hardiness to which the tree is acclimated. This frost event kills seedlings and saplings less than 2m in height. Adult trees lose all their foliage and flowers at such temperatures during the frost sensitive period following bud burst. Such frost event not immediately kills adults but may cause that reserves are depleted required to build-up new foliage which then causes the death of the tree.
- if due to competition crowns of adjacent tree overlap to such a degree that the edge of a crown reaches the stem of the suppressed tree, then this tree receives a 100% mortality probability. See below in section 'Crown volume and –radius' for the description of increment of crown radius and overlap of crowns between adjacent trees.
- if the maximum number of trees that can be supported on the plot area is exceeded, calculated over all individual trees of all tree species, exceeds the maximum number of

trees as determined by the -2/3 self-thinning rule from Reinecke (in (Zeide 1987)). This self-thinning rule is applied in the ForGEM model to seedlings and saplings less than 2m in height only.

$$n_{max} = 10^{(\theta \cdot log_{10}(\bar{W}))}$$
Eqn. Mort 2

- if the tree approaches its maximum age. Age dependent mortality is based upon a Weibull distribution function. It depends on the species-specific maximum age, at which 95% of the trees are dead, and a period before that maximum age at which the population is 95% alive, but begins to decline. The cumulative density function of a Weibull distribution takes the following form:

$$CDF_{Weibull} = 1 - exp^{-\left(\frac{x}{\alpha}\right)^{\gamma}}$$
Eqn. Mort 3

$$\alpha = \frac{x_{start}}{-ln(1-v_{start})^{\frac{1}{\gamma}}}$$
Eqn. Mort 4

$$\gamma = \frac{ln\left(\frac{ln(1-v_{max})}{ln(1-v_{start})}\right)}{ln\left(\frac{1-x_{max}}{1-x_{start}}\right)}$$
Eqn. Mort 5

Thus, the probabilities of death are such that 5% of the population is dead at age x_{start} (CMxAge-CMrtPhs), and 95% is dead at Age=CMxAge. CMxAge is a location parameter that is, however, not equal to the maximum attainable age of the species. CMrtPhs is the age dependent mortality phase and scales the width of the distribution. Age dependent mortality is determined once a year, at the 1st of January.

Table Mortality 1. Variables of the mortality sub-model

Symbol	Variable name	Description	Unit
x_{start}	xStart	Age at which age related mortality begins	yr
x_{max}	xEnd	Maximum tree age	yr

v_{start}	vStart	Fraction of trees dead at x_{start} (0.05)	-
v_{max}	vMax	Fraction of trees dead at v_{max} (0.95)	-
n_{max}	MxN	Maximum number of trees per unit area	# m^{-2}
$\overline{W}$		Average seedling weight	kg individual^{-1}

Table Mortality 2. Parameters of the mortality sub-model.

Symbol	Parameter name	Description	Unit
θ	CThn	Self-thinning parameter	-
$T_{h,0}$	CFrostThresholdTemp	Temperature threshold of de-hardened tree below which tree is damaged	°C
P_h	CFrostSensitivePeriod	Duration of frost sensitive period around budburst	d
v_{max}	CMxAge	Age at which 95% of the trees are dead due to age related mortality	yr
v_{phase}	CMrtPhs	Period before maximum age from which age related mortality sets in	yr

Table Mortality 3. Parameters values for the mortality sub-model

Parameter name	Default	Deciduous Broadleaved	Evergreen Needleleaved	Fagus sylvatica	Picea abies	Pinus sylvestris	Quercus spec.
CFrostSensitivePeriod[a]	10						
CFrostThresholdTemp[a]		-2	-4				
CThn[b]	3/2						
CMrtPhs[c]				150	50	150	250
CMxAge[c]				350	200	300	450

[a] (Kramer et al. 2008a); [b] (Zeide 1987); [c] (Schelhaas 2005)

3.2.1. Annual cycle

In dynamic models of the annual cycle of tree, the key state variable is *the state of development*, *S(t)*. It quantifies the phase of a given attribute of the annual cycle. The state of development can either describe physiological attributes of the annual cycle or quantify the annual ontogenetic cycle of trees. Physiological attributes includes frost hardiness (Repo

et al. 1990, Leinonen 1996) or photosynthetic capacity of needles (Pelkonen and Hari 1980) Mäkelä et al. 2004) of evergreen conifers.
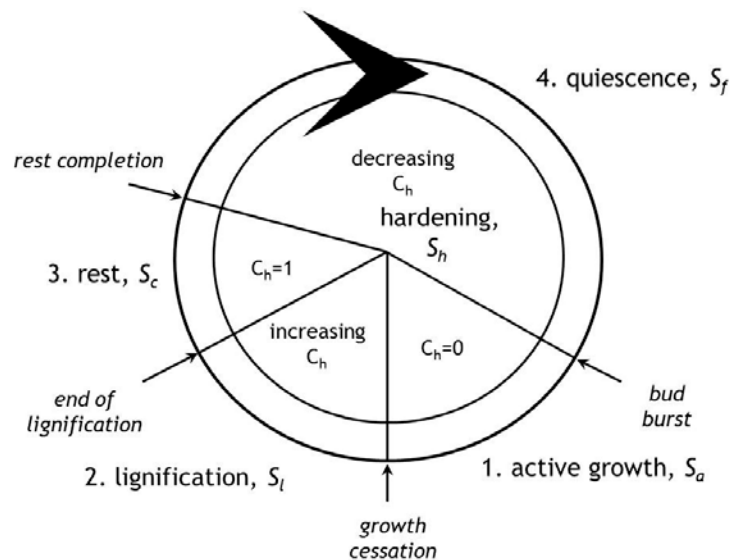
Figure AnnualCycle 1. Annual cycle of trees of boreal and temperate zone. The outer circle describes fixed sequence of ontogenetic development and phenological events. The inner circle describes frost hardiness as trait with partly fluctuating development, whereby the competence of hardening depends on the state of ontogenetic development of the fixed sequence cycle. Redrawn from Leinonen (1996b).

As in any other dynamic model, the time course of the state of development is simulated by first calculating the value of its first time derivative, i.e. the value of *the rate of development, R(t)*, and then integrating *R(t)* over time (Hari et al. 1970, Hari 1972). The effect of environmental factors on phenology is modelled via environmental responses of the *R(t)*. Details and full referencing of the approach to model the annual cycle of development of trees can be found in (Hänninen and Kramer 2007, Kramer and Hänninen 2009).

3.2.1.1. Bud burst and flowering

The date of bud burst is simulated in ForGEM as a two stage process: rest followed by a period of quiescence. The state of rest is tracked by the state variable S_r and that during quiescence with S_o (with the subscript o referring to ontogenetic development. The rest phase ends if S_r attains a critical value ($S_r = S_r^*$). Similarly quiescence end if S_o attains a critical value ($S_o = S_o^*$), at which moment bud burst is predicted to occur. The equations determining the rate development of S_r and S_o as function of ambient temperature ($T(t)$) are, respectively:

$$R_r(t) = \begin{cases} 0, T(t) < T_{r,\min} \\ \dfrac{T(t) - T_{r,\min}}{T_{r,opt} - T_{r,\min}}, T_{r,\min} \leq T(t) \leq T_{r,opt} \\ \dfrac{T(t) - T_{r,\max}}{T_{r,opt} - T_{r,\max}}, T_{r,opt} \langle T(t) \leq T_{r,\max} \\ 0, T(t) \rangle T_{r,\max} \end{cases}$$

Eqn. Pheno 1

and

$$R_o(t) = \begin{cases} 0, T(t) < T_{o,\min} \\ \dfrac{1}{1 + e^{(a_o \cdot (T(t) + b_o))}}, T(t) \geq T_{o,\min} \end{cases}$$

Eqn. Pheno 2

The start day of flowering is assumed to be the same date as the predicted day of bud burst. The duration of flowering is described in ForGEM as a species specific value.

3.2.1.2. Leaf fall

During the growing season a period of active growth followed by a period of lignification is discerned in the ForGEM model, characterised by the state of active growth (S_a) and that of lignification (S_l). The rate of development of these states are in both cases described by a simple temperature sum model

$$R_a(t) = \begin{cases} 0, T(t) < T_b \\ T(t) - T_b, T(t) \geq T_b \end{cases}$$

Eqn. Pheno 3

$$R_l(t) = \begin{cases} 0, T(t) < T_b \\ T(t) - T_b, T(t) \geq T_b \end{cases}$$

Eqn. Pheno 4

The phase of active growth ends if S_a attains a critical value ($S_a = S_a^*$), thereby starting the lignification phase which ends when S_l attains a critical value ($S_l = S_l^*$). In case of deciduous trees, leaf fall predicted to occur the day at which lignification ends.

3.2.1.3. Annual cycle of frost hardiness

During winter, the needles of evergreen coniferous trees harden to withstand frost. The change in the state of hardiness, S_h, is described by a stationary state S_h, which is attained when environmental conditions are stable for a prolonged period, and a time constant, τ_h:

$$R_h(t) = \frac{1}{\tau_h} \cdot \left(\hat{S}_h(t) - S_h(t) \right)$$

Eqn. Frost 1

The stationary state is characterized by a minimal level of hardiness, which is attained during the growing season; a competence function indicating the ability of the tree to harden, as trees cannot harden during the growing season; and two functions determining the stationary state of hardiness depending on the change in temperature and photoperiod.

$$\hat{S}_h(t) = \hat{S}_{h,\min} + C_h(t) \cdot \left(\Delta \hat{S}_{hT}(t) + \Delta \hat{S}_{hP}(t) \right)$$

Eqn. Frost 2

The competence to harden depends on the ontogenetic phase, with phase = 1: active growth, phase = 2: lignification; phase 3: rest; phase 4: quiescence.

$$C_h(t) = \begin{cases} MAX\left(0, 1 - \frac{S_o(t)}{S_h^*}\right), Phase = 1 \\ \frac{S_l(t)}{S_l^*}, Phase = 2 \\ 1, Phase = 3 \\ MAX\left(0, 1 - \frac{S_o(t)}{S_{o,h}^*}\right), Phase = 4 \end{cases}$$

Eqn. Frost 3

The dependency of the stationary state of hardiness depending on the change in temperature and photoperiod is described below.

$$\Delta \hat{S}_{hT}(t) = \begin{cases} \Delta \hat{S}_{hT,\min}, & T(t) \rangle T_{h,1} \\ \Delta \hat{S}_{hT,\max} \cdot \left(1 - \dfrac{T_{\min}(t) - T_{h,2}}{T_{h,1} - T_{h,2}}\right), & T_{h,2} \leq T(t) \leq T_{h,1} \\ \Delta \hat{S}_{hT,\max}, & T(t) \langle T_{h,2} \end{cases}$$

Eqn. Frost 4

$$\Delta \hat{S}_{hP}(t) = \begin{cases} \Delta \hat{S}_{hP,\min}, & NL(t) \langle NL_{h,1} \\ \dfrac{\Delta \hat{S}_{hP,\max}}{NL_{h,2} - NL_{h,1}} \cdot \left(NL(t) - NL_{h,1}\right), & NL_{h,1} \leq NL(t) \leq NL_{h,2} \\ \Delta \hat{S}_{hP,\max}, & NL(t) \rangle NL_{h,2} \\ 0, & Phase = 1 \wedge C_h = 0 \end{cases}$$

Eqn. Frost 5

Needle damage occurs if the ambient temperature drops below the level of frost hardiness of the needles. This needle damage then results in a fraction of needle area lost due to frost:

$$d_f = a_f + b_f \cdot e^{c_f \cdot S_h(t)}$$

Eqn. Frost 6

$$D(t) = \frac{1}{1 + e^{d_f \cdot (S_h(t) - T_{\min}(t))}}$$

Eqn. Frost 7

3.2.1.4. Annual cycle of photosynthetic capacity

Because of hardening is the photosynthetic capacity of needles is very low in winter time and only recovers during spring. The recovery of photosynthetic capacity is described as follows in the ForGEM model:

$$R_p = \frac{1}{\tau_p} \cdot \left(\frac{1}{1 + c_p \cdot a_p^{-(\hat{S}_p - S_p)}} - \frac{1}{1 + c_p \cdot a_p^{(\hat{S}_p - S_p)}} \right)$$

Eqn. PhotoCap 1

With the stationary state of photosynthetic capacity as simple function of ambient temperature:

$$\hat{S}_p(t) = b_p \cdot T(t)$$

Eqn. PhotoCap 2

Table Pheno 1.Variables for sub-model of the annual cycle

Symbol	Variable name	Description	Unit
C_h	Ch	Competence for stationary state of frost hardiness to respond to temperature or photoperiod	-
C_o	Co	Competence for ontogenetic development	-
D	D	fraction of foliage damaged by frost	-
$\Delta \hat{S}_{hT}$	dcShT	Change of stationary state of frost hardiness due to change in temperature	°C
$\Delta \hat{S}_{hP}$	dcShP	Change of stationary state of frost hardiness due to change in photoperiod	°C
K_p	Kp	Efficiency of the actual photosynthetic capacity relative to the annual maximum level at similar environmental conditions	
NL	NL	Night length	h d-1
R_a	Ra	Rate of change of active growth	°Cd d-1
R_h	Rh	Rate of change of frost hardiness	°C d-1
R_l	Rl	Rate of change of lignification	°Cd d-1
R_o	Ro	Rate of ontogenetic development	FU d-1
R_p	Rp	Rate of change or recovery of photosynthetic capacity	d-1
R_r	Rr	Rate of change of rest	CU d-1
$\hat{S}_h$	cSh	Stationary state of frost hardiness	°C
$\hat{S}_p$	cSp	Stationary state of recovery of photosynthetic capacity	°C
S_a	Sa	State of active growth	°Cd
S_h	Sh	State of frost hardiness	°C
S_l	Sl	State of lignification	°Cd
S_o	So	State of ontogenetic development	FU
S_p	Sp	State of recovery of photosynthetic capacity	
S_r	Sr	State of rest	CU
T		Average daily temperature	°C
T_{min}		Minimum daily temperature	°C

Table Pheno 2. Parameters for sub-model of the annual cycle

Symbol	Parmeter name	Description	Unit
a_f	af	Coefficient for effect of frost hardiness damage on amount of foliage	
a_0	ao	Coefficient for ontogenetic development	
a_p	ap	Coefficient for rate of recovery of photosynthetic capacity	
b_f	b0	Coefficient for effect of frost hardiness damage on amount of foliage	
b_o	bf	Coefficient for ontogenetic development	
b_p	bp	Coefficient for stationary state of recovery of photosynthetic capacity	
c_f	CaP	Coefficient for effect of frost hardiness damage on amount of foliage	
c_p	CaT	Coefficient for rate of recovery of photosynthetic capacity	
Ca_T	cf	Competence of state of active growth to respond to temperature	
Ca_P	cp	Competence of state of active growth to respond to photoperiod	
$\Delta \hat{S}_{hP,\min}$	cSh_min	Minimum change of stationary state of frost hardiness with a change in photoperiod	
$\Delta \hat{S}_{hP,\max}$	dcShP_max	Maximum change of stationary state of frost hardiness with a change in photoperiod	
$\Delta \hat{S}_{hT,\min}$	dcShP_min	Minimum change of stationary state of frost hardiness with a change in temperature	
$\Delta \hat{S}_{hT,\max}$	dcShT_max	Maximum change of stationary state of frost hardiness with a change in photoperiod	
$NL_{h,1}$	dcShT_min	Lower limit of effective range of photoperiod to change frost hardiness	
$NL_{h,2}$	NLh_1	Upper limit of effective range of photoperiod to change frost hardiness	
$\hat{S}_{h,\min}$	NLh_2	Minimal state of frost hardiness	

$S^*_{o,h}$	sSo_h	Critical state of ontogenetic development where competence of stationary level of frost hardiness to respond to change in temperature or photoperiod is zero	
S^*_o	sSo	Critical state of ontogenetic development to end quiescence	
S^*_p	sSp	Critical state of recovery of photosynthetic capacity so that full competence of recovery is attained	
S^*_r	sSr	Critical state of ontogenetic development to end rest	
S^*_a	sSa	Critical state of active growth to end active growth phase	
S^*_l	sSl	Critical state of lignification to end lignification phase	
τ_h	Tau_h	Time constant for rate of change of frost hardiness	
τ_P	Tau_p	Time constant for rate of recovery of photosynthetic capacity	
T_b	Tb	Base temperature for accumulation of thermal time	
$T_{h,1}$	Th_1	Upper limit of effective range of temperature to change frost hardiness	
$T_{h,2}$	Th_2	Lower limit of effective range of temperature to change frost hardiness	
$T_{o,min}$	To_min	Minimum temperature for rate of change of ontogenetic development	
$T_{r,max}$	Tr_max	Maximum temperature for rate of change of rest	
$T_{r,min}$	Tr_min	Minimum temperature for rate of change of rest	
$T_{r,opt}$	Tr_opt	Optimum temperature for rate of change of rest	
	CFloweringDuration	Flowering duration relative to flowering start day	d
	CFloweringStartDay	Flowering start day relative to predicted day of leaf bud burst	d
	CLeaffallDay	Average day of leaf fall	DoY
	CSeedfallDay	Average day of seed fall	Doy

Table Pheno 3. Parameters values for sub-model of the annual cycle.

Parameter name	Default	Evergreen Needleleaved	Fagus sylvatica	Picea abies	Pinus sylvestris	Quercus spec.
ao [b]			-0.1	-0.14	-0.11	-0.17
af [a]		-0.1435				
ap		2				
b0 [b]			-33.1	-35.9	-37.6	-16.2
bf [a]		-1.4995				
bp		600				
CaP	0					
CaT	1					
cf [a]		0.1071				
cp [c]		100				
cSh_min [a]		-4.5				
dcShP_max		-18.5				
dcShP_min		0				
dcShT_max		-47				
dcShT_min		0				
NLh_1		8				
NLh_2		16				
sSa			510	510	510	510
sSl			300	300	300	300
sSo [b]			3.6	1.6	2.4	11.7
sSo_h [a]		4.5				
sSp [a]		6500				
sSr			117.6	82.5	85.3	112.2
Tau_h		4				
Tau_p		0.000416				
Tb			5	5	4.4	5
Th_1		10				
Th_2		-16				
To_min [b]	0					
Tr_max [b]			77	16.3	16.5	58.9
Tr_min [b]			-19.4	-11.4	-13.8	-20.6
Tr_opt [b]			-0.2	0.1	-1.2	-0.8
CFloweringDuration	10		5			
CFloweringStartDay	0					
CLeaffallDay	305					
CSeedfallDay	304					

[a] (Leinonen et al. 1995); [b] (Kramer 1994); [c] (Pelkonen and Hari 1980)

3.2.1.5. Production, dispersal and survival of seeds

The production of seeds is based on the approach developed in (Kramer 2001, Kramer et al. 2006a). The reproduction of trees is described by: (1) the maximum production of seeds by an individual tree; (2) the variability of the production of seeds between years; (3) the seed dispersal distance and (4) survival and fraction of viable seeds. The literature shows a wide variation of values for the maximum seed production of forest trees (Fenner 1985, Fenner 1992, Schopmeyer 1974, Siegl 1990, Willson 1983, Young and Young 1992, Youngblood and Max 1992, Zasada 1978). These values are based on trees that have attained their maximum crown dimensions. The actual seed production of a tree was determined by multiplying the maximum seed production by the ratio of the actual to maximum crown size. Between-year variability in seed production rates was stochastically simulated based on the empirical distribution of seed crop levels found by (LaBastide and Van Vredenburch 1970). However, their 8-scale empirical distribution of seeds was pooled into an equidistant 4-scale distribution indicating a very bad, moderate, fairly good and very good seed production. These classes rare represented in the model as 0-10%, 10-40%, 40-70% and 70-100% seed production relative to the maximum seed production. Each of these classes have an empirical frequency distribution. Seed production is thus a stochastic process. This is simulated in the ForGEM model by drawing 2 samples from a random uniform distribution. The first random number determines the class of seed production, whilst the second random number determines the number of seeds from that class.

$$r \sim \begin{cases} U_{0-10} \\ U_{10-40} \\ U_{40-70} \\ U_{70-100} \end{cases} \qquad \qquad \textit{Eqn Seed 1}$$

$$N_{sd} = c N_{sd,max} \cdot \frac{V_{cn}}{V_{cn,max}} \cdot r \qquad \qquad \textit{Eqn Seed 2}$$

$$V_{cn,max} = 2\pi \cdot R_{cn,max}^2 \cdot L_{cn,max} \qquad \qquad \textit{Eqn Seed 3}$$

These seeds are subsequently dispersed over the simulated area. Based on the literature referred to above, we came to the distribution of distances over which the seeds were distributed as indicated based on an Weibull probability density (Bakker 1980, Bossema 1979, Bouman 2000, Estrada and Fleming 1986, Fleming and Estrada 1993, Jansen 2003, Karlsson 2001, Murray 1986).

$$f(x; \lambda, k) = \begin{cases} \frac{k}{\lambda} \left(\frac{x}{\lambda} \right)^{k-1} e^{-(x/\lambda)^k} & x \geq 0, \\ 0 & x < 0, \end{cases}$$
Eqn Seed 2

where $k > 0$ is the shape parameter and $\lambda > 0$ is the scale parameter of the distribution.

A generic value for all tree species on the decay rate of seeds during the winter of 0.15 per month was used, as very limited information is available on demographic factors that cause seed mortality following seed dispersal. For the fraction of viable seeds of total seed production, some information was found in the literature resulting in the following values: Betula: 0.73, Fagus: 0.80, Picea: 0.61, Pinus: 0.85, Pseudotsuga: 0.61, Quercus: 0.81 (Fenner, 1985, 1992; Hester et al., 1991; Schopmeyer, 1974; Young and Young, 1992).

Table Seed 1. Variables of the seed production, -dispersal and –survival sub model.

Symbol	description	unit
N_{sd}	Number of seeds	$\# \, m^{-2}$
V_{cn}	Crown volume	$m^3 \, tree^{-1}$
$V_{cn,max}$	Maximum crown volume	$m^3 \, tree^{-1}$

Table Seed 2. Parameters of the seed production, -dispersal and –survival sub model.

Symbol	Parameter name	Description	unit
$R_{cn,max}$	CMxRds	Maximal crown radius	m
$L_{cn,max}$	CMxLngCn	Maximal crown length	m
	CF0_10MxPrdNSd[b]	Fraction of maximum number of seeds produced in 'very bad' masting year	
	CF10_40MxPrdNSd[b]	Fraction of maximum number of seeds produced in 'moderate' masting year	
	CF40_70MxPrdNSd[b]	Fraction of maximum number of seeds produced in 'fairly good' masting year	
	CF70_100MxPrdNSd[b]	Fraction of maximum number of seeds	

		produced in 'very good' masting year	
	CMxPrdNSd[c]	Maximal number of seeds produced by fully grown adult tree	
	CNSdPerFlower[c]	Number of seeds per flower	#
	cLocationSeedDispersion	Parameter of seed dispersal function	
λ	cScaleSeedDispersion	Parameter of seed dispersal function	
k	cShapeSeedDispersion	Parameter of seed dispersal function	

Table Seeds 3. Parameter values for the seed production, dispersal, survival sub model.

Parameter name	Default	Evergreen Needleleaved	Fagus sylvatica	Picea abies	Pinus sylvestris	Quercus spec.
CMxRds[a]			20	15	12	15
CMxLngCn[a]			18	8	8	8
CF0_10MxPrdNSd[b]	0					
CF10_40MxPrdNSd[b]			0.66	0.79	0.11	0.32
CF40_70MxPrdNSd[b]			0.24	0.21	0.89	0.66
CF70_100MxPrdNSd[b]			0.1	0	0	0.03
CMxPrdNSd[c]			18000	70000	25000	15000
CNSdPerFlower[c]	1	50	2			
cLocationSeedDispersion	0					
cScaleSeedDispersion			40	40	50	40
cShapeSeedDispersion	1					

[a] (Kramer 2001); [b] (Kramer et al. 2006a)

3.2.2. Allocation

Newly formed net primary production (NPP) is allocated with priority to reserves and foliage. It is assumed that the maximum weight of the reserve pool is equal to weight of the foliage. Thus, based on the reserve pool can a tree be completely defoliated once. To determine the maximum reserve pool, an optimal leaf density is calculated based on a species-specific maximum leaf area index and crown length.

$$\rho^*_{fl} = \frac{\Lambda_{max}}{L_{cn}} \qquad \qquad Eqn\ Alloc\ 1$$

Depending on the volume of the canopy thus the optimum amount of foliage and thereby the maximum reserve pool can be determined even if there is actually no foliage on the tree.

The reserves become depleted when NPP does not cover costs for respiration. As soon as NPP exceeds respiration, the reserve pool is refilled again. Also the build-up of the foliage in spring of deciduous trees depletes the reserve pool.

The amount of NPP allocated for foliage growth depends on crown expansion. The NPP allocated to foliage is the amount required to fill the new crown volume with foliage at optimal density. If there is insufficient NPP to do so, height growth is reduced such that the expansion of the crown fits with the NPP available to fill that crown volume with foliage at optimal density.

$$W_{fl}^{*} = \cdot \rho_{fl}^{*} \cdot \sigma_{fl} \cdot \frac{dL_{cn}}{dt}$$

Eqn Alloc 2

For the allocation of assimilates among the other tree components, we assume that the internal development of partitioning ratios depends on the dimensions of the trees only (Grote 1998). This assumption can be derived from pipe model theory and the principle of a functional balance between tree components (Mäkelä and Hari 1986, Valentine 1988). We derived the partitioning ratios of the weights of foliage, branch, stem and roots with total shoot biomass using biomass data obtained from literature (see: (Van Hees 1997, Van Hees and Clerkx 2003, Van Hees et al. 1996)). On a log–log scale, a polynomial function was fitted, relating the ratio of a plant component with the stem to the total shoot biomass.

$$\ln\left(\frac{W_{fl}}{W_{st}}\right) = C_1 + C_2 \cdot \ln(W_{sh}) + C_3 \cdot \ln(W_{sh})^2 + C_4 \cdot \ln(W_{sh})^3$$

Eqn Alloc 3

$$\ln\left(\frac{W_{br}}{W_{st}}\right) = C_5 + C_6 \cdot \ln(W_{sh}) + C_7 \cdot \ln(W_{sh})^2 + C_8 \cdot \ln(W_{sh})^3$$

Eqn Alloc 4

$$\Rightarrow \frac{W_{st}}{W_{sh}} = \frac{1}{1 + \ln\left(\dfrac{W_{fl}}{W_{st}}\right) + \ln\left(\dfrac{W_{br}}{W_{st}}\right)}$$

Eqn Alloc 5

Total root weight shoot should be 17.5% of the total tree weight (above and belowground), and allocation to the roots is calculated accordingly. Initially 35% of the total plant weight is assigned to the roots. The fractions of NPP allocated to the other plant components are derived such that the tree strives for partitioning ratios between plant components as indicated by Eqns Alloc 3-5.

Table Alloc 1. Variables of the allocation sub-model. These variables are attributes of the Tree object.

Symbol	Description	Unit
L_{cn}	Length of the tree crown	m
dL_{cn}/dt	Change in crown volume	$m^{-2} d^{-1}$
ρ^*_{fl}	Optimal foliage density	m^{-2} foliage m^{-3} crown
W^*_{fl}	Foliage weight at optimal foliage density	kg foliage $tree^{-1}$
W_{fl}	Foliage weight	kg tree-1
W_{br}	Branch weight	kg tree-1
W_{st}	Stem weight	kg tree-1
W_{fr}	Fine root weight	kg tree-1
W_{cr}	Coarse root weight	kg tree-1
W_{rs}	Reserve weight	kg tree-1

Table Alloc 2. Parameters of the allocation sub-model

Symbol	Parameter name	Description	unit
C_i	C_iAll	Allocation coefficient	-
σ_{fl}	cSLA	Specific leaf area	m^{-2} foliage g^{-1} DM
Λ_{max}	cMxLai	Maximum leaf area index	m^{-2} foliage m^{-2} soil

Table Alloc 3. Parameters values for the allocation sub-model

Parameter name	Fagus sylvatica	Picea abies	Pinus sylvestris	Quercus spec.
C1All	-1.204	-1.0711	-1.1734	-1.1145
C2All	-0.3404	-0.2005	-0.1762	-0.3041
C3All	-0.0232	-0.0119	-0.0137	-0.0123

C4All	0	-0.0011	-0.0028	0
C5All	-0.5272	-1.0793	-1.1929	-0.561
C6All	-0.1256	-0.0536	-0.0208	0.0965
C7All	-0.0315	-0.0419	-0.0368	-0.0619
C8All	0.0034	0.0031	0.0022	0.004
cSLA	22	5	5	15
cMxLai	6	6	4	4

3.2.3. Structural tree features

Structural features consider tree height, and the volume and diameter of both the stem and crown. In this section the dynamics of these structural features are described.

3.2.3.1.   Height

We used the Chapman-Richard function for height increment of the trees. This function is a generalization of the Von Bertalanffy's growth model (Pienaar and Turnbull 1972), which is based on fundamental allometric relationships between both anabolic and catabolic rates and the volume of an organism.

$$H = H_{max} \cdot \left(1 - e^{C7 \cdot t}\right)^{C_8}$$

$$\Rightarrow \frac{\partial H}{\partial t} = C_7 \cdot C_8 \cdot H \cdot \left(\frac{e^{C_7 \cdot t}}{1 - e^{C_7 \cdot t}}\right) \qquad\qquad Eqn.\,Height\,1$$

where height *H* is in metres and *t* the tree age in years.

3.2.3.2.   Stem diameter and volume

For diameter increment we also used an allometric approach, as is used in virtually all forest growth models (Landsberg and Waring, 1997; Zianis et al., 2005). To derive diameter increment, we expressed volume as power function of both diameter and height (Peichl and Arain, 2007, their Eqn. 3.):

$$V = D^{C1} \cdot H^{C2} \cdot e^{C3}$$

$$\Rightarrow \frac{\partial D}{\partial t} = \frac{D}{C_1} \cdot \left\{ \frac{1}{V} \cdot \frac{\partial V}{\partial t} - \frac{C_1}{H} \cdot \frac{\partial H}{\partial t} \right\} \qquad \text{*Eqn Diameter 1*}$$

Where, volume V is in dm^3 and diameter D in cm. *e* is the exponent of the natural logarithm. The volume of the stem is based on the weight and density of the stem, ρ_s (Duursma et al., 2007, their Eqn. 2):

$$V = \frac{W_s}{\rho_{sw}} \qquad \text{*Eqn Volume 1*}$$

3.2.3.3. Crown volume and –radius

For the dynamics in volume and radius of the crowns of trees we adopt the approach developed by Schelhaas et al. (2007). In the ForGEM model the crown is represented by two cylinders, with equal crown length and the same centre represented by the coordinates of the crown position. The outer cylinder is determined by the actual crown radius and can only increase in size. The inner cylinder is a 'virtual crown' that can both expand and decrease in size, depending on the competition with neighbouring crowns. If there is no crown overlap with any of the adjacent trees, the actual and the virtual crowns coincide and expand in the same rate. The decrease of the virtual, inner, crown is the consequence of an increase in overlap with the crowns of adjacent trees, either from the same or of other tree species. The virtual crown volume is determined as a reduction of the actual crown volume proportional to both the overlap in crowns and the amount of foliage each tree has in the shared crown volume. The virtual crown thus also has a virtual crown radius which is less than the actual crown radius.

$$V'_{cn,i} = V_{cn,i} - \sum_j \left(O_{cn,ij} \cdot \frac{\Lambda_i}{\Lambda_i + \Lambda_j} \right) \qquad \text{*Eqn Crown 1*}$$

$$R'_{cn} = \sqrt{\frac{V'_{cn}/L_{cn}}{\pi}} \qquad \text{*Eqn Crown 2*}$$

In case a tree is surrounded by competitors that still expand their crowns, the virtual radius of the suppressed tree continues to decrease. If the crown radii of the surrounding tree

extend to the degree that they reach the stem of the suppressed tree, the virtual crown radius of the tree becomes zero. In this situation assume the supressed tree dies (see Mortality section).

The maximum increase of the projected crown area (Maximum Percentage Crown Area Increment, %CAI$_{MAX}$, % per year) of the outer cylinder is expressed as a logarithmic function of the projected crown area. The maximum increase is then modified according to the ratio between virtual crown volume and actual crown volume, indicating the competition status of the tree.

$$\left(\frac{\frac{dA_{cn}}{dt}}{A_{cn}}\right)_{max} = 1.25 \cdot \beta \cdot \left(\frac{\ln(A_{cn})}{\ln(R_{cn,max} \cdot \pi)} - 1\right) \qquad \text{Eqn Crown 3}$$

$$\frac{\frac{dA_{cn}}{dt}}{A_{cn}} = \frac{V'_{cn}}{V_{cn}} \cdot \left(\frac{\frac{dA_{cn}}{dt}}{A_{cn}}\right)_{max} \qquad \text{Eqn Crown 4}$$

The parameter *b* can be fitted to growth and yield tables. The factor 1.25 is introduced in the model to compensate for the effect of crown competition that is already present in stands of normal density in yield tables. See Schelhaas et al. (2007) for the description how this factor is derived.

3.2.3.4.   Horizontal and vertical root distribution

Both the roots and the foliage have a horizontal distribution to determine the competition for light and water, respectively. Roots also have a vertical distribution, whereas the foliage is assumed to have a uniform vertical in the canopy. This fraction of either foliage or roots at a given distance of the distance from the stem depends on the diameter of the crown.

$$f(d, D_{cn}) = e^{-\delta_1 \cdot \left(\frac{d-\delta_0}{D_{cn}}\right)^{\delta_2}} \qquad \text{Eqn DistanceDist 1}$$

C0vDstRt   = C0DstRt

C1vDstRt   = 2.5*C1DstRt

C2vDstRt = C2DstRt

Table Structure 1. Variables of the sub-models on structural tree features. These variables are attributes of the Crown object

Symbol	Description	unit
A_{cn}	Projected crown area	m^2
D_{cn}	Diameter of the crown	m^2
L_{cn}	Crown length	m
R_{Rcn}	Crown radius	m
R'_{cn}	Virtual crown radius	m
V_{cn}	Crown volume	m^3
V'_{cn}	Virtual crown volume	m^3
$O_{cn,ij}$	Crown volume overlap between tree *i* and tree *j*	m^3
$\left(\dfrac{\frac{dA_{cn}}{dt}}{A_{cn}}\right)_{max}$	Maximum relative increment of crown area	-
$\dfrac{\frac{dA_{cn}}{dt}}{A_{cn}}$	Actual relative increment of crown area	-

Table Structure 2. Parameters of the sub-models on structural tree features

Symbol	Parameter name	Description	Unit
	C0DstRt	Offset parameter of horizontal distribution function of root	
	C1DstRt	Scale parameter of horizontal root distribution function	
	C2DstRt	Shape parameter of horizontal root distribution function	
	C0vDstRt	Offset parameter of vertical distribution function of root	
	C1vDstRt	Scale parameter of vertical root distribution function	
	C2vDstRt	Shape parameter of vertical root distribution function	
	C1Dbh	Parameter volume-dbh function	
	C2Dbh	Parameter volume-dbh function	

	C3Dbh	Parameter volume-dbh function	
	C7Hgh	Parameter height growth function	-
	C8Hgh	Parameter height growth function	-
β	cCrownExpansion	shape parameter for crown expansion rate (per year)	yr^{-1}
$ρ_{sw}$	CDnsWd	Wood density	kg m^{-3}
	cExponentTaperFunction	rc of the relation ln(power)=intercept + rc * ln(TreeHeight/Diameter0)	-
	cInterceptTaperFunction	intercept of the relation ln(power)=intercept + rc * ln(TreeHeight/Diameter0)	-
	CFHwSt	Fraction weight of hardwood to weight of sapwood	0 < F < 1
	CMxHgh	Maximal tree height	m
	CMxHghWhw	Maximum height of heartwood formation	m
	CMxLngCn	Maximum length of crown	m
	CMxRds	Maximum crown radius	m
	CMxRSrf	Maximal rate of increase in projected crown surface	m2/ind/yr

Table Structure 3. Parameter values of the sub-models on structural tree features

ParameterName	Default	Fagus sylvatica	Picea abies	Pinus sylvestris	Quercus robur	Quercus spec_
C0DstFl	0					
C0DstRt	0					
C1Dbh		1.86116	1.75055	1.82075	1.82628	1.82628
C1DstFl	1					
C1DstRt	1					
C2Dbh		1.04313	1.10897	1.07427	1.11342	1.11342
C2DstRt	2					
C3Dbh		-3.05257	-2.75863	-2.88085	-3.04885	-3.04885
C7Hgh		-0.01766	-0.02642	-0.035	-0.01336	-0.01336
C8Hgh		1.333	1.612792	1.5998	0.96667	0.96667
cCrownExpansion		0.0861	0.1379	0.123		0.0942
CDnsWd		579	400	420	580	580
cDnsWdGrn		1070	800	850	1025	
cExponentTaperFunction		-0.1664	-0.3126	-0.2212	-0.1963	

56

CFHwSt	0.8				
cInterceptTaperFunction		0.201	0.0019	0.0178	0.0695
CMxHgh		57	42.494	31.558	47.315	47.315
CMxHghWhw	14				
CMxLngCn		20	15	12	15	15
CMxRds		18	8	8		8
CMxRSrf		0.444000444	0.16214	0.1827		0.338791643

3.3. Eco-physiology

Net primary production is the fraction of gross photosynthesis available for growth after the carbon cost for respiration are accounted for. Light intercepted by the canopy is the primary driver of photosynthesis, however, the availability of water, nutrients and ambient atmospheric CO_2 concentration as well as the prevailing temperature determine the rate of photosynthesis and thereby growth of individual trees. Nutrient availability and uptake is not dynamically simulated in the version of the ForGEM model described here. Thus, tissue nutrient concentrations are kept constant in the model but do affect the value of many parameters (see below).

3.3.1. Photosynthesis

3.3.1.1. Instantaneous rates of photosynthesis and transpiration

We use the standard Farquhar model (Farquhar et al. (1980); Von Caemmerer and Farquhar 1981) to describe photosynthesis, including nitrogen-dependency of Jmax and Vcmax; (Forstreuter 2002) and the Leuning model of stomatal conductance (Leuning (1995)).
The rate of net photosynthesis is determined by the constraints imposed either by the rate of carboxylation or the rate of electron transport, minus the cost of processes in the leaf that are not related to responses to light, i.e. dark respiration:

$$A_n = min(V_c, V_J) - R_d \qquad \text{Eqn. Photo 1}$$

The rate of carboxylation is described by a two-substrate (CO_2 and O_2) Michaelis-Menten function, above a the CO_2 compensation point in absence of mitochondrial respiration (Γ^*):

$$V_c = \frac{V_{c,max} \cdot (c_i - \Gamma^*)}{c_i + k_c \cdot \left(1 + \dfrac{o_i}{k_o}\right)} \qquad \text{Eqn. Photo 2}$$

The rate of electron transport is described by an saturating curve of internal CO_2. The value 4 in the denominator converts electrons to CO_2 as 4 electrons are required to reduce the carbon in carbon dioxide to sugars (i.e. from $C^{(4+)}O_2^{(2-)}$ to $C_6^{(0)} H_{12}^{(+)} O_6^{(2-)}$).

$$V_J = \frac{J \cdot (c_i - \Gamma^*)}{(c_i + 2 \cdot \Gamma^*)} \qquad \text{Eqn. Photo 3}$$

Electron transport in the foliage is driven by intercepted light following an empirical curve with initial light use efficiency, α, and maximum value J_{max} (Tenhunen et al. (1976) in Forstreuter (2002)):

$$J = \frac{\alpha \cdot I}{\sqrt{1 + \left(\dfrac{\alpha \cdot I}{J_{max}}\right)^2}} \qquad \text{Eqn. Photo 4}$$

J_{max} and $V_{c,max}$ are linearly related (Kattge and Knorr 2007):

$$J_{max}(T_{ref}) \qquad = r_{J,V} \cdot V_{c,max}(T_{ref}) \qquad \text{Eqn. Photo 5}$$

Both J_{max} and $V_{c,max}$ linearly depend on leaf nitrogen concentration, which can be described by the nitrogen dependency of $V_{c,max}$ (Evans 1989):

$$V_{c,max} = a_{V_{c,max}} + b_{V_{c,max}} \cdot N \qquad \text{Eqn. Photo 6}$$

Internal [CO_2] is described by a function of leaf assimilation and stomatal conductance to CO_2 (g_c):

$$c_i = c_a - \frac{A_n}{g_c} \cdot P_{atm}$$

Eqn. Photo 7

The dependency can be resolved through the widely-observed correlation between stomatal conductance and leaf photosynthesis (Wong, Cowan, & Farquhar 1979), by representing leaf stomatal conductance as (Leuning 1995):

$$g_c = g_0 + a \cdot \frac{A_n}{c_a - \Gamma^*} \cdot \frac{D_0}{D_0 + D}$$

Eqn. Photo 8

where g_0 is leaf stomatal conductance in the dark, Γ^*, is compensation point for CO_2, the parameter D_0 captures stomatal response to air vapor pressure deficit (D) and a is an empirical parameter which is a function of soil water content:

$$a = \frac{a_{max}}{1 + \left(\frac{1 - SWR}{\theta_1}\right)^{\theta_2}}$$

Eqn. Photo 9

where the soil water ratio, SWR ranges between 1 at field capacity and 0 at wilting point. The shape of the response to soil water content follows Landsberg and Waring (1997).

The ratio of internal to external CO_2 concentration and thus be expressed as a linear function of air vapor pressure deficit D, and a non-linear function of soil water ratio:

$$\frac{c_i}{c_a} = \left(\frac{a - P_{atm}}{a}\right) - \left(\frac{P_{atm}}{a \cdot D_0}\right) \cdot D$$

Eqn. Photo 10

Finally, if we assume transpiration to be imposed transpiration (i.e. if we neglect the effects of aerodynamic resistance), instantaneous leaf transpiration (E) can be expressed as:

$$E = 1.56 \cdot g_c \cdot \frac{D}{P_{atm}}$$

Eqn. Photo 11

where the factor 1.56 accounts for the different diffusivities of water and CO_2 in air.

The temperature dependence of the photosynthetic parameters is described following Farquhar & Wong (1984) for the parameters k_c, k_o and R_d (Eqn 9):

$$p(T) = p(T_{ref}) \cdot \exp\left(\frac{H_a \cdot (T - T_{ref})}{R \cdot T \cdot T_{ref}}\right)$$

Eqn. Photo 12

The temperature dependence of for J_{max} and V_{Cmax} is calculated based on Johnson et al. (1942)

$$p(T) = p(T_{ref}) \cdot H_d \cdot \exp\left(\frac{H_a \cdot (T - T_{ref})}{R \cdot T \cdot T_{ref}}\right) \cdot \frac{1 + \exp\left(\frac{T_{ref} \cdot \Delta S - H_d}{T_{ref} \cdot R}\right)}{1 + \exp\left(\frac{T \cdot \Delta S - H_d}{T \cdot R}\right)}$$

Eqn. Photo 13

From which it can be derived that the optimal temperature is:

$$T_{opt} = \frac{H_d}{\Delta S - R \cdot \ln\left(\frac{H_a}{H_d - H_a}\right)}$$

Eqn. Photo 14

Based on an analyses on 36 plant species Kattge and Knorr (2007) find that acclimation of photosynthesis to ambient temperature depends on the temperature sensitivity of $r_{J,V}$ and ΔS of both J_{max} and $V_{c,max}$:

$$r_{J,V} = a_{J,V} + b_{J,V} \cdot T_{growth}$$

Eqn. Photo 15

$$\Delta S_J = a_{\Delta S_J} + b_{\Delta S_J} \cdot T_{growth}$$

Eqn. Photo 16

$$\Delta S_{V_{c,max}} = a_{\Delta S_{V_{c,max}}} + b_{\Delta S_{V_{c,max}}} \cdot T_{growth}$$

Eqn. Photo 17

This mechanism result in a shift in the temperature optimum of J_{max} and $V_{c,max}$ based on average ambient temperatures.

Table Photo 1. Variables of the coupled photosynthesis, conductance, transpiration sub-model.

Symbol	Description	Unit
A_n	Rate of net photosynthesis	$\mu mol\ CO_2\ m^{-2}$ foliage s^{-1}

V_c	Carboxylation limited rate of gross leaf photosynthesis	μmol CO_2 m^{-2} foliage s^{-1}
V_J	Electron transport limited rate of gross leaf photosynthesis	μmol CO_2 m^{-2} foliage s^{-1}
R_d	Dark respiration of the leaf	μmol CO_2 m^{-2} foliage s^{-1}
c_i	Internal CO_2 concentration	ppm (μmol CO_2 mol air^{-1})
	<u>Abiotic drivers</u>	
P_{atm}	Atmospheric pressure	Pa
N	Foliar nitrogen concentration	g N m^{-1} foliage
I	Incoming short-wave radiation intercepted by the foliage	μmol quanta m^{-2} foliage
c_a	Ambient CO_2 concentration	*ppm* (μmol CO_2 mol^{-1} air)
T	Temperature	*K*
D	Vapor pressure deficit	*Pa*
SWR	Soil water ratio, relative soil water content between wilting point and field capacity	m^3 water m^{-3} soil

Table Photo 2. Parameters of the coupled photosynthesis, conductance, transpiration sub-model.

Symbol	Parameter name	unit
$V_{c, max}$	Maximal carboxylation rate	μmol CO_2 m^{-2} foliage s^{-1}
J_{cmax}	Maximal electron transport rate	μmol CO_2 m^{-2} foliage s^{-1}
k_c	Michaelis-menten coefficient for carboxylation	μmol CO_2 mol^{-1}
k_o	Michaelis-menten coefficient for oxygenation	mmol O_2 mol^{-1}
Γ^*	CO_2 compensation point	*ppm (μmol CO_2 mol^{-1} air)*
$H_a(k_c)$	Activation energy for k_c	J mol^{-1}
$H_a(k_o)$	Activation energy for k_o	J mol^{-1}
ΔS	Change in entropy	J mol^{-1} C^{-1}
α	Quantum yield	*(μmol CO_2 m^{-2} foliage s^{-1}) · (μmol fotons m^{-2} foliage s^{-1})$^{-1}$*

Symbol	Parameter name	ParameterDescription	Unit	ReferenceCode
θ_1	c1SoilWaterContent2StomatalConductance	Coefficient of dependency of gs to soil water ratio	m3 H20 / m3 soil	Landsberg & Waring 1997
θ_2	c2SoilWaterContent2StomatalConductance	Coefficient of	-	Landsberg &

Towards the Sustainable Management of Forest Genetic Resources FORGER FP7- 289119

		dependency of gs to soil water ratio		Waring 1997
Γ^*	CCO2CompensationPointAtRefTmp	CO2 compensation point at reference temperature	ppm	
g_0	CCuticularConductanceCO2	Leaf cuticular conducance for CO2	mol m-2 s-1	Leuning 1995
Ha	cHaOfCO2CompensationPoint	Activation energy of GammaStar	J mol-1	
	cHaOfJMax	Activation energy of Jmax	J mol-1	
	cHaOfKc	Activation energy of Kc	J mol-1	
	cHaOfKo	Activation energy of K0	J mol-1	
	cHaOfRd	Activation energy of Ri	J mol-1	
	cHaOfVcMax	Activation energy of Vcmax	J mol-1	
Hd	cHdOfJMax	De-activation energy of Jmax	J mol-1	
	cHdOfVcMax	De-activation energy Vcmax	J mol-1	
$r_{J,V}$	cIntercept_JMaxToVcMax	Intercept of dependency of Jmax to VcMax at T=25C to ambient growing condidtions, to describe acclimation to temperature	-	Kattge & Knorr 2007
$a_{\Delta SJ}$	cInterceptDeltaS_JMax	Intercept of entropy term (deltaS) for Jmax to ambient growing conditions to describe acclimation to temperature	J mol-1 K-1	Kattge & Knorr 2007
$a_{\Delta SVc,max}$	cInterceptDeltaS_VcMax	Intercept of entropy term (deltaS) for VcMax to ambient growing	J mol-1 K-1	Kattge & Knorr 2007

62

		conditions to describe acclimation to temperature		
$a_{Vc,max}$	cInterceptVcMaxToNitrogen	Intercept from Vcmax to foliage nitrogen (on a leaf area basis)	mu mol CO2 m-2 foliage 2-s	
k_c	cKcAtRefTmp	Michaelis Menten constant for carboxylation rate	umol CO2 mol-1	
k_o	cKoAtRefTmp	Michaelis Menten constant for oxygenation rate	mmol O2 mol-1	
	cPAR_Watt2Quanta	Conversion of photosynthetic radiaton in Watt m-2 to mu mol quanta m-2 s-1	mu mol quanta J-1	Goudriaan & Van Laar 1994
α	cQuantumEfficiency	Light conversion efficiency based in incoming radiation	mol CO2 mol-1 quanta	
$Rd_{Vc,max}$	cRd2VcMaxRatioAtRefTmp	Dependence of Rd to VcMax at reference temperature	(mu mol CO2 m-2 foliage s-1) (mu mol CO2 m-2 foliage s-1) -1	Leuning et al. 1995
	cRdAtRefTmp	mitochondrial respiration at reference temperature	mu mol CO2 m-2 foliage s-1	
	cSlope_JMaxToVcMax	Slope of dependency of Jmax to VcMax at T=25C to ambient growing	C-1	Kattge & Knorr 2007

		condidtions, to describe acclimation to temperature		
$b_{\Delta SJ}$	cSlopeDeltaS_JMax	Slope of entropy term (deltaS) for Jmax to ambient growing conditions to describe acclimation to temperature	J mol-1 K-1 C-1	Kattge & Knorr 2007
$b_{\Delta Vc.max}$	cSlopeDeltaS_VcMax	Slope of entropy term (deltaS) for VcMax to ambient growing conditions, to describe acclimation to temperature	J mol-1 K-1 C-1	Kattge & Knorr 2007
$b_{Vc,max}$	cSlopeVcMaxToNitrogen	Slope from Vcmax to foliage nitrogen	mu mol CO2 g-1 N s-1	
a	cStomatalConductance2Assimilation	Parameter in response of stomatal conductance to assimilation rate, at field capacity	Pa	Leuning 1995
a_{max}	cStomatalConductance2SoilWaterContent	Parameter in response of stomatal conductance to volumetric soil water content	m3 (soil) / m3 (water)	Granier 1994
D_0	cStomatalConductance2VPD	Parameter in response of stomatal conductance to vapor pressure deficit	Pa	Leuning 1995

Table Photo 3. Parameter values of the coupled photosynthesis, conductance, transpiration sub-model.

Parameter name	*Default*	*Deciduous Broadleaved*	*Evergreen Needleleaved*
c1SoilWaterContent2StomatalConductance	0.6		

c2SoilWaterContent2StomatalConductance	7		
CCO2CompensationPointAtRefTmp	40		
CCuticularConductanceCO2		0.04	0.01
cHaOfCO2CompensationPoint	29000		
cHaOfJMax		60498	69830
cHaOfKc	59500		
cHaOfKo	35900		
cHaOfRd	46390		
cHaOfVcMax		61154	66438
cHdOfJMax	200000		
cHdOfVcMax	200000		
cIntercept_JMaxToVcMax	2.59		
cInterceptDeltaS_JMax	659.7		
cInterceptDeltaS_VcMax	668.39		
cInterceptVcMaxToNitrogen		5.4	34.05
cKcAtRefTmp	404		
cKoAtRefTmp	248		
cQuantumEfficiency	0.8		
cRd2VcMaxRatioAtRefTmp	0.0089		
cRiAtRefTmp	0.02281		
cSlope_JMaxToVcMax	-0.0035		
cSlopeDeltaS_JMax	-0.75		
cSlopeDeltaS_VcMax	-1.07		
cSlopeVcMaxToNitrogen		30.38	9.71
cStomatalConductance2Assimilation	438910		
cStomatalConductance2VPD	2000		
CTmpRef_C	25		
WntGrn		0	1

3.3.1.2.   Respiration

Both maintenance and growth respiration are considered in the ForGEM model. The rate of maintenance respiration of living tree tissue is based on the nitrogen concentration of the plant component above a nitrogen threshold value. Growth respiration is based on a fixed

proportion of the net primary production that is required to convert assimilated to plant dry matter (Penning de Vries et al. 1974, Penning de Vries 1975). Maintenance respiration strongly depends on temperature, whereas the temperature dependency of growth respiration is determined by the temperature dependency of net primary production.

$$R_M = \sum_z f(T) \cdot \eta_z \cdot (N_z - H_{z,0})$$ *Eqn Resp 1*

$$R_G = \alpha \cdot NPP$$ *Eqn Resp 2*

$$f(T) = Q_{10}^{(T - T_{ref})/T_{ref}}$$ *Eqn Resp 3*

Table Respiration 1. Variables of the respiration sub-model

Symbol	description	unit
R_M	Rate of maintenance respiration	kg C tree^{-1} d^{-1}
R_G	Rate of growth respiration	kg C tree^{-1} d^{-1}
N_z	Nitrogen concentration	kg N kg^{-1} C
T	Temperature	°C

Table Respiration 2. Parameters of the respiration sub-model.

Symbol	Description	unit
η_z	Respiration coefficient	kg C kg^{-1} N d^{-1}
H_z	Offset of nitrogen dependency of maintenance respiration	kg N kg^{-1} C
T_{ref}	Reference temperature for temperature response function	m^{-2} foliage g^{-1} DM
Q_{10}	Maximum leaf area index	m^{-2} foliage m^{-2} soil
z	foliage, branches, sapwood, fine roots	

Table Respiration 3. Parameter values of the respiration sub model.

Symbol	Parameter name	value
α	cEfficiencySugars2DryMatter	0.8
Q_{10}	CQ10	2.5
T_{ref}	CTmpRef_C	25
η_{fl}	cRespiration2NitrogenFlAtRefTmp	0.5042

η_{fr}	cRespiration2NitrogenFrAtRefTmp	0.361267
η_{sw}	cRespiration2NitrogenSwAtRefTmp	0.1268
H_{fl}	cRespiration2NitrogenFlAtRefTmpInt	0.0042
H_{fr}	cRespiration2NitrogenFlAtRefTmpInt	0
H_{sw}	cRespiration2NitrogenFlAtRefTmpInt	0

3.3.2. Light interception and diurnal integration of leaf gas-exchange

Light is distributed over trees in a 20x20 grid cell regardless their exact position, but taking into account the vertical distribution of the foliage. Foliage is assumed to be distributed equally within a crown. The vertical distribution of foliage over a grid cell is thus determined by absence or presence of individual tree crowns. The vertical distribution of foliage is represented as by vertical layers, where the limits of the layers are determined by the top heights and crown bases of all trees present in the grid cell. The thickness of each layer is variable, depending on the exact positions of the individual crowns, but within the layer the amount of foliage is constant.

Total photosynthetic active radiation absorbed by tree n (PAR_n, MJ d^{-1}) is calculated as:

$$PAR_n = fI_n \times R_{in} \times (1 - \rho) \times fPAR \qquad \text{\textit{Eqn. Light 1}}$$

PAR_n is based on the fraction of radiation absorbed by tree n (fI_n), which is the sum of the absorbed radiation per layer:

$$fI_n = \sum_1^m fI_{m,n} \qquad \text{\textit{Eqn. Light 2}}$$

fI_n in its turn depends on the radiation absorbed in layer m by individual tree n:

$$fI_{m,n} = \frac{LA_{m,n}}{LA_m}(1 - e^{-k\,LA_m}) \qquad \text{\textit{Eqn. Light 3}}$$

LA_m is the leaf area in layer m over all individual that have foliage in that layer:

$$LA_m = \sum_1^n LA_n t_m \qquad\qquad\qquad \textit{Eqn. Light 4}$$

LA$_n$ is then the average leaf area per meter crown of individual *n*:

$$LA_n = \frac{W_{fl}\, SLA}{H - Cn_b} \qquad\qquad\qquad \textit{Eqn. Light 5}$$

Note that *f* indicates the weighted leaf area either of a tree or of a tree in a layer and can thus exceed unity.

Table Light 1. Variables of the light interception sub model

Symbol	Description	unit
CB$_n$	the crown base of tree *n*	m
fl$_m$	fraction radiation absorbed by layer *m*	-
fl$_{m,n}$	fraction radiation absorbed by the part of the crown of tree *n* present in layer *m*	-
fPAR	fraction of incoming radiation that is photosynthetically active	-
fT$_m$	fraction radiation transmitted by layer	m
H$_n$	top height of tree *n*	m
LA$_m$	leaf area in layer *m*	m^2 foliage
LA$_{m,n}$	leaf area of tree *n* in layer *m*	
LA$_n$	average leaf area per meter crown length for tree *n*	m^2 foliage m^{-1} crown length
R$_{in}$	incoming radiation	MJ m^{-2} d^{-1}
WF$_n$	foliage weight of tree *n*	kg

Table Light 2. Parameters of the light interception sub model

Symbol	Parameter name	Description	unit
SLA	CSla	specific leaf area	m^2 kg
t_m	-	thickness of layer *m*	m
k	CExt	extinction coefficient in leaves	-
ρ	rho	canopy reflectivity	-

Table Light 3. Parameter values of the light interception sub model

ParameterName	Default	Fagus sylvatica	Picea abies	Pinus sylvestris	Quercus spec_
CSla		22	5	5	15

CExt	0.7
rho	0
t_m	1

3.3.3. Soil water balance

The amount of water in the soil is determined by the incoming rain not intercepted and evaporated by the canopy, the uptake of water by trees for transpiration and evaporation of water from the soil surface. Capillary rise and drainage is not considered by the current model. Water in access of the water holding capacity of the soil is removed from the system ('tipping bucket').

3.3.3.1. Evaporation of water from the soil

Soil evaporation is the loss of water from the surface of the soil to the atmosphere. The calculation of evaporation from the soil in ForGEM is based on Kergoat (1998). Equation 11 in Kergoat states:

$$E_{soil} = \frac{\Delta\, R_n^{soil}+\frac{\rho \cdot C_p}{r_a^{soil}}\cdot D}{L_v \cdot \left(\Delta+\gamma \cdot \left(1+\frac{r_s}{r_a^{soil}}\right)\right)} \cdot \tau_{day} \qquad \text{Eqn Evap 1}$$

The evaporation can be separated in a radiation term ($E_{soil,R}$) and an air moisture term ($E_{soil,M}$):

$$E_{soil,R} = \frac{\Delta \cdot R_n^{soil}}{L_v \cdot \left(\Delta+\gamma \cdot \left(1+\frac{r_s}{r_a^{soil}}\right)\right)} \cdot \tau_{day} \qquad \text{Eqn Evap 2}$$

$$E_{soil,M} = \frac{\frac{\rho \cdot C_p}{r_a^{soil}}\cdot D}{L_v \cdot \left(\Delta+\gamma \cdot \left(1+\frac{r_s}{r_a^{soil}}\right)\right)} \cdot \tau_{day} \qquad \text{Eqn Evap 3}$$

The saturated vapour pressure curve is (Goudriaan et al. 1977 in Kropff & van Laar, 1993 p70 (5.8)):

$$e_s = 0.611e^{(17.4T_a/(T_a+239))}$$

Eqn Evap 4

Δ is the derivate of this function:

$$\Delta = \frac{239 \times 17.4\ e_s}{(T_a+239)^2}$$

Eqn Evap 5

r_s increases as the soil dries out:

$$r_s = r_s^{min} \frac{W_f - W_{wp}}{W_a - W_{wp}}$$

Eqn Evap 6

Table Evap 1. Variables of the soil evaporation model

Symbol	Description	unit
E_{soil}	evaporation from the soil	m d^{-1}
Δ	temperature derivative of the saturated vapour pressure curve	kPa C^{-1}
R_n^{soil}	net radiation at the soil level	W m^{-2}
r_s	soil surface resistance, as a function of the wetness of the soil	s m^{-1}
τ_{day}	day length	s

Table Evap 2. Parameters of the soil evaporation model

Symbol	Parameter name	Description	unit	Default
ρ	AirDensity	air density	kg m^{-3}	1.226
Cp		specific heat of air	J kg-1 C-1	1013
Lv	cEvaporationHeat	latent heat of vaporization of water	J kg-1 H$_2$0	2.45·10e6
γ	cPsychrCoeff	psychrometric constant	Pa C^{-1}	67
r_a^{soil}	SoilAtmResistance	aerodynamic resistance of the soil	s m^{-1}	100
$r_{s,min}$	SoilSurfaceResistanceMin	Minimum soil surface resistance	s m^{-1}	50

3.4. Genetics

Forest genetic models include a genetic map representing the location of loci and genetic markers at the chromosomes of the species. This can either be based on bi-parental inheritance, to simulate inheritance of genetic information from the cell-nucleus, or based on uni-parental inheritance to simulate inheritance of genetic information from chloroplasts

and mitochondria in the cytoplast. Such a representation of the genetic map can thereby represent observed nuclear- and cytoplasmic genetic markers obtained from sequencing of the genome of the species of interest. This allows simulating the dynamics of these genetic markers observed in a forest (Kramer K.; van der Werf 2010). To connect genetic information to an observed or theoretical phenotype, one or more loci and one or more alleles are considered in these models. For quantitative genetic traits, multiple loci with multiple alleles are considered to be able to represent a broad range of values of the phenotype. To initialize a genetic model, the number of loci and alleles per locus need to be set, as well as initial allele frequencies and allelic effects for the traits under selection. Usually neutral traits are considered, which are not under selection, as detailed genetic information is often missing. An impact analysis of environmental change of forest management then provides an upper estimate of the genetic diversity maintained in the forest. However, no assessment of a rate of adaptation can be made. If adaptive traits are considered, an allelic effect needs to be assigned to each allele and for all loci considered, as well as possible interactions between alleles and between loci (Falconer and Mackay 1996). In the most complicated genetic system also loci are considered that affect the phenotypic value of multiple traits.

The genetic processes included in mechanistic forest genetic models are immigration, emigration, selection, and mutation (Hartl and Clark 1997). *Mutation* is only relevant when simulating over a very large number of generations or for very large populations. As we focus on forest genetic models as tool for forest management, mutation is not considered here.

Immigration and emigration refers for forest stands to gene flow by dispersal of pollen and seeds toward and from the stand. Forest genetic models describe gene flow in considerable detail either between individual trees, between and among patches, or over the landscape, depending on the spatial scale of the model. The use of genetic markers made it possible to do a parental analysis both to determine which tree fathered a seed collected from a mother tree, to assess pollen dispersal, and to determine from which mother tree the seed originated from which a seedling established, to assess seed dispersal. Using the distance between father and mother tree and between mother tree and seedling,

elaborate statistical dispersal kernels are calibrated for both short distance dispersal and long distance dispersal. For the dispersal of seeds, dispersal kernels are developed dispersal by wind, birds, mammals and other dispersal strategies.

Selection in forest genetic models refers to the loss of genetic diversity due to differential selection pressure at one or more stages of the tree's life cycle. This is done either as a result of differences in the genetic composition of trees or population of trees for particular traits, or directly related to differences in the tree's fitness depending on the whole tree's phenotypic value. In the former approach the following the stages of the life cycle considered to be under selection: male and female fertility in production of gametes; fecundity; and viability of seedlings and trees resulting in differential mortality. In the latter approach an optimal phenotypic value is assumed for particular environmental conditions.

3.4.1. Quantitative genetics of functional traits of trees

The genetic control of individual functional traits is modelled by additive-linear relationship between the allelic effect (i.e. '*allele dose*') and the phenotypic value of the trait (Liu, 1998). In the simulation the genetic part of each trait is determined by a given initial number of loci. The contribution of a locus to the phenotype is proportionally to the effects of its alleles, which do not change during the course of the simulation, and the frequencies of the alleles, which do change during the course of the simulation. The contribution of each locus on the phenotypic value of the individual is independent from other loci. I.e. there is no epistasis between loci. However, loci can be linked with a user-defined recombination fraction. Each locus has initially 2 alleles, which is kept constant during the simulation. This means that there is neither mutation, nor immigration of new alleles for a particular loci. However, gene flow of known alleles per locus between populations can be simulated. To obtain the actual phenotypic value of a traits, a random/environmental component is added to the value characterised by the genetic system. A user-defined initial heritability determines the additive genetic variance as fraction of the total phenotypic variance. During the course of the simulation genetic variation can be lost, resulting in a reduction of the heritability of the

trait. Thus, the following aspects of the genetic model need to be quantified for the initialisation of the ForGEM model:

- the initial frequencies of the alleles for each locus contributing to the phenotypic values of the trait

- the initial genetic and non-genetic variances

- the allelic effects or 'allele dose' of each allele

If measured of otherwise observed values for these aspects are not available, they are determined by statistical methods during the initialisation of the model. These methods are described below. Observed values can always be used to overrule the statistically derived values.

Evolutionary forces such as selection, random genetic drift, migration and mutation, act upon these frequencies and modify them through time. These genetic processes are modelled in the ForGEM model in detail.

3.4.1.1.   Initializing allele frequencies

For polymorphic loci in trees, the distribution of the frequency of alleles over all loci that determining a trait is typically U-shaped. This means that alleles are either very common (allele frequency approaching unity) or very rare (allele frequency approaching zero), but rarely have a frequency in the population of around 0.5 (e.g. Hamrick, 2004; Chakraborty et al., 1980). In absence of observations on the frequency distribution of alleles of adaptive traits to initiate the genetic model, an equilibrium allele frequency distribution of neutral traits is used Crow and Kimura, 1970). This equilibrium distribution of allelic frequencies (x) can expressed as (Nei, 1987, p. 367):

$$\phi\left(x\right) = \frac{\Gamma\left(M + M'\right)}{\Gamma\left(M\right)\Gamma\left(M'\right)}\left(\left(1 - x\right)^{M-1}x^{M'-1}\right)$$

Eqn Genetics 1

With:

$M = 4 \cdot N_e \cdot v$

$M' = M / (k - 1)$

N_e effective population size

v mutation rate per locus and per generation

k the number of alleles per locus

$\Gamma()$ gamma function

M can also be estimated from the average heterozygosity (H). If a large number of loci are examined, then: $M = H/(1-H)$. The figure below presents an example of the shape of this equation for different values of H and k.
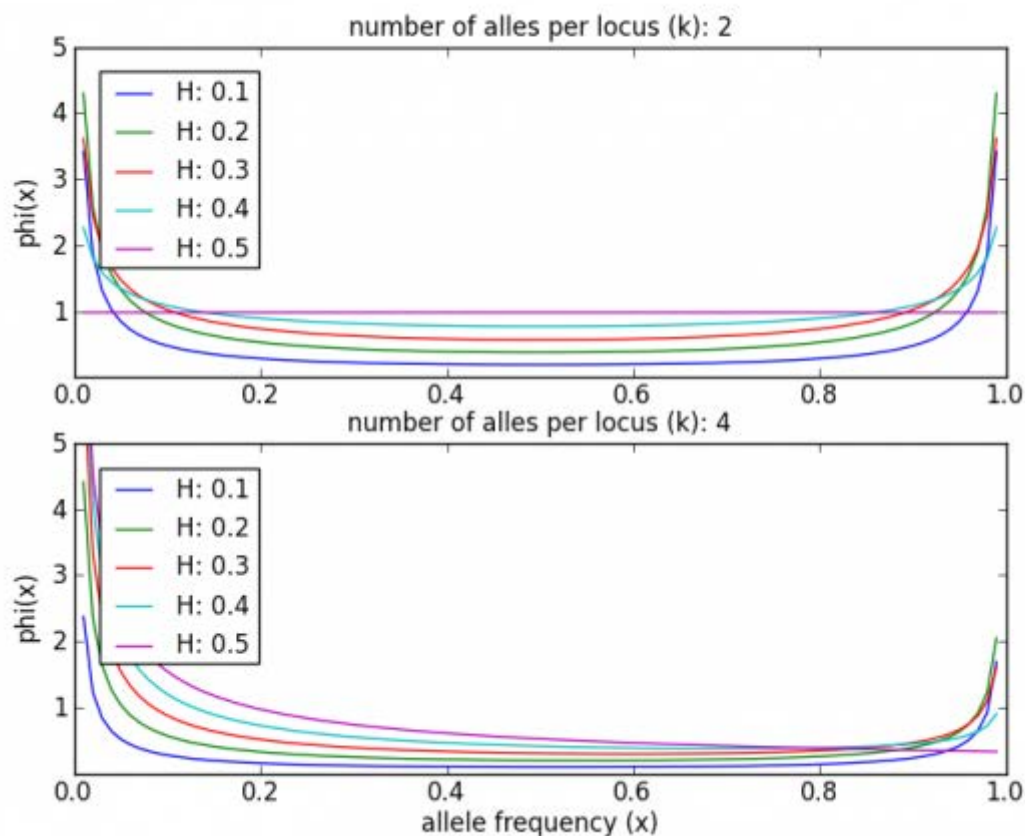

Figure Genetics 1. Example of the equilibrium distribution of allele frequencies in a population for neutral traits. H = 0.25 and k = 2 (typical values for isozyme data)

Note that in Figure 1 the number of loci is undetermined as Eqn. 1 represents the distribution of allele frequencies over a very large number of loci. To arrive at initial allele frequencies for an actual number of loci (e.g. 5), most conveniently the cumulative distribution of & phi(x) is calculated and the allele frequencies for the actual number of loci are determined at the quantile values of the cumulative distribution. i.e. every 20% quantile in case of 5 loci.

To obtain the cumulative distribution of $\varphi(x)$, $\varphi(x)dx$ is numerically integrated between 0 and 1 (extreme are excluded because $\varphi(x) \rightarrow \infty$ when $x \rightarrow 0$ or $x \rightarrow 1$):

$$\int_{0+}^{1-} \phi(x)\,dx \cong \sum_{x=0.000001}^{0.999999} \phi(x)\,\Delta x \cong 1$$

Eqn Genetics 2

then compute a cumulative distribution function, *p*, of *φ(x)x'* as:

$$p = \phi_{cumul} = \sum_{0.000001}^{x} \phi(x)\,\Delta x$$

Eqn Genetics 3

To compute the allele frequency for a given number of loci, the inverse of the integral of $\phi(x)$ is required, where $\phi(x)$ is the distribution of allele frequencies of all loci in a population. This inverse can be obtained by linear interpolation after evaluating $\phi(x)$ over a large number of x-values.

As an example, to choose the 5 initial allelic frequencies (nLoci = 5; k = 2 and k=4) equally spaced points in the first half of distribution of cumulative *φ(x)* are selected, other half is determined by the other allele. Examples of Eqn. 2 for nLoci = 5 and k = 2 or k = 4 are presented in Figure 2.
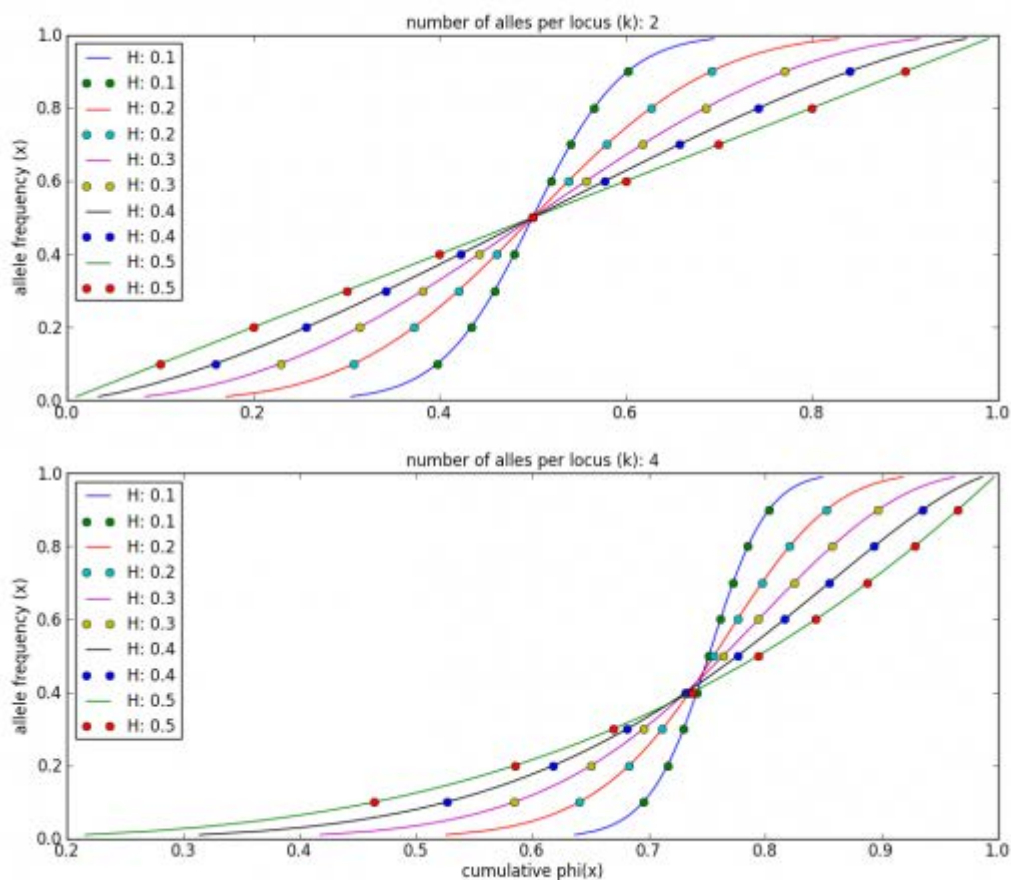
Figure Genetics 2. Cumulative distribution of ϕ(x) and relative allelic frequencies (x). Dots indicate interpolated values for a 5 locus genetic system (the allele frequencies > 0.5 are 1 - the allele frequencies < 0.5).

These 5 points are the 10th, 20th, 30th, 40th and 50th percentile of the cumulative distribution. In case H = 0.25 and k = 2, their relative frequencies are 0.006, 0.044, 0.141, 0.299, 0.499. In this way, 5 allelic frequencies are obtained that take into account the natural distribution of frequencies, with many of loci with low (or high) allele frequencies and few loci with allele frequencies around 0.5.

3.4.1.2. Initializing allelic effects

For the ForGEM model, it is necessary to assign allelic effects to each of the alleles that compose the genotype of the individual tree. Allelic effects are kept constant during the entire simulation. If information is lacking on the actual number of loci, the number of alleles and the allelic effects that determine quantitative phenotypic traits, a statistical approach is taken. This is done by designing for each trait a genotype distribution over the population such that the observed mean and variance of the phenotypic trait of the population are attained, under the constraint that the allele frequencies follow the U-shaped initial distribution. If information becomes available on the QTLs or candidate genes of the phenotypic traits considered, this statistically procedure can be replaced by actual data on the genetic make-up of these traits for a particular population.

The approach followed in ForGEM to obtain the observed mean phenotypic value is as follows:

- assign initially arbitrary allelic effects of *i* = +1 and *j* = -1 to each of the alleles *i* and *j* of all loci
- calculate mean and variance under the constraint of the U-shaped distribution of allele frequencies
- scale allelic effects such that the distribution of phenotypic values over all possible genotypes is normalised (mean equals zero, variance equals unity)
- add the mean and multiply with the additive genetic variance of the functional trait in question

The mean and variance of a genotype then become:

$$m = \sum_{l=1}^{Nloci} pi + qj$$

Eqn Genetics 4

$$var = \sum_{l=1}^{Nloci} p(i - m)^2 + q(j - m)^2$$

Eqn Genetics 5

This assignment of +1 and -1 values can be done for all alleles in a multi-locus 2 allele system.

The following steps are made to arrive at a mean of zero, and a variance of unity for the whole population. First, we make expectations zero by offset and sum of individual effects.

$$m = \sum_{l=1}^{nLoci} p(i-c) + q(j+c) = 0$$

$$=> \sum_{l=1}^{nLoci} pi - \sum_{l=1}^{nLoci} pc + \sum_{l=1}^{nLoci} qj + \sum_{l=1}^{nLoci} qc = 0$$

$$=> \sum_{l=1}^{nLoci} (pi + qj) - c \sum_{l=1}^{nLoci} (p-q) = 0$$

$$=> m - c \sum_{l=1}^{nLoci} (p-q) = 0$$

$$=> c = \frac{m}{\sum_{l=1}^{nLoci}(p-q)}$$

$$var = \sum_{l=1}^{nLoci} p(i-m-c)^2 + q(j-m+c)^2$$

$$=> var = \sum_{l=1}^{nLoci} p(i-c)^2 + q(j+c)^2$$

This leads to a large number of possible allelic values. Arbitrarily, the first combination of allelic effects that yield the lowest expectancy (m) is selected. This is $(i-c)$, thus the standardized allelic effect, e, with $m_e = 0$ and $var_e = 1$ is described by:

$$e = \frac{i-c}{\sqrt{var}}$$

Table Genetics. Example of vectors with allele frequency and effects for a 5-locus di-allele genetic system. p: allele frequency; i or j: initial arbitrary effects of opposite sign but equal in value; i-c or j+c: centralized effects such that mean equals zero; allelic effects with lowest expectancy; standardized allelic effects (e) such that variance equals zero. m: mean of allele effects, var: variance of allele effects, $c \left(= \frac{m}{\sum_{l=1}^{nLoci}(p-q)} \right)$: scalar to attain m=0.

Locus	Allele	p	initial effects: (i, j)	centralized effects: (i-c, j+c)	standardized effects: (i-c, j+c)/√(var)
1	A	0.005	1	1.080	0.489
2	B	0.043	-1	-0.920	-0.417
3	C	0.138	-1	-0.920	-0.417
4	D	0.298	1	1.080	0.489
5	E	0.500	-1	-0.920	-0.417
1	a	0.995	-1	-1.080	-0.489
2	b	0.957	1	0.920	0.417
3	c	0.862	1	0.920	0.417
4	d	0.702	-1	-1.080	-0.489
5	e	0.500	1	0.920	0.417
	m		0.243	0.000	0.000
	var		5.000	4.872	1.000
	c		-0.08031331		

With the standardized allele effects e (last column in table A1) and the probabilities p (p_a, p_b, ...p_E) the phenotypic value for that trait for individual trees to initialize the stand are calculated in the ForGEM model as follows. With: h^2 : heritability; V_g : genetic variance; V_e : environmental variance; V_t : total variance (=V_g + V_e).

1. Calculate the genetic variance V_g and environmental variance V_e from the total variance V_t and heritability h^2: $V_g = h^2 \times V_t$ and $V_e = V_t - V_g$. h^2 and V_t should thus be known for the trait.

2. Multiply standardized allelic effects e with sqrt(V_g) to obtain allele effects E having expected variance of V_g.

3. Determine genotypes of individual trees by randomly sampling 2 gametes for each locus using the probabilities *p*.

4. The phenotypic value for the trait is obtained by summing the allelic effects *E* over all loci and alleles representing the trait, adding the overall population mean, and adding the environmental deviate with variance V_e and expectation of 0.

If there are also observations of the trait on individual trees, the phenotypic values and alleles obtained in 4. are reassigned to closest matching tree. *E.g.*, if phenological observations on individual trees are available, the tree with earliest bud burst obtains the set of alleles resulting in the earliest bud burst, i.e. the genotype with the most alleles with negative effects. If such observations are not available, phenotypic values are assigned randomly over the trees of the stand. The initial phenotypic value of a trait for an individual tree is determined by making 2 independent draws from the above probabilities per locus. Each drawing results in an allele from which the allelic value is known. Subsequently, the allelic effects over all loci and alleles are added, resulting in the total phenotypic value of the trait.

3.4.1.3. Probability of combining parent trees

The probability that gametes of a mother tree M_i and father tree F_j meet can be estimated by the fraction pollen of F_j that arrive at the position of M_i, relative to the contribution to all other known and unknown father trees. The amount of pollen of any father tree arriving at the position of a mother tree depends on the amount of pollen produced by the father tree, the distance between the target mother tree and all possible father trees, the wind direction relative to the orientation between the mother and the father, and the overlap in flowering phenology between the father and the mother trees. The general equation for the decline of the amount of pollen with distance is (Degen 1996):

$$y = y_0 \cdot e^{-b \cdot d}$$

Eqn Pollen 1

With:

b slope parameter indicating the rate of decline of the amount of pollen

d distance from father tree

y_0 maximum number of pollen produced by the father tree, at *d=0*

The processes affecting these 3 parameters are described in this section. It is thereby assumed that there is no incompatibility between genotypes.

3.4.1.3.1. Fraction of pollen from father tree arriving at target mother tree

The direction of the wind affects the slope parameter, whereas the overlap in flowering phenology between the target mother tree M_i and *k* potential father trees determines which portion of the pollen emitted by the father tree F_j can actually pollinate a given flowering mother tree. Thus, the fraction of F_j pollen arriving at position M_i can be described as:

$$P(M_i \times F_j) = \frac{y_0(F_j) \cdot e^{-b(M_i,F_j) \cdot d(M_i,F_j)} \cdot t(M_i,F_j)}{\sum_k \left(y_0(F_k) \cdot e^{-b(M_i,F_k) \cdot d(M_i,F_k)} \cdot t(M_i,F_k) \right) + E_{M_i}}$$

Eqn Pollen 2

With:

b(Mᵢ,Fⱼ) slope parameter effected by of wind direction

d(Mᵢ,Fⱼ) distance between mother tree M_i and father tree F_j

y₀(Fⱼ) amount of pollen of father tree F_j at distance *d= 0*

t(Mᵢ,Fⱼ) effect of phenology, *i.e.* overlap in flowering phenology

E_{Mi} amount of external pollen arriving at mother tree M_i

The effect of wind direction on the slope parameter, *b(Mᵢ,Fⱼ),* is calculated as follows:

$$b(M_i, F_j) = b_0 + m \cdot \cos(\alpha_w - \alpha)$$

Eqn Pollen 3

With:

b(M_i,F_j) direction-dependent slope parameter

b_0 slope parameter when *cos(x) = 0*, *i.e.* at wind direction perpendicular to direction of M_i to F_j tree

α_w main wind direction

α direction from F_j tree to M_i tree

m magnitude parameter

The distance between parental trees, *d(M_i, F_j)*, is based on the Euclidean distance between mother tree, *i,* and father tree, *j* :

$$d(M_i, F_j) \;=\; \sqrt{\left(x_i - x_j\right)^2 + \left(y_i - y_j\right)^2}$$

Eqn Pollen 4

With *x* and *y* indicating the *x*- and *y*- co-ordinates of the parent trees.

The effect of phenology on flowering overlap between mother and father trees, *t(M_i,F_j)* is calculated as follows:

$$t(M_i, F_j) = \begin{cases} |tM_i - tF_j| \leq tFL & \longrightarrow \frac{tFL - |tM_i - tF_j|}{tFL} \\ |tM_i - tF_j| > tFL & \longrightarrow 0 \end{cases}$$

Eqn Pollen 5

With:

t(M_i, F_j) fraction of overlap of flowering between M_i and F_j trees, relative to the flowering duration of the M_i tree

tFL duration of flowering of trees

tM_i timing of flowering of mother tree M_i

tF_j timing of flowering of father tree F_j

It is assumed that the duration of flowering of trees, *tFL*, is the same for all genotypes.

3.4.2. Genetic statistics

In this section an overview of common population-genetic statistics is presented as output of genetic models. The population statistics, within and among populations, include diversity measures, differentiation measures between populations, heterozygozity and fixation, and F-statistics. The statistics described in this section are obtained from Hanssen (2000) and Hattemer (1991). Details on the use and interpretation can be found there and in (Gregorius 1978, Gregorius 1977, Gregorius 1986, Gregorius 1987, Gregorius 1988).

3.4.2.1.   Diversity measures

3.4.2.1.1.   Genetic variety

The genetic variety can be measured as the number of different alleles or different genotypes in population (Gregorius 1977, Gregorius et al. 1985).

3.4.2.1.2.   Genetic diversity

The genetic diversity characterizes the heterogeneity of the distribution of genetic variants in a population of a sample therefrom (Hattemer 1991). It can thus be measured the allelic diversity of the *k*-th locus or genotype diversity of a deme.

$$v_k = \frac{1}{\sum_{i=1}^{n_k} \left(p_i^k \right)^2}, \qquad 1 \leq v_k \leq n \qquad\qquad \textit{Eqn. GenStat 1}$$

where

- *n* number different genetic types (alleles, genotypes)
- *p* frequency of i-th genetic type

v equals unity if there is only 1 genetic type, and equals *n* if every all genetic types are equally frequent (Gregorius 1978).

3.4.2.1.3. Mean effective number of alleles

In case of allele diversity, v_k can be considered as the effective number of alleles for locus k if n_k alleles occurs with frequencies p_i^k (i=1, … n_k). (Hattemer 1991). Thus, the mean effective number of alleles is the harmonic mean of v_k at m loci.

$$\overline{v} = m \cdot \frac{1}{\sum_{k=1}^{m} \frac{1}{v_k}}, \qquad 1 \leq v \leq \frac{1}{n} \sum_{k=1}^{n} n_k \qquad \text{\textit{Eqn GenStat 2}}$$

3.4.2.1.4. Hypothetical gametic multi-locus diversity

The diversity of the gametic output of populations is a special case of diversity and characterizes the adaptive potential of sexually reproducing populations (Gregorius 1978). It is hypothetical in the sense that the absence of fertility selection is assumed as well as the independence of the distributions of alleles at different loci (*i.e.* no linking) (Hattemer 1991).

$$v_{gam} = \prod_{k=1}^{m} v_k, \qquad 1 \leq v \leq \prod_{k=1}^{m} n_k \qquad \text{\textit{Eqn GenStat 3}}$$

where

- *m* the number of unlinked loci

- *v_k* the allelic diversity for the *k*-th locus

v_{gam} is thus a measure for effective number of the multiloci gametes that can be produced in a population (Gregorius 1978).

3.4.2.1.5. Actual heterozygosity

$$H_a = \sum_{i \neq j} P_{ij} \qquad \text{\textit{Eqn GenStat 4}}$$

where

- *P_{ij}* the frequency of genotype with alleles *i* and *j*, with *i* ≠ *j*

- H_a indicates the fraction of observed heterozygotes in the population

3.4.2.1.6. Fixation index

The fixation index indicates for the locus considered the surplus or deficit of heterozygotes compared to Hardy-Weinberg-equilibrium.

$$F = \frac{H_e - H_a}{H_e}, \qquad -1 \le F \le 1 \qquad\qquad \textit{Eqn GenStat 5}$$

where

- H_e the expected heterozygosity based on Hardy-Weinberg-equilibrium

3.4.2.2.   Differentiation measures

3.4.2.2.1.   Genetic distance between demes

The differentiation between two demes is characterized by counting the number of genetic variants which the demes do not share. Thus, the allelic differentiation between demes *X* and *Y* represents the genetic distance between the demes (Gregorius 1974, Gregorius & Roberts 1986).

$$d_{xy} = \frac{1}{2} \cdot \sum_{i=1}^{n} \left| x_i - y_j \right|, \qquad 0 \le d_{xy} \le 1 \qquad\qquad \textit{Eqn GenStat 6}$$

where

- x_i and y_j genetic frequencies (of alleles at a given locus or of a genotype). of deme *X* and *Y*.

If the genetic distance equals zero, then both populations have the same alleles or genotypes with the same frequency. d_{xy} equals unity if both populations have no alleles or genotypes in common (Gregorius 1974, 1978, 1984). Note that the genetic distance is a

symmetrical statistic ($d_{xy} = d_{yx}$). and that the distance between population *X* and *Y* cannot exceed the sum of their distances to a third population *Z* ($d_{xy} \leq d_{xz} + d_{yz}$) (Hattemer 1991).

3.4.2.2.2.   Genetic differentiation among demes

This statistic represents the genetic distance between a deme and its complement, *i.e.* the union of all other demes (Gregorius 1985).

$$D_j = \frac{1}{2} \cdot \sum_{i=1}^{n} \left| p_i^{(j)} - \overline{p}^{(j)} \right|, \qquad\qquad 0 \leq D_j \leq 1 \qquad\qquad \textit{Eqn GenStat 7}$$

where

- $p_i^{(j)}$ frequency of allele or genotype *i* in deme *j*

- and $\overline{p}^{(j)}$ average allele or genotype frequency in the complement of deme *j*

The substructure of the complement has no influence of *D,* as different complement can yield the same $\overline{p}^{(j)}$. Thus, identical *D's* do not necessarily indicate the demes with an identical genetic structure. However, *vice versa* demes with an identical genetic structure do possess an identical genetic structure (Hattemer 1991).

3.4.2.2.3.   Average genetic differentiation

The average genetic differentiation among *m* demes is the weighted mean of D_j

$$\delta = \sum_{j=1}^{m} D_j \cdot c_j, \qquad\qquad 0 \leq \delta \leq 1 \qquad\qquad \textit{Eqn GenStat 8}$$

where

- *m* number of populations

- c_j relative size of deme *j*. (Gregorius 1984, 1988)

δ attains zero if all demes have the same genetic structure, and reaches unity if all demes considers in pairs have no gene in common (Hattemer 1991).

3.4.2.2.4. Differentiation within a population

The concept of differentiation can also be applied within a population by considering each individual in that population a deme. The number of identical individuals can be counted and expressed relative to the number of other genetic types.

$$\delta_T = \frac{N}{N-1} \cdot \left(1 - \sum_{i=1}^{n} p_i^2\right) = \frac{N}{N-1} \cdot \left(1 - \frac{1}{v}\right), \qquad 0 \leq \delta_T \leq 1 \qquad \text{\textit{Eqn GenStat 9}}$$

where

- N the sample size

- p_i frequency of genetic type (allele or genotype)

δ_T indicates the total genetic difference between all individuals of a population. δ_T equals zero if all individuals of the population are of the same genotype, and δ_T equals unity if all individuals are different (Gregorius 1987, 1988). δ_T represents the probability that two individuals samples from the sample population without replacement represent the same variant (Hattemer 1991).

Note that all differentiation measures range between zero and unity, whereas the genetic diversity measures range between unity and the number of genetic types, *n* (Gregorius 1987).

3.4.2.2.5. F-statistics

F-statistics measure the degree of deviation of genotypic frequencies from those expected under random mating in structured populations (Falconer 1996), (Weir & Cockerham, 1984. ref in (Larsen 1996)).

F_{IS} : Inbreeding coefficient of an individual relative to its on subpopulation. Measures inbreeding due to non-random mating in a sub-population. Within population fixation index.

F_{ST} : Average inbreeding of the subpopulation relative to the whole population, or correlation between two randomly chosen alleles in a sub-population relative to the alleles in the whole population. Measures inbreeding due to correlation among alleles cause by their occurrence in the same sub-population. Between populations fixation index.

F_{IT} : Inbreeding coefficient of an individual relative to the whole population, or correlation between gametes for the total population. Measures the extend of inbreeding in the entire population (for neutral alleles). Total fixation index.

Note that:

- in a random mating population: $F_{IS} = 0$ and $F_{IT} = F_{ST}$
- if all populations are genetically identical: $F_{ST} = 0$ and $F_{IS} = F_{IT}$

3.5. Conclusions

The ForGEM model is continuously in development and both model description and its parametrisation change over time. The version that is presented above is the one that is used for the analyses for the FORGER project to meet the aims of WP 3 on the use and management of forest genetic resources. Therefore only the parameter values of *Fagus sylvatica, Quercus spp., Pinus sylvestris,* and *Picea abies* are presented in this report. The model is also being applied on other tree species that are not being analysed in the context of the FORGER project.

The full content of the model description and parametrization will be presented at the ForGEM wiki (http://vle-models.wur.nl/wiki/index.php/ForGEM_-_Forest_Genetics,_Ecology_and_Management) such that modifications of both the model description and parameter values can be dynamically updated. A large part of the model description is already available at that website.

Towards the Sustainable Management of Forest Genetic Resources FORGER FP7- 289119

4. Process-model initialization

The aim of this work is to be able to simulate ForGEM anywhere in Europe, as well as at the full European scale, without the need of extensive parameterisation and initialisation. The tasks to initialize the ForGEM model are the following:

- for the stand: to develop an algorithm to convert existing stand data (EFISCEN-Space 1x1km2, digitally available national records for: Spain, Portugal, France, Italy, Germany, Netherlands, E-Europe, Baltic states, United Kingdom, Scandinavia), Tröltsch map at 1x1km2 (2010 REF); EUFGIS data on species distribution

- for the climate: to develop an algorithm to convert existing data climate data in format suitable for the model, throughout Europe. Based on CRU database, select 1 climate change scenario.

- for the soil: to develop algorithm to convert existing soil data in format that is suitable for the model.

- for forest management: to develop forest management schemes for 4 species, at pan-European scale (2 - 3 per location), including transfer of FGM. This activity will also be based on current case studies in the EU projects MOTIVE and EFORWOOD in which similar information is collected at the pan-European scale for the EFISCEN model.

- for genetics: the initialization of selected phenotypic traits (phenology, water use, based on literature studies as far as available). This activity will profit from a recently started national project on the genetic base of adaptive traits.

Details on the initialisation of each of these aspects is described below.

4.1. Stand

4.1.1. Input required

Towards the Sustainable Management of Forest Genetic Resources FORGER FP7- 289119

The user requests a simulation for a specific location in Europe, corresponding to grid cells as used in ISI-MIP (see Appendix Selection of sites and scenarios). The user can provide extra search criteria:

- One or more tree species that should be present in the plot to be selected.
- Plots within a certain radius from the selected location, with the possibility to select an azimuth sector (defined by min and max degree).

4.1.2. Plot selection procedure

If no location search criteria is specified, a random NFI plot is drawn according to the procedure for the Synthetic European Forest Structure Database (Hengeveld in prep.), i.e. using the forest inventory region as a basis (Figure 4.1). The user gets the original information of the selected plot, plus the number of plots that were selected given the search criteria. The NFI plot database is basically the same as the one described in (Hengeveld et al. 2012).
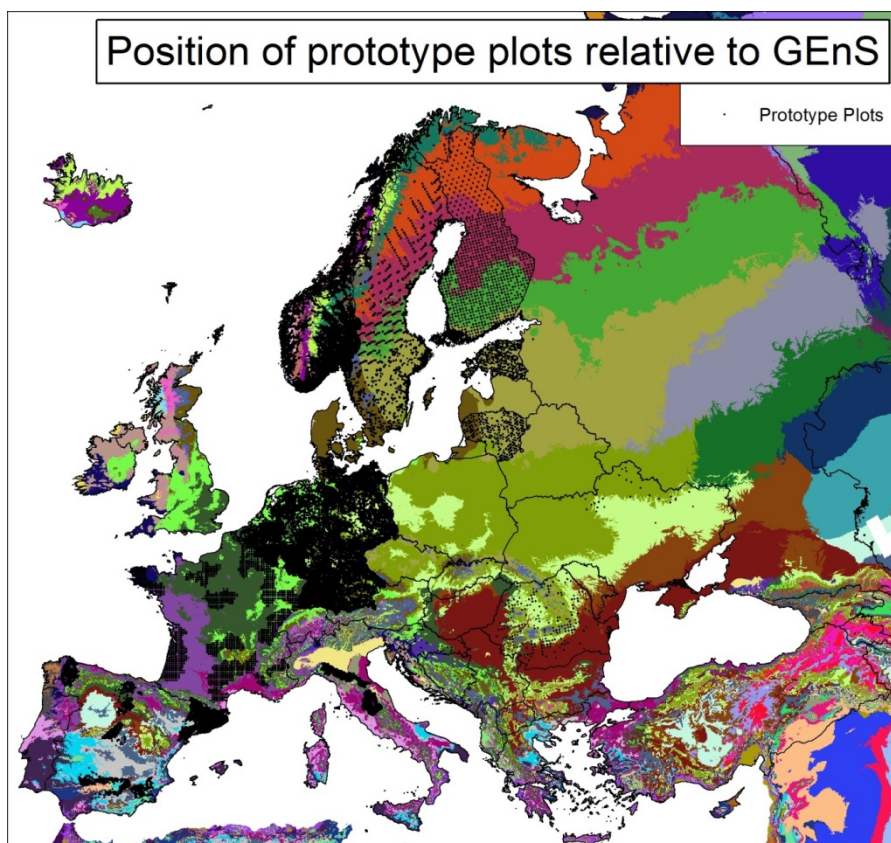
Figure 4.1. Distribution of NFI plots over Europe, positioned at the Global Environmental Stratification map (Metzger et al. 2013).

4.1.3. Generation of initial stand

The NFI plot data contains at least the variables tree species, stem number (N/ha), average height (m), average dbh (cm), basal area (m2/ha) and volume (m3/ha). One plot may contain more than one cohort, which is differentiated by tree species and/or height. For the initialisation, only stem number, average height and dbh are used. Initialisation is done using the Generate function as programmed in NSM. A variation around the average values of height and diameter is determined either determined from the data in the NFI plot , or by a pre-set coefficient of variation of 25%. If the NFI data does not contain information on crown dimensions, values on maximal dimensions from the parameters database is used. In case additional information is available this is used as well (for example minimum and maximum

diameter and/or height). The age of the tree is estimated from its height, using the age-height relationship (Richards curve) of the highest site class available for Dutch conditions (Jansen et al. 1996). This will in many cases result in an underestimation of the actual age. This error is deemed acceptable as age is only used in ForGEM to determine age-dependent mortality, which will be overruled by competition and harvest effects for most simulations. Age is estimated on the individual heights and thus varies per individual tree. In case age is given for the NFI plot, it is assumed to be the same for all trees in a cohort. Simulation plots are 100x100m. See Figure 4.2 for an example of a generated plot and its diameter distribution, compared to the values measured on individual trees in an observation plot.
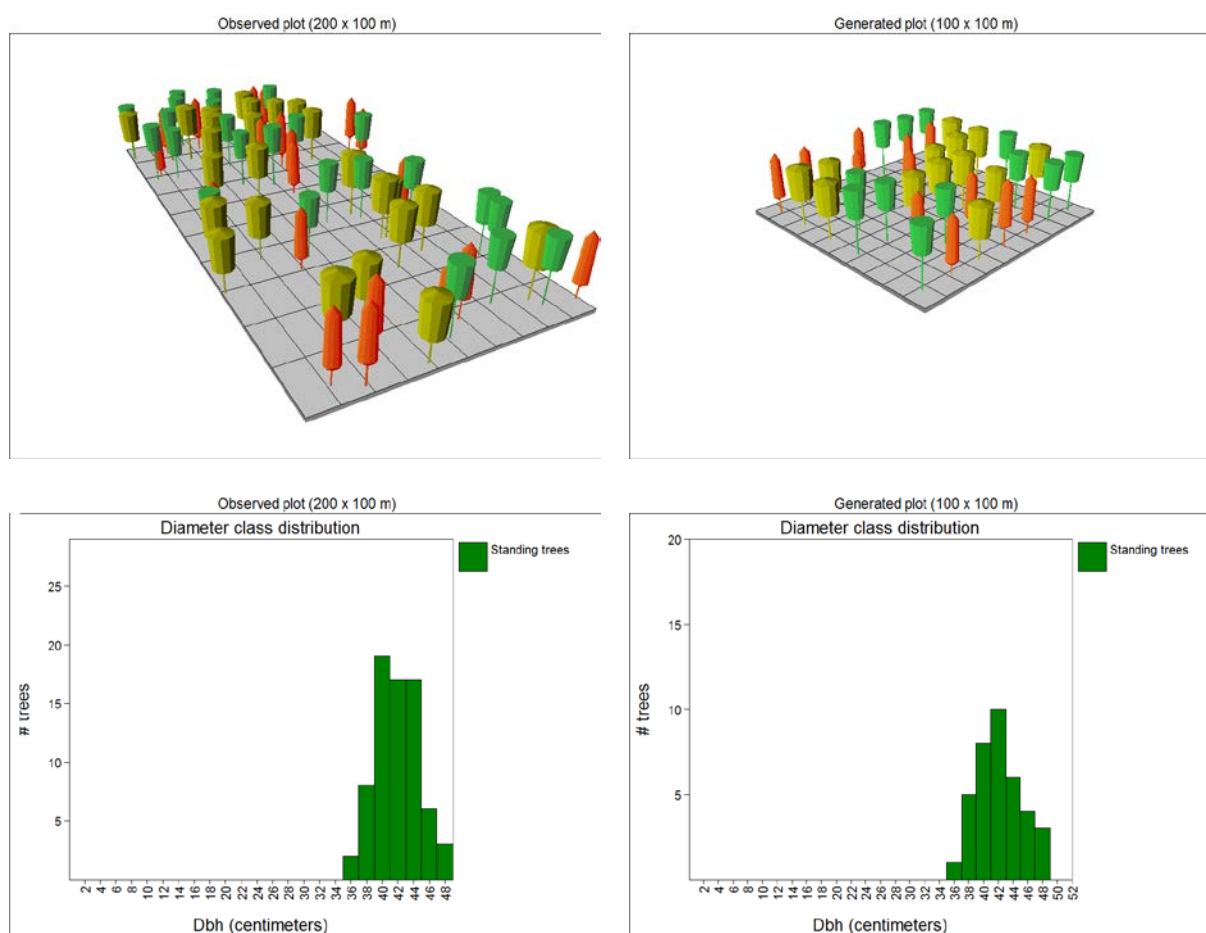
Figure 4.3. Visualisation of a stand used to initialise the ForGEM model. Spatial distribution of trees and diameter distribution of observed plot with individually measured trees, and the same representation of a generated plot based on stand statistics (density per species, mean

and coefficient of variation of height and diameter at breast height) of the observed plot. Several representations of a plot can be generated at the European scale with a 1 x 1 km resolution. Note that spatial structure is not accounted for in the generated plot. Yellow trees – *Quercus robur*; Orange trees – *Fagus sylvatica*; Green trees – *Fraxinus excelsior*. Visualized with Stand Visualisation System SVS, (McGaughey 1997).

4.1.4. Derivation of additional parameters

The tree species map (see Figure 2.1) can optionally be used to determine the gene flow from outside the simulated area, for all tree species. Gene flow by both seed dispersal then depend on the presence of a species in the 1x1km grid cell. As fixed amount of seeds or fraction of pollen with the same genetic composition as the initial stand is then included in the current stand.

4.2. Climate

Daily meteorological data for incoming radiation, minimum and maximum temperate, precipitation, vapour pressure deficit, relative humidity and wind speed are obtained from the ISI-MIP website (http://www.pik-potsdam.de/research/climate-impacts-and-vulnerabilities/research/rd2-cross-cutting-activities/isi-mip/input-data). This data is made available in NetCDF. The I/O module of the ForGEM model is developed such that it can read and write NetCDF formatted files (v4). See Figure 4.3 for examples of the pan-European distribution of some daily meteorological variables.
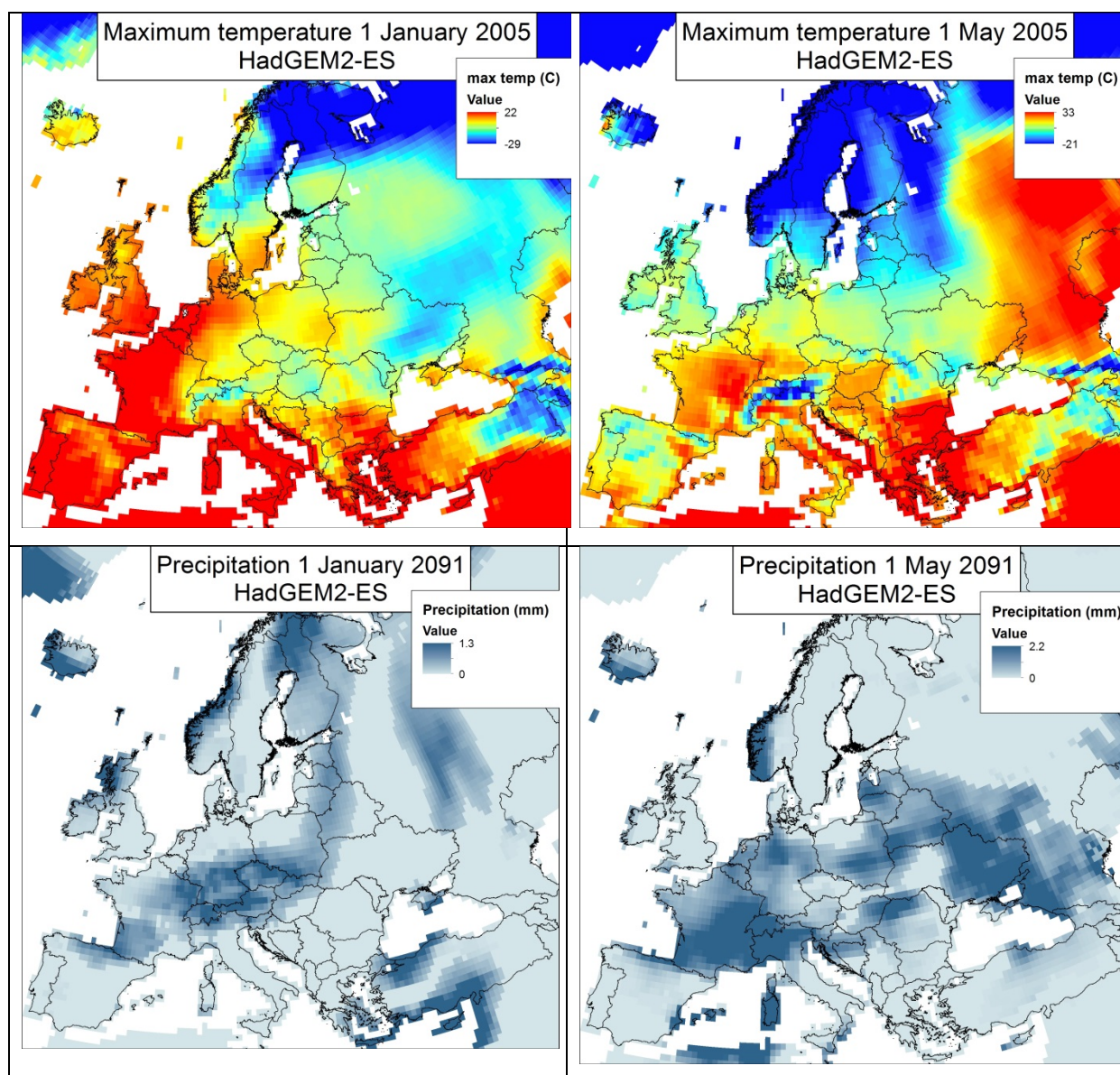
Figure 4.3. Example of European distribution of daily meteorological variables, i.c. maximum temperature and precipitation.

4.3. Soil

Soil characteristics required are those to determine water availability according to pedo-transfer functions (Wösten et al. 1999, Wösten et al. 2001), including texture, soil organic matter and bulk density. The soil maps of the explanatory variables are available at Alterra. See the original literature for a representation of the maps.

4.4. Forest management

In the ForGEM model, a broad array of forest management scenarios can be composed by the user. A forest management scenario consists of one or more sub-scenarios. Each sub-scenario is defined by a management intervention type (making gaps, thinning, shelter cut, clear cut, planting etc.). For each sub-scenario, the user defines when to start and to when finish the sub-scenario, and indicate a number of management intervention type specific parameters. E.g. gap size in case of a sub-scenario using the Gap making management intervention type. It is thus possible to have different sub-scenarios of the same management intervention type within the same scenario. However, in such cases the sub scenarios must be separated in time. For example, large gap making during the first 100 years of the simulation, followed by making small gaps during the remainder of the simulation. When a new sub scenario starts, all information on the old sub scenario of the same type is lost (overwritten with new values). Gaps according to the first Gap making sub scenario will therefore not be effectuated as soon as a new Gap making sub scenario starts. To calculate parameters for the different management interventions, a grid is put over the simulation area. For example, the gap size in a Gap making sub scenario can be defined as a fixed number of grid cells. The size of the grid cell is user-defined, or is proportionate to the area size, e.g. by indicating a number of equally sized grids.

In this section, the management intervention type specific parameters are described. For each management intervention type, first the 'Input' that the user needs to supply are listed. In the subsequent 'Implementation' section the consequences of the inputs are described. Typically, the user inputs are provided by the forest management database. Based on the forest management module of the ForGEM model, a number of forest management approaches, indicating the most likely form of forest management at a particular location in Europe, are quantified.

Table 4.1. Definition of Forest Management Approaches in allowed actions (Duncker et al. 2012).

Decision	Basic principle by FMA				
	Intensity scale				
	FMA1 Passive "Unmanaged forest nature reserve"	FMA2 Low "Close-to-nature forestry"	FMA3 Medium "Combined objective forestry"	FMA4 High "Intensive even-aged forestry"	FMA5 Intensive "Short rotation forestry"
1. Naturalness of tree species composition	Only species characteristic of the potential natural vegetation (PNV)	Native or site adapted species	Tree species suitable for the site	Tree species suitable for the site	Any species (not invasive)
2. Tree improvement[†]	No	Not genetically modified or derived from breeding programmes	Trees from tree breeding but not genetically modified	Trees from tree breeding but not genetically modified	Genetically modified or breeding
3. Type of regeneration	Natural regeneration / natural succession	Natural regeneration (planting for enrichment or change in tree species composition)	Natural regeneration, planting and seeding	Natural regeneration, planting and seeding	Planting, seeding and coppice.
4. Successional elements	Yes	Yes	Temporarily	No	No
5. Machine operation	No	Extensive	Medium	Intensive	Most intensive
6. Soil cultivation	No	No (only to introduce	Possible (mainly to	Possible	Yes

Towards the Sustainable Management of Forest Genetic Resources FORGER FP7- 289119

		natural regeneration)	promote natural regeneration)		
7. Fertilisation / Liming	No	No (only if devastated soil)	No (only if devastated soil)	Possible	Yes
8. Application of synthetic protective agents	No	No	Possible as a last resort	Possible	Possible
9. Integration of nature protection	High	High	High	Medium	Low
10. Tree removals	No	Stem (solid volume)	Stem and crown (solid volume)	Up to whole tree	Whole tree and residues
11. Final harvest (and main silvicultural) system	No	Mimics natural disturbances, Single Stem Selection Group Selection Irregular Shelterwood	All possible, Seed Tree Strip Shelterwood Group Shelterwood Uniform Shelterwood Coppice with standards	All possible, clear-cut (long rotation) preferably used	All possible, Coppice Clear fell (shorter rotation)
12. Maturity	No intervention	Long rotation length ≥ age of max. MAI	Med. rotation length ≈ age of max. MAI	Short rotation length ≈ age of max. financial return (low interest rate)	Shortest rotation length ≤ age of max. MAI or ≈ age of max. financial return (high interest rate)

FMA1 is defined as a strict nature reserve, without any management. In ForGEM this is implemented by only specifying General management parameters (Table 2), but without any other interventions. In general, plots with exotic species would not be labelled as having an FMA1 type of management. But in case this happens, it means that non-indigenous species will remain in the stand and can only be eliminated by natural processes.

In **FMA2** forest management is allowed, but only aimed at enhancing the ecological functioning of the forest, with a low management intensity. The management cycle is therefore set to 10 years (Table 4.2). Each time non-indigenous species are removed. This more or less reflects the current natural range of the species and does not tolerate natural expansion of species outside their current range, for example due to climate change. Every 50 year a few gaps will be created to emulate small-scale natural disturbance processes. The total gap size is 5% of the simulated area. Gaps are between 200 and 800 m2 and at least 10m wide, with a preference for smaller gaps. Gaps are preferentially located at spots where most light reaches the forest floor. Existing gaps might thus be enlarged, or nothing is done if the gap is of sufficient size. Occurrence of natural regeneration is not a criterion. A gap will remain labelled as gap until the trees reach half their maximum attainable size. After that the area will be available for creation of a new gap. No soil scarification is applied and all (advanced) regeneration up to 5m tall is left untouched. Of the harvested wood (either from removal of certain species or the creation of gaps), 20% of the trees with a breast-height diameter of more than 15cm are extracted as harvest. The rest of the stem volume, branches and foliage of the felled trees remain in the forest.

FMA3 is characterised as combined-objective forestry. Besides wood production, other functions as biodiversity, recreation and protection of soil and groundwater are integrated into the management. Forest management intensity is characterised as medium, implemented in ForGEM as a management cycle of 10 years (Table 3). Regeneration of the simulated stand is done by a type of shelter wood felling. If the trees reach on average their target diameter (in general 60cm) the number of trees is reduced to about 25, depending on the tree species. In case of a mixture, a weighted average is calculated. No soil scarification is applied, and all trees smaller than 5m are retained. At the next management intervention the density is reduced to 10 trees per ha. These trees will be left as seed source, and for biodiversity and recreational purposes. At the same time, the density of the natural regeneration is assessed. If this is below 2000 trees per ha, trees will be planted until this density is reached. This will be done with the tree species best adapted to the site, as assessed from the tree species map. After the regeneration reaches a height of 8m, the stand will be thinned every 10 years. A mixed stand is aimed at, with 60% of the basal area contributed by the dominant species. The dominant species is assessed based on the actual situation of the stand and may thus change over time. The remaining 40% is distributed over the other tree species that are present. The number of trees to be removed are based on the crown space that is needed per tree, which is based on Dutch yield tables. Trees are removed randomly. From the felled trees, only those with a minimum diameter of 10cm are extracted. However, 20% of them are left in the forest as deadwood for biodiversity purposes. No branches or foliage are extracted.

FMA4 is intensive even-aged management. In ForGEM, this is implemented as a 5-year management cycle (Table 3). After clear-felling, the soil is prepared and planted with 3500 trees per hectare. At 6m height a tending is carried out, where numbers are reduced to 2000 trees per ha, where 20% admixture of other species is allowed. Thinnings are carried out every management cycle until the trees have reached the target diameter of 60cm. Thinnings are done using the crown space method. Only a small fraction (10%) of the

harvested trees (>10cm) remain in the forest. 50% of the branches of the felled trees are removed, but no foliage.

FMA5 is more intensive than FMA4. This is reflected by a 4-year management cycle, higher planting density (5000 trees per hectare), higher tending density (2500 per hectare) and an earlier harvest (target diameter 40cm) (Table 4.3). No admixture is allowed. All biomass is removed from the site, except half of the foliage.

Table 4.2. Definition of forest management parameters in ForGEM for FMA3, FMA4 and FMA5.

	General Management	FMA3	FMA4	FMA5
General management	cManagementInterval	10	5	4
	cMinimumCuttingHeight	5	2	2
	cMinimumHarvestDiameter	10	5	0
	cLeaveDeadwoodAtHarvest	0.2	0.1	0
	cLeaveBranchesAtHarvest	1	0.5	0
	cLeaveFoliageAtHarvest	1	1	0.5
Additional planting	cLowestDensity	20	35	50
	cDesiredDensity	20	35	50
	cTimeSinceHarvest	1	0	0
Tending	cMainSpeciesTargetPercent		80	100
	Density at height 6m		20	25
Thinning	cThinningInterval	1	1	1
	cMethod	1	1	1
	cMainSpeciesTargetPercent	60	80	100
Shelterwood	cHeightCriterium	0.5		
	cSoilScarification	0		
	cTargetDiameter	60		
	cInterval	1		

	cGeneralDensity	25		
	cEndDensity	10		
Clearcut	cHeightCriterium		0.5	0.5
	cSoilScarification		1	1
	cTargetDiameter		60	40

4.5. Genetics

The genetic system can be initialised (initial allele frequencies and assigning allelic effects) either by taking a statistical approach or by using observed allele frequencies and allelic effects for Quantitative Trait Loci (QTLs) or Candidate Genes (CGs) determined in experimental populations (Brendel et al. 2008). We currently assume on theoretical considerations that initially the allele frequency distribution follows a U-shaped beta distribution, *phi*. (Figure 4.7). The U-shape indicates that there are many alleles with either a very low or a very high frequency, and few alleles have a frequency around 0.5. The allele frequency distribution is a function of the heterozygosis of the traits (H) and the number of alleles (k) (Nei 1987). Inverting the cumulative distribution of *phi* leads to the initial allele frequencies (Figure 4.8, see (Kramer et al. 2008a) for details). Reasonable values for quantitative traits are: number of loci, *nLoci* =10, H=0.25 and k=2 (Kramer et al. 2008a).

See: http://vle-models.wur.nl/wiki/index.php/Initialisation_of_the_genetic_system for a full description of the initialisation of the genetic system in ForGEM.
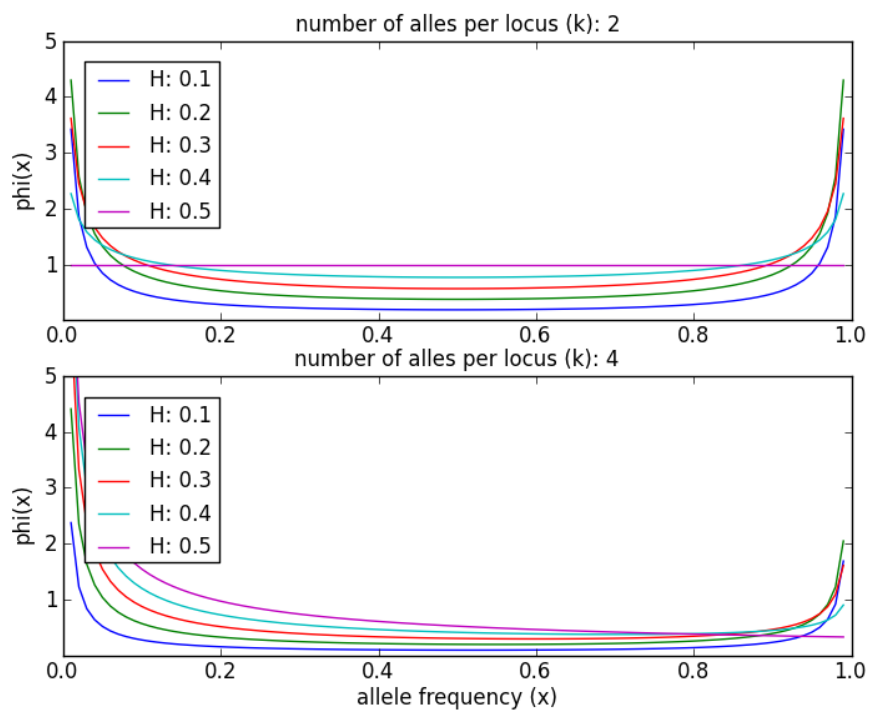
Figure 4.4. Theoretical allele frequency distribution, phi, for different values of heterozygosis (H) and number of alleles per locus (k) (Nei, 1987).

Towards the Sustainable Management of Forest Genetic Resources FORGER FP7- 289119
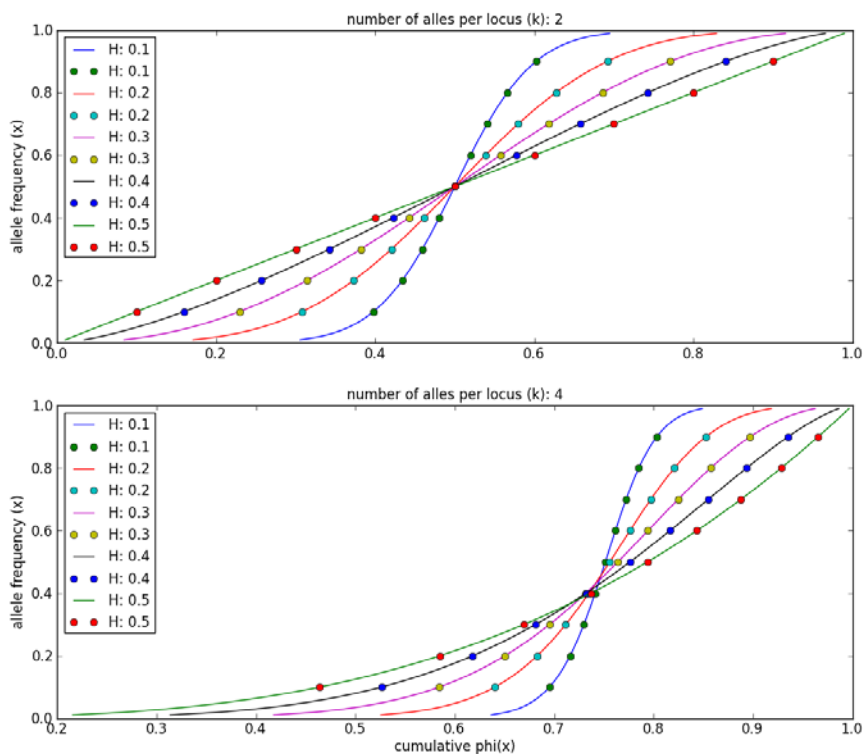
Figure 4.5. Allele frequencies to initialise the ForGEM model for different values of heterozygosis (H) and number of alleles per locus (k). The dots indicate the allelic effects for a 10-locus trait evenly spaced over cumulative phi(x).

Allelic effects are determined in the ForGEM model by first assigning +1 and -1 values to the two alleles of di-allelic multi-locus traits and subsequently normalising the allelic effects (mean of zero, variance of unity) under the constraint of the U-shaped distribution of allelic frequencies as indicated above. Figure 4.9 shows the decline in allelic effect with increasing number of loci for a di-allelic genetic system with symmetric allelic effects. Genotypic values for a model parameter are attained by adding the observed mean and multiplying with the observed variance of the parameter. Phenotypic values are attained by enhancing the genotypic values with an environmental deviate based on the heritability of the trait.
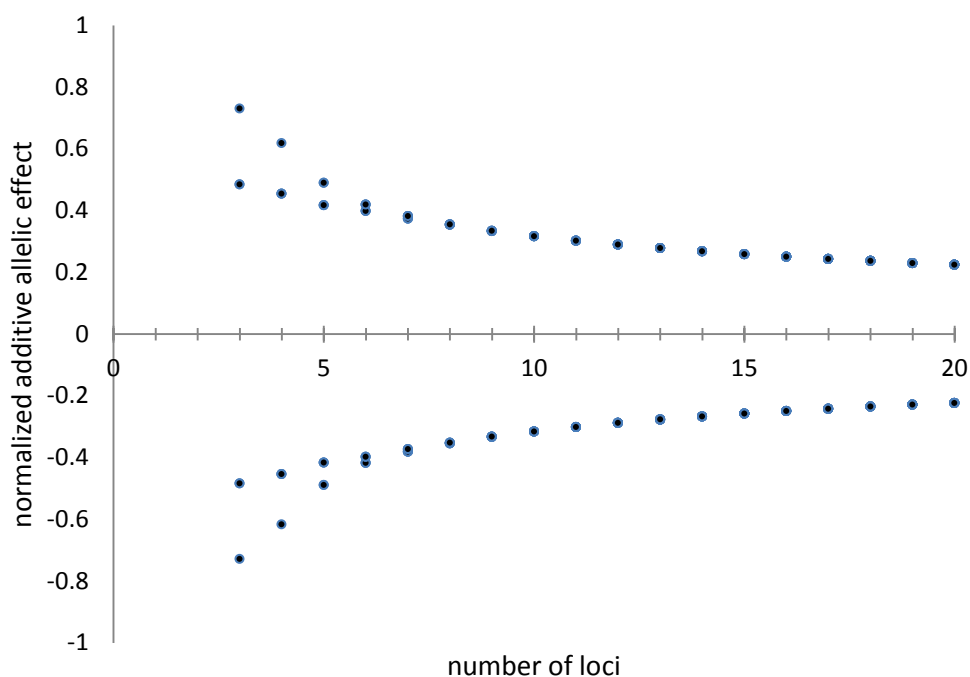
Figure 4.6. Normalised additive allelic effects assigned to di-allelic multi-locus traits, under the constraint of the distribution of allelic frequencies as indicated in Figs. 4.1 and 4.2 with k=2 and H=0.25. With a low number of loci (*nLoci* < 7) two symmetric allelic effects are attained. At higher values for the number of loci per trait, all alleles have virtually the same effect on the genotype.

Towards the Sustainable Management of Forest Genetic Resources FORGER FP7- 289119

5. Process-model validation

The following analyses were performed to validate the ForGEM model:

- sensitivity analyses to the environmental drivers: temperature, precipitation and ambient CO2 concentration. The default values of these drivers were compared to growth and yield data
- validation to productivity patters over Europe
- sensitivity analyses to foliar N-content

5.1. Sensitivity analyses of model output to environmental drivers

5.1.1. Simulation setup

The aim of the sensitivity analysis is to test the response of the ForGEM model to the environmental drivers temperature, CO_2 and water, excluding interactions between environmental drivers. The simulation location is assumed to be in the Netherlands at the Veluwe (52.15N 5.45E). Daily weather time series are obtained from the MARSOP database from the JRC (www.marsop.info) for the grid cell where the Veluwe area is located. For each simulation year, a randomly chosen weather year is used from the series that is available (1975-2009). Where applicable, these series are manipulated according to the specific scenario (described below). In the default settings, CO_2 concentration is defined as 36 Pa partial CO_2 pressure at a total air pressure of 1013 hPa, thus equal to 355 ppm.

Simulations were done for 4 species: *Fagus sylvatica* (beech), *Quercus robur* (oak), *Pinus sylvestris* (Scots pine) and *Picea abies* (Norway spruce). The starting point for the simulations is derived from species-specific information of stand variables at age 40 from the yield tables of Jansen et al. (1996) (Table 5.1). For all species, the highest yield class available was used. Stem density was reduced to 75% of that in the yield table to avoid mortality due to self-thinning during the 10 year simulation. For each species, 5 initial stands of 1 ha each were produced using the procedure *Generate* each time using a different random seed. It is

known that the current procedure implemented in InitTree underestimates the crown radii. Therefore, after the generation of the initial stands, the crown radius of the individual trees was adapted using the required distance between the trees as described in the thinning procedures (see Chapter 4. Process-model initialization).

Table 5.1. Stand-level variable values used as starting point for the simulations

species	N	h	CV	DBH	CV	age	yield class	#replicates
Pinus sylvestris	440	17.9	0.1	23.5	0.1	40	12	5
Picea abies	401	20.7	0.1	27	0.1	40	16	5
Quercus robur	488	17.7	0.1	18.8	0.1	40	9	5
Fagus sylvatica	581	18.6	0.1	18.5	0.1	40	12	5

The sensitivity analysis consist of a simulation under normal conditions (further labelled as "average"), and 2 simulations (low/high) per driver that is tested (temperature, CO_2 and water). Table 5.2 shows the values applied for each of the sensitivity simulations. Interactions between the drivers are not tested. Temperature change is implemented by applying the specified temperature offset to the daily temperatures from the input weather series. Precipitation change is implemented as a multiplication of daily precipitation values with the respective factor. Thus, rainfall *patterns* are not changed, only the overall level of precipitation. Different levels of CO_2 concentration are implemented as ratios relative to the current level, i.e. respectively 0.7, 1 and 1.27 arriving at concentrations of respectively 249, 355 and 451 ppm. Thus, for each species a set of 7 simulations are performed. All simulations were done for a period of 10 years, with 5 replicates, where each replicate started with the respective new initial situation as outlined above. No management was applied during the simulation and no ground vegetation is present in the simulations.

Table 5.2. Changes in drivers for the sensitivity analysis

Driver	Range and step size	Explanation	Unit
T	-2, 0, +2	Temperature, offset to	^0C

		observations	
c_a	249, 355, 451	ambient CO_2 concentration, overriding default value	ppm
P	50%, 100%, 150%	Precipitation, multiplication of rainfall factor per daily values observed	kg m-2 (=mm)

The simulations were done using a specific single parameterisation per species as described in Chapter 3 Process-model parametrization. The model version used is without genetics (#UNDEF _GENETICS) and not allowing seeds to be produced (#DEFINE _NO_FLOWERS). Note that afterwards changes were made to the code regarding frost damage to foliage, these were not implemented yet in these runs.

5.2. Results

5.2.1. Wood production

Wood production (W) is calculated as the difference in standing stock (V) between start and end of the simulation, plus the total mortality (M) occurring during the simulation, divided by the length of the simulation (t):

$$W = \frac{(V_0 - V_t) + \sum_0^t M}{t}$$

Thus, we get an estimate of the average annual productivity (m^3 ha^{-1} yr^{-1}).

Fagus sylvatica

Quercus robur
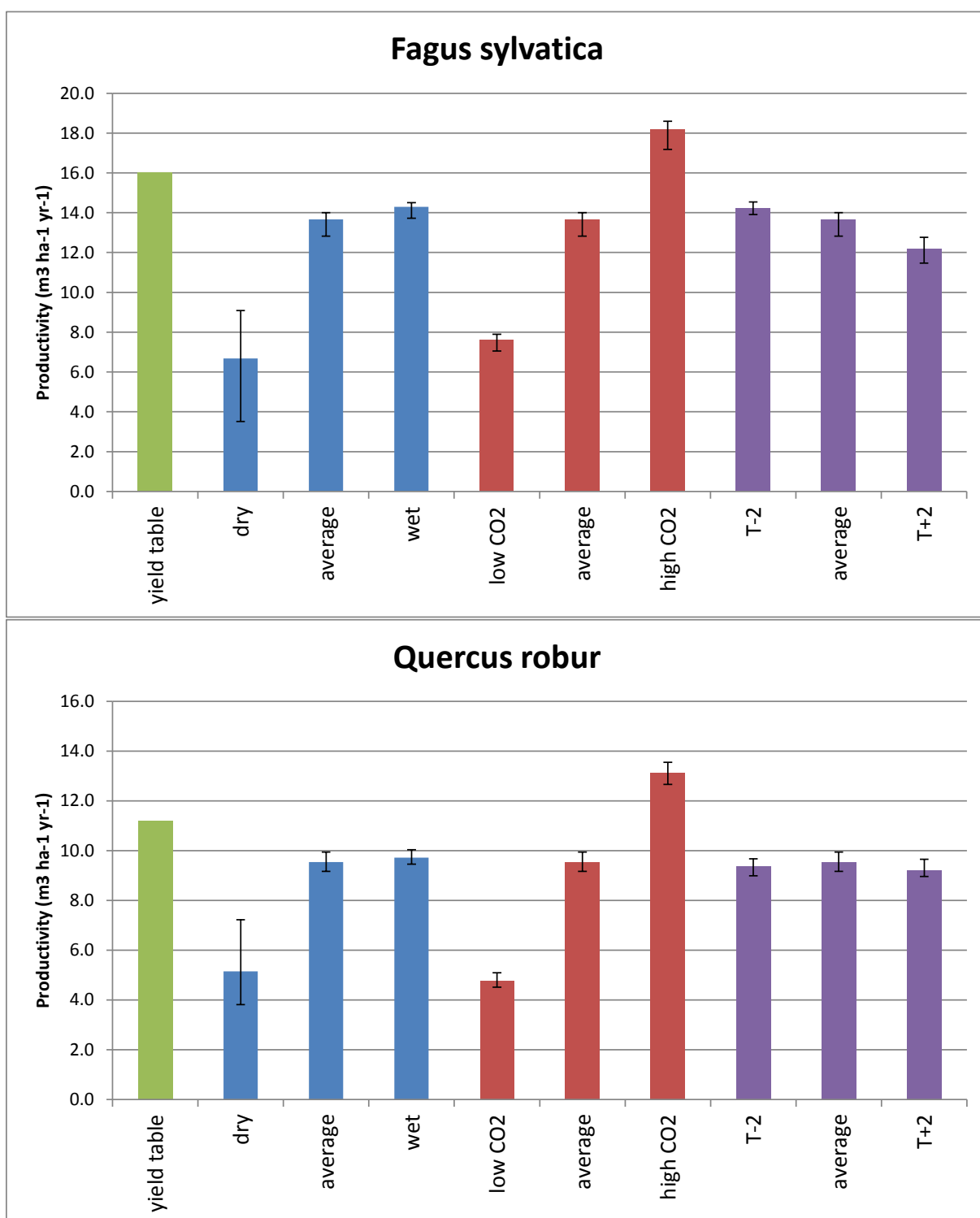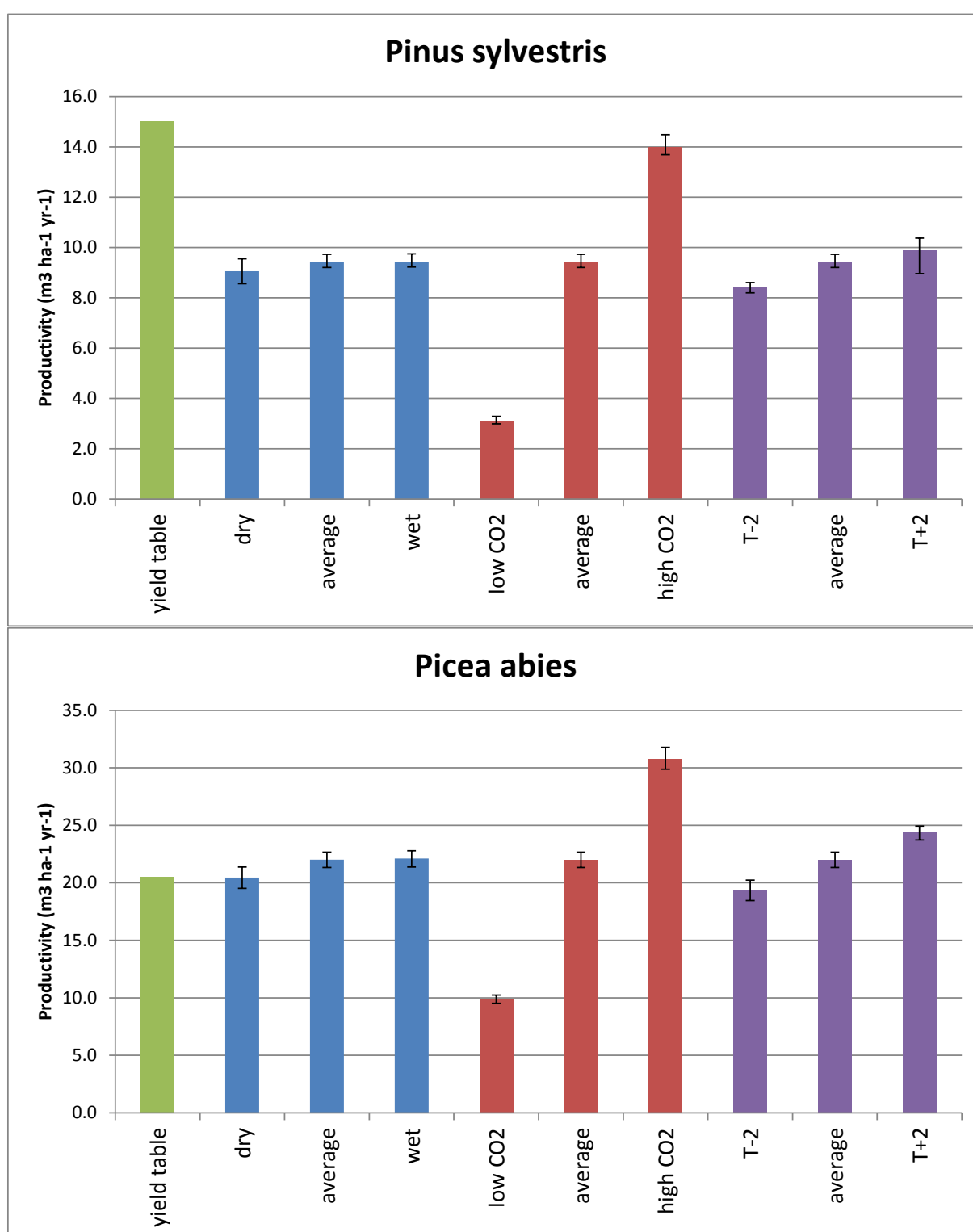
Figure 5.1. Observed production of wood (m^3 ha^{-1} yr^{-1}) averaged over the 10 year simulations. Bars show the minimum to maximum range of the 5 replicates. Mortality only occurred in the simulation of the dry scenario for Fagus sylvatica (in 1 out of 5 replicates)

and for Quercus robur (2 out of 5 replicates). The green bar ("yield table") shows the respective value from the yield table.

The observed level of wood productivity agrees rather well with that calculated from the yield tables ("yield table" in Figure 5.1) for Picea abies. For the broadleaved species the simulations are slightly lower, and for Pinus sylvestris the productivity level is considerably underestimated by the model.

The conifers hardly show a reaction to changes in water availability, while the productivity of the broadleaved species is clearly decreased at decreased water availability, with even mortality in some of the replicates. Increased water availability leads only to a slightly increased productivity.

All species show an almost linear positive response to CO_2 concentration. Conifers show a positive response to temperature, while Quercus robur shows no real response, and Fagus sylvatica shows a negative response. This negative response might be related to increased water demand (and thus water limitation) at higher temperatures.

5.2.2. Water use – average scenario

We studied the water use of the different species by calculating the average monthly values of each of the components of the water balance. The change in soil storage was calculated as the difference between the precipitation reaching the soil and the water used for transpiration, soil evaporation and the water that leaked through the soil.

Figure 5.2 shows the monthly water use in each simulation under average conditions. Shown is the canopy interception, soil evaporation, transpiration and leaching, as well as monthly precipitation (shown as negative values) and changes in the soil water storage. Annual totals are shown in Table 5.3. Monthly precipitation varies between the species as a consequence of the randomly drawn weather, but a small peak in mid-summer and early winter (November/December) is visible for all species. Transpiration occurs only when foliage is present, but is low in wintertime for conifers. Soil evaporation increases with

temperature, but is clearly affected by the flushing of the broadleaves. In spring and summer, water use is higher than precipitation, causing a reduction in soil water storage. In autumn and winter soil water storage is refilled again. Pinus sylvestris has the lowest transpiration and Fagus sylvatica the highest (Table 5.3).

Picea abies has a low soil evaporation due to its high and year-round crown cover. Pinus sylvestris has the highest soil evaporation due to its low LAI. Broadleaves are intermediate, with relative high LAI during the growing season and no foliage at all during winter and, more importantly, early spring.

Towards the Sustainable Management of Forest Genetic Resources FORGER FP7- 289119
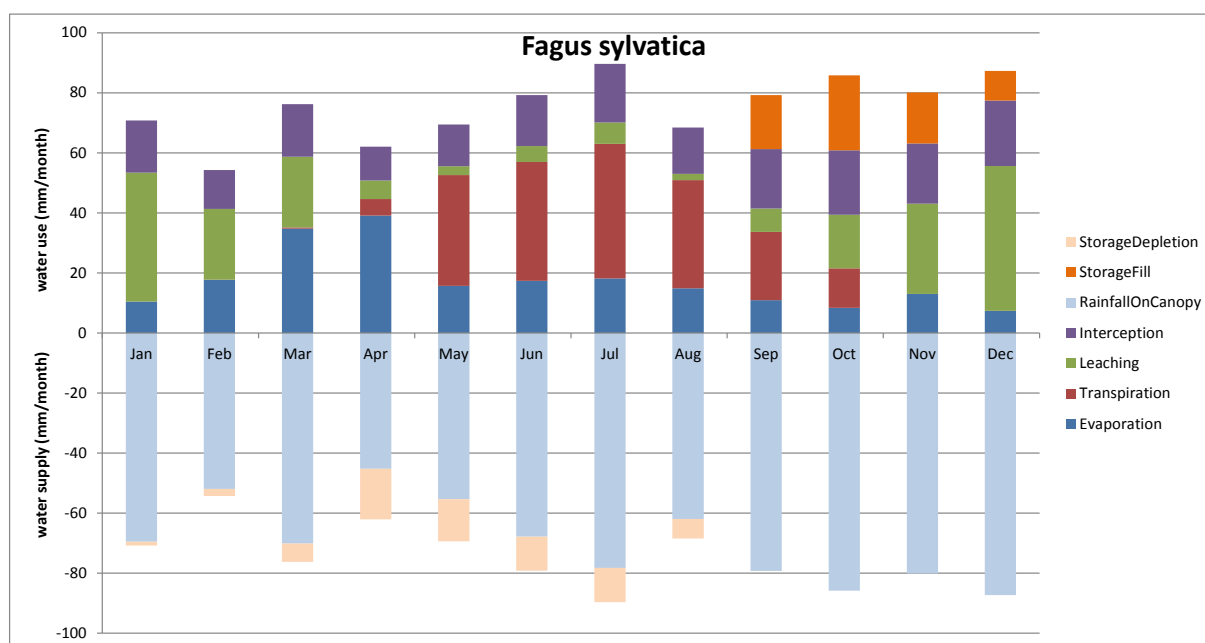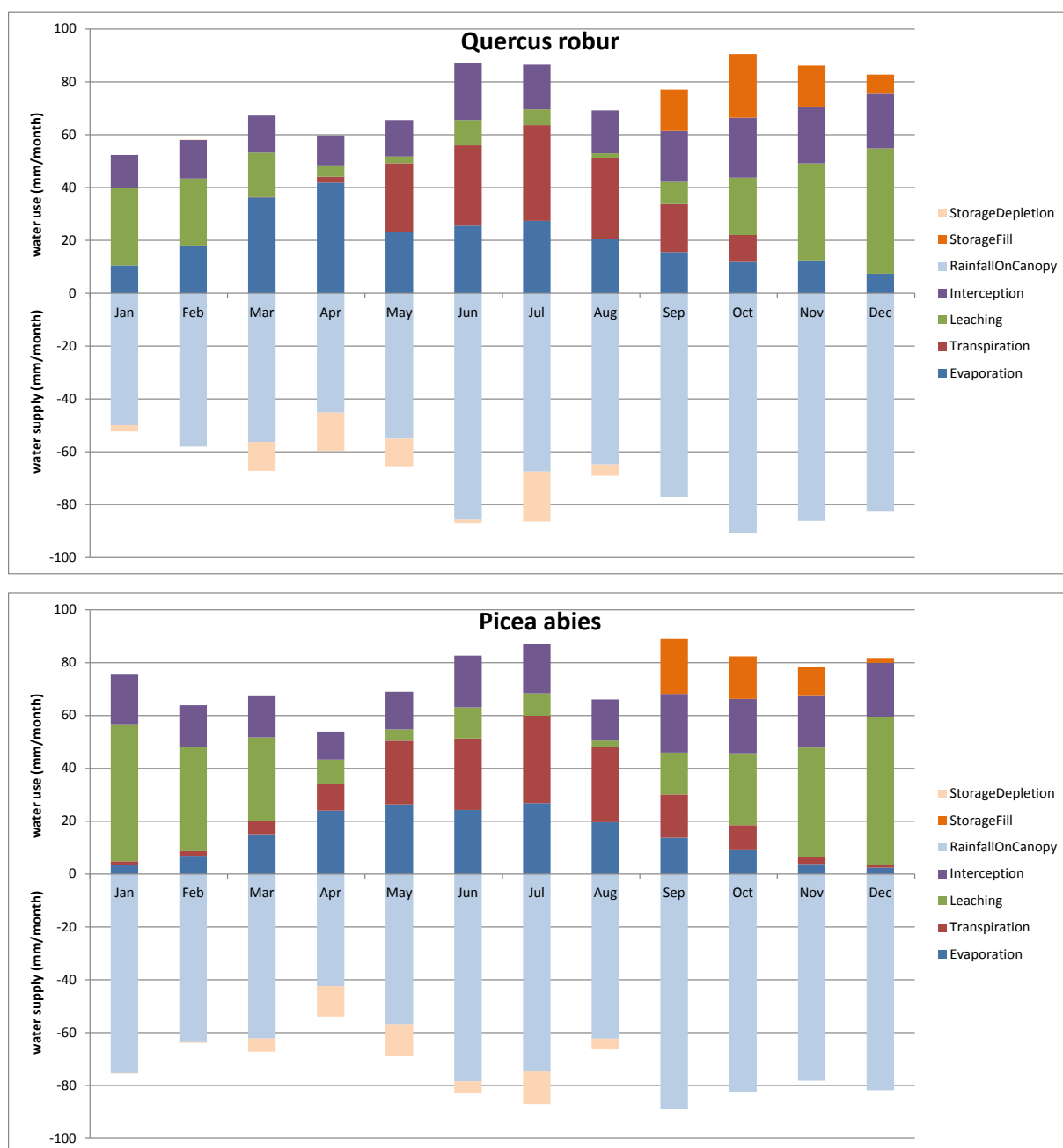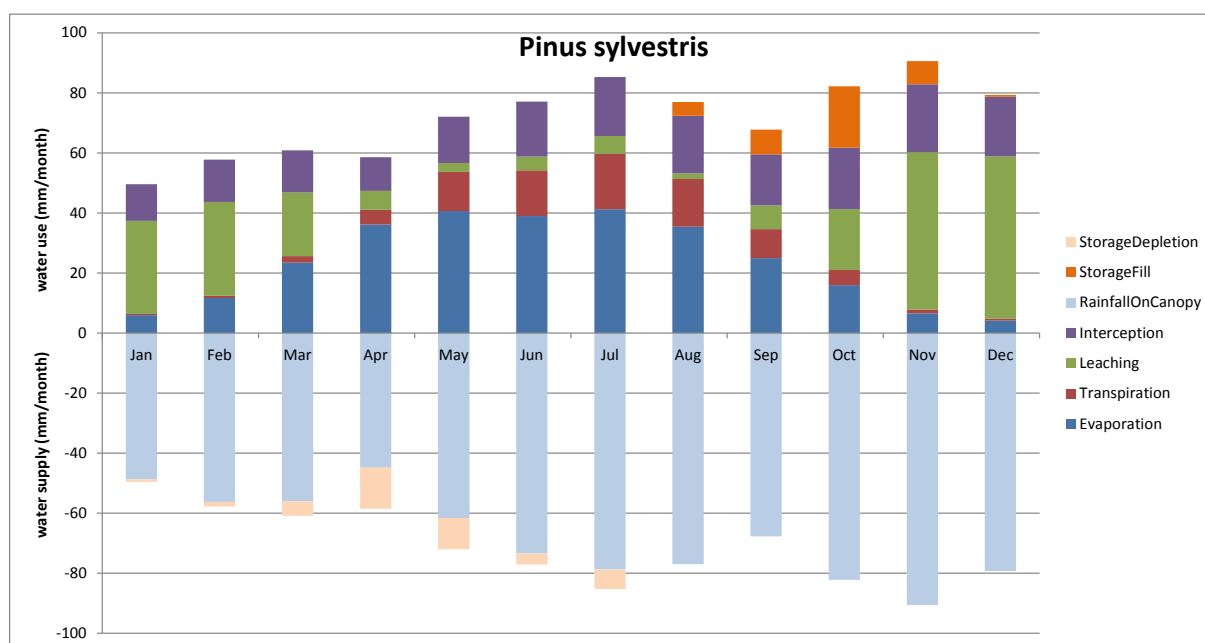
Figure 5.2. Annual cycle of water use for the simulations under average conditions for the 4 species (average of 5 replicas).

Table 5.3. Comparison of annual water use (mm/yr) in the average scenario for each of the 4 species.

Species	Soil evaporation	Transpiration	Leaching	Interception
Fagus sylvatica	208	199	218	208
Quercus robur	250	154	210	205
Pinus sylvestris	285	87	240	204
Picea abies	176	160	299	212

5.2.3. Water use – conifers

In general, the simulated transpiration is low. This is certainly affected by the absence of ground vegetation. Inclusion of a ground vegetation layer would increase the transpiration component, and reduce soil evaporation because less light reaches the ground. According to (http://edepot.wur.nl/300885), about 2/3 of the total precipitation is evaporated or

transpired. In the simulations this is on average 71%, including soil evaporation, plant transpiration and assuming all intercepted precipitation is evaporated. The monthly values in winter agree in pattern and magnitude with the measured and simulated figures they present, but in summertime our simulated values are somewhat lower. According to (http://www.stowa.nl/Upload/publicaties/STOWA%202010%2036%20LR.pdf) total annual evaporation of soil and intercepted precipitation plus transpiration in Loobos (Pinus sylvestris) was 496mm, while we simulated 576mm for Pinus sylvestris. They do not separate between plant transpiration and soil and wet canopy evaporation, but Elbers (pers. com.) estimates the tree transpiration component at 50-70% of the total of soil evaporation and tree transpiration, while we have 23% for Pinus sylvestris. For the period 1995-1998, annual data of the water balance components are available (Table 5.4). From the 5 replicas for both Pinus sylvestris and Picea abies, we extracted the simulated annual data for those years were one of the weather series of the corresponding years were used. Only 1996 and 1997 were present in the random series for Pinus sylvestris (Figure 5.3). Simulated tree transpiration plus soil evaporation corresponds well with measured evapotranspiration, but most likely tree transpiration is too low (19-30% transpiration and 70-81% soil evaporation in the simulations). Simulated interception (fixed at 25% of total precipitation) is in the same order as the measurements (average 27%).

Probably the simulated Scots pine stand is less dense than the stand at Loobos, with simulated LAI values (reported at January 1 of each simulation year) in the range 0.98-1.35, while the actual LAI does not exceed 1.8 (see: http://www.climatexchange.nl/projects/boshydrologie/Info-den-loc_n.htm).

Table 5.4. Measured values at Loobos, NL, Scots pine
(http://www.climatexchange.nl/projects/boshydrologie/Meet-den-jaar_n.htm)

Measurement period	*1995*	*1996*	*1997*	*1998*
Precipitation	843 mm	722 mm	787 mm	1266 mm
Interception	185 mm	194 mm	241 mm	368 mm
Evapotranspiration	423 mm	344 mm	441 mm	333 mm
Runoff	-	-	-	-
Precipitation surplus	235 mm	184 mm	105 mm	565 mm

Towards the Sustainable Management of Forest Genetic Resources   FORGER FP7- 289119
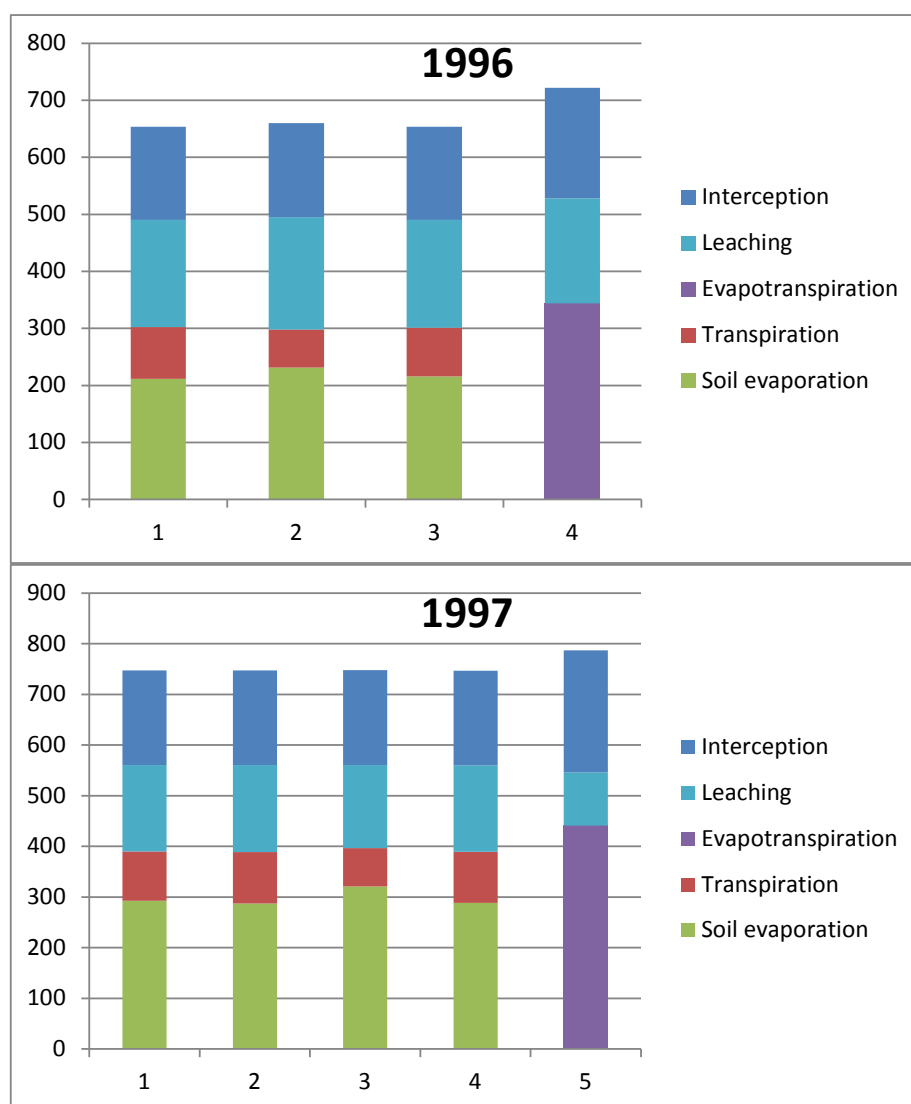
Figure 5.3. Simulated annual water balance (Pinus sylvestris) in the individual years where the corresponding year was used as weather, compared to the measured values at Loobos (right column).

For Picea abies we used the same approach as for Pinus sylvestris, with the same site, since no other measured evergreen conifers site was available for comparison. For Picea abies, the transpiration component is 44-50% of total evapotranspiration. Total simulated evaporation is well in range with the measured value, but still a bit lower than measured for 1995 and 1997, like for Scots pine in 1996 and 1997. Interestingly, the total evapotranspiration of Picea abies in 1997 is lower than for Pinus sylvestris. Apparently, the higher LAI (simulated values 2.25-2.87) of Picea abies decreases the soil evaporation more than it increases the foliage transpiration.
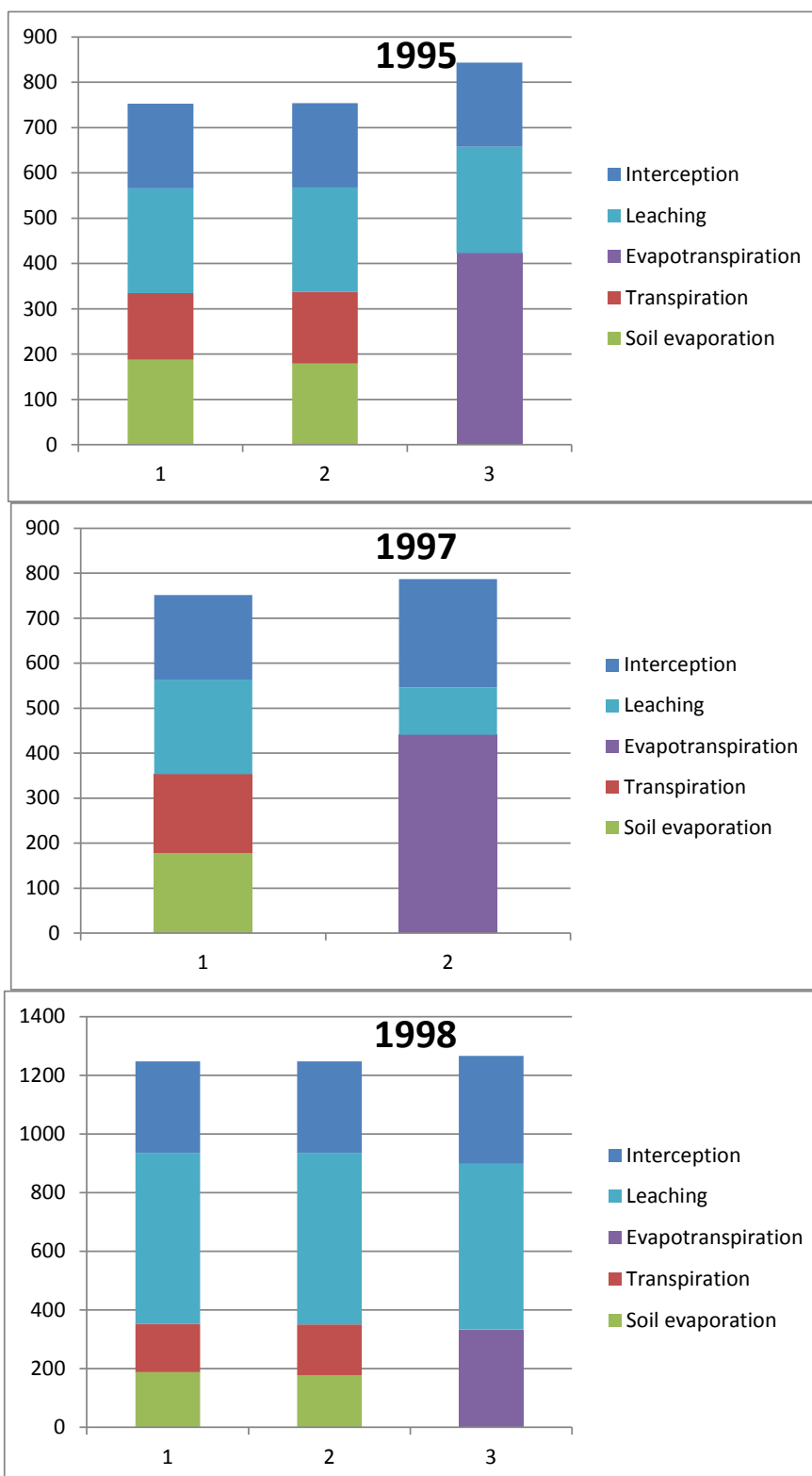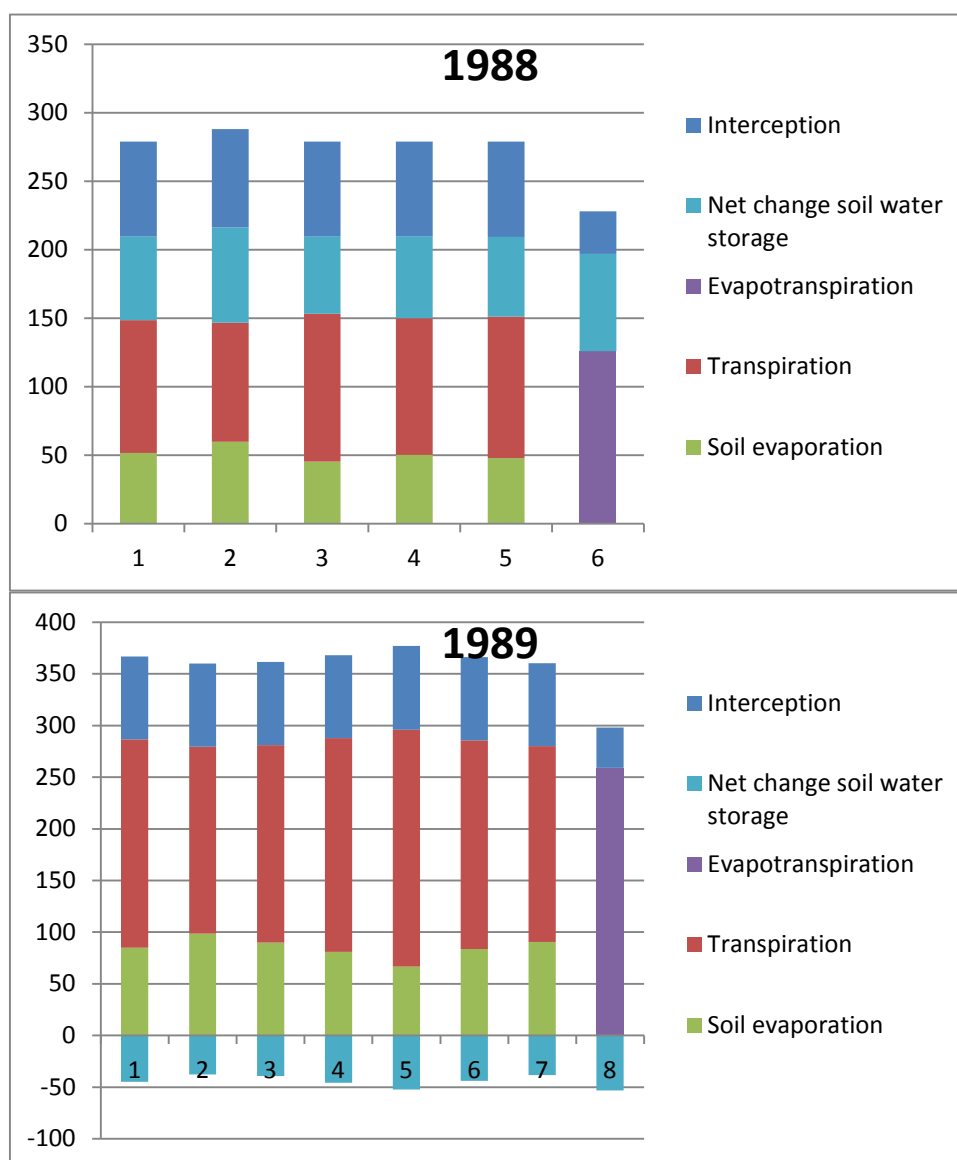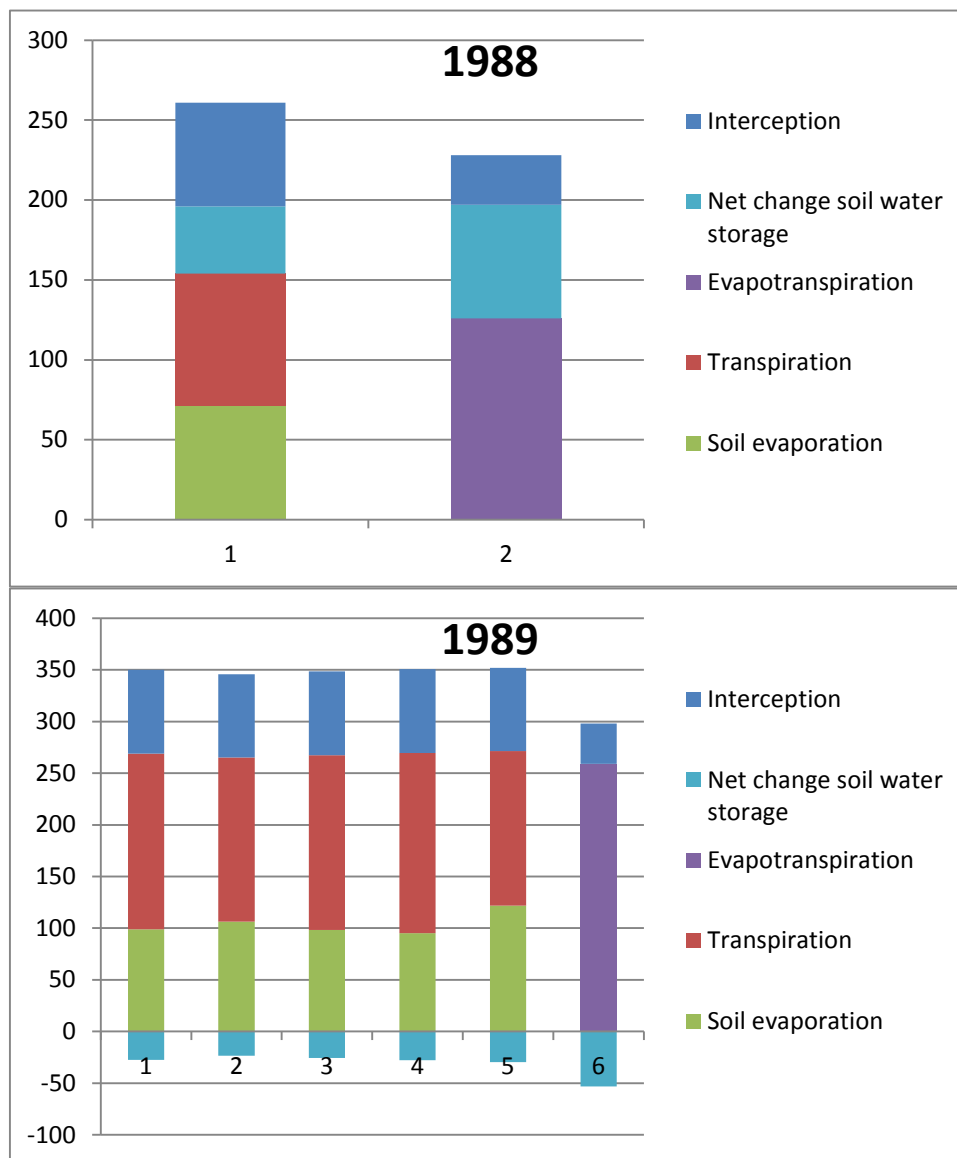
Figure 5.4. Simulated annual water balance (Picea abies) in the individual years where the corresponding year was used as weather, compared to the measured values at Loobos (Pinus sylvestris, right column).

5.2.4. Water use – broadleaves

For the broadleaves we did a similar comparison with measured data as for the conifers as described above. Comparison data are available as partial (summer) measurements in Quercus rubra (http://www.climatexchange.nl/projects/boshydrologie/Info-eik-loc_n.htm), LAI max at 4.9. Note that for 1988 the simulated period is 10 days longer than the measurement period due to difficulties in extracting data from the simulations. We calculated the change in soil water storage as the difference in soil water content between start and end of the comparison period plus the simulated leakage.

The precipitation in ForGEM is higher than the measured values, probably caused by differences in local showers between the locations of the respective measurement stations. For both species and both years, the sum of simulated transpiration and soil evaporation exceeds the measured evapotranspiration by 2-22%, for 1988 generally more (19-22% on average) than for 1989 (4-10% on average). This is partly related to the longer simulation period, but this would account only for about 5% of the difference. Simulated interception is too high in all scenarios, 14-16% of the precipitation in the measurements against the fixed 25% in ForGEM.

Simulated change in soil water storage is of the same sign as the measurements, but underestimated in all simulations. The underestimation is larger for Quercus than for Fagus. In general, the underestimation in soil water storage change is related to the too high water use for soil evaporation and plant transpiration. For 1989 the underestimation of soil water depletion is also related to the higher precipitation in the simulations.

Table 5.5. Measured values at Edesebos, NL, Quercus rubra
(http://www.climatexchange.nl/projects/boshydrologie/Meet-eik-jaar_n.htm)

Measurement period	11-07-1988 till 01-10-1988	01-05-1989 till 01-11-1989
Precipitation	228 mm	245 mm
Interception	31 mm	39 mm
Evapotranspiration	126 mm	259 mm
Runoff	-	-
Precipitation surplus	71 mm	-53 mm

Figure 5.5. Simulated annual water balance (Fagus sylvatica) in the individual years where the corresponding year was used as weather, compared to the measured values at Ede (Quercus rubra, right column).

Figure 5.6. Simulated annual water balance (Quercus robur) in the individual years where the corresponding year was used as weather, compared to the measured values at Ede (Quercus rubra, right column).

5.2.5. Water use – sensitivity

Figure 5.7 shows the annual water use in the different sensitivity scenarios. As expected, total precipitation (the total of all components) is clearly different in the dry and wet scenarios and comparable in the other scenarios. Dry conditions hardly affect the

Towards the Sustainable Management of Forest Genetic Resources   FORGER FP7- 289119

transpiration rates in conifers, only the broadleaves show a somewhat reduced transpiration. Soil evaporation is reduced to some extent, while leaching is strongly reduced. Wet conditions mainly increase leaching, indicating that sufficient water is available for tree growth already under average conditions, and even under dry conditions in case of the conifers.

Varying CO_2 concentrations does not visibly affect the transpiration rates, but transpiration is increased by 1-2mm for all species under low CO_2 concentrations and decreased by 3-5mm under high CO_2 concentrations. Temperature change has a strong effect on transpiration, while soil evaporation is only slightly affected.
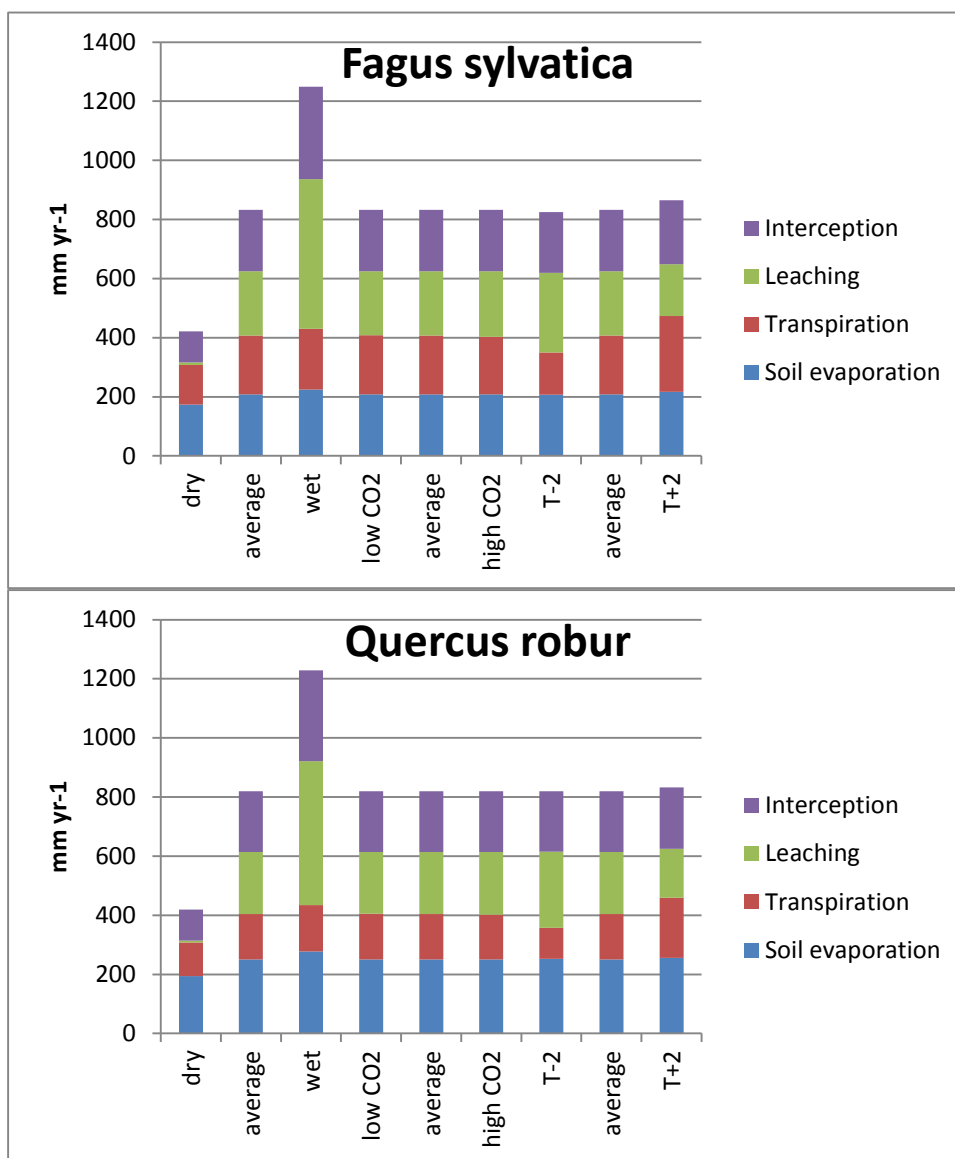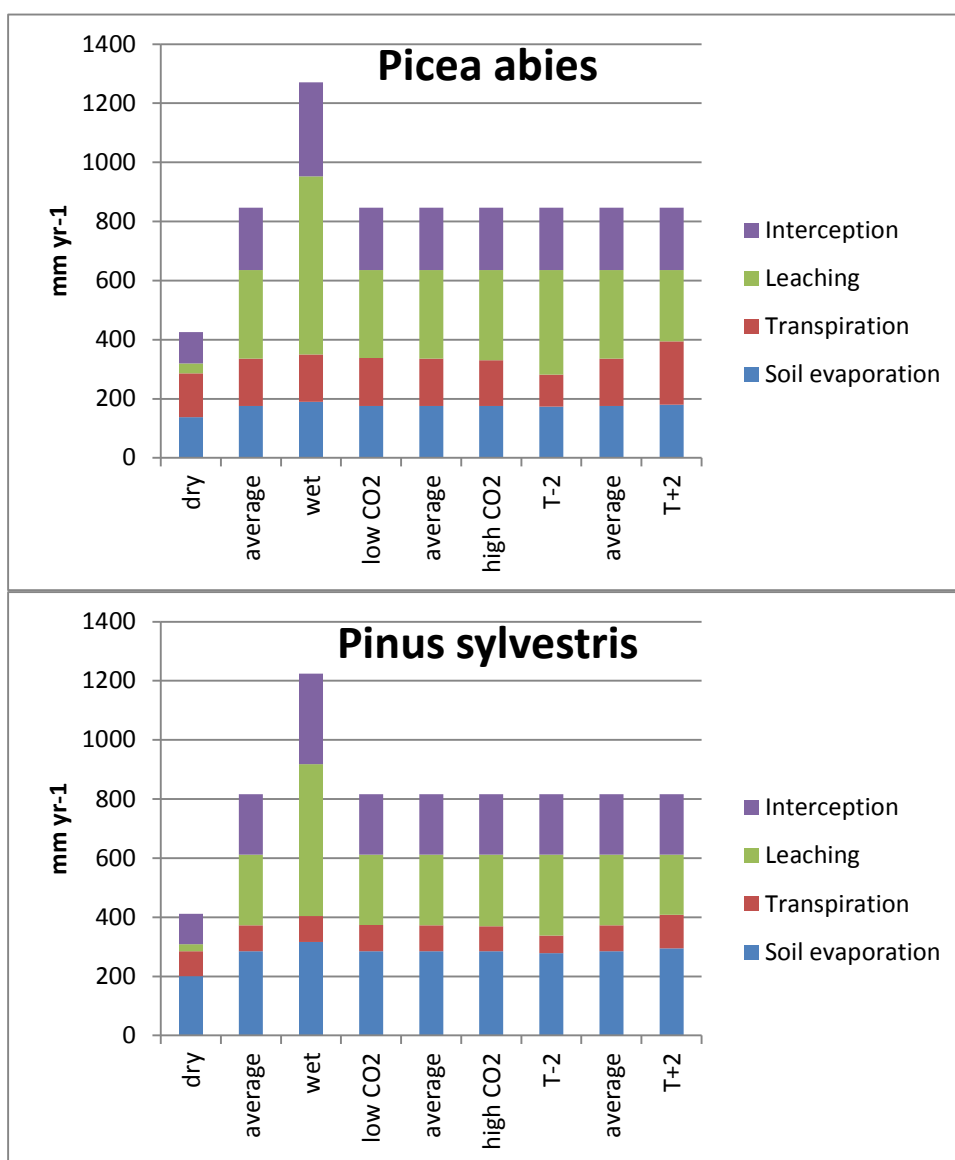
Figure 5.7. Water use in the different simulations (average of 5 replicas).

5.3. Validation of simulated productivity patterns over Europe

5.3.1. Simulation setup

The aim of this validation exercise is to test how well ForGEM is able to simulate productivity of the 4 species (oak, beech, Scots pine, Norway spruce) over a gradient of climate conditions in their area of occurrence in Europe. As starting point, we used a generated stand, based on the first age reported in the highest site class available in Janssen et al (1996). For Quercus, the trees are 10 years old, for the other species 15. These stands are dense, with 4000-5000 stems per hectare. All replicates start with the same initial stand. The weather was taken from unforced GCM-output from the ISIMIP series, for the period 1951-1980, with randomly drawn weather years for the simulation (bced_1960_1999_hadgem2-es_historical_1951-1980_detrended). All simulations were done for 100 years, without any management. Originally, the plan was to simulate management by applying stem density trajectories according to local growth and yield tables. However, this did not work out as expected, since at most locations mortality occurred before management was applied. This is probably related to different dynamics in crown expansion across Europe, as compared to the situation in the Netherlands where it was calibrated.

The simulated locations (7 or 8 per species) were chosen to span the range of growing conditions for each species, but not at the real margins of their distributions. Figures 5.8-5.11 show the selected locations, with the corresponding climate characteristics in Table 5.6. For comparison of the simulated productivity, we selected for each location the lowest and highest yield table available and computed the average annual productivity from the difference in volume at the start and end of the yield table, plus the accumulated thinnings. A maximum period of 100 years was applied in case the yield tables spanned a longer time frame. If the tables spanned a shorter period, simulation outputs were evaluated over the corresponding time span (according to the length of the highest yield table). Simulated productivity was calculated from volume increase and volume of accumulated mortality as described in the previous chapter. For additional comparison we extracted the average increment for the corresponding species for the first 5-year time step as simulated by the

EFISCEN model (Schelhaas et al. 2007) in the EFSOS II simulations (UNECE/and FAO 2011). EFISCEN is calibrated on increment data from the national inventories and is thus expected to be quite close to the actual increment from the inventory (~0.5m3/ha/yr tolerance). For the Netherlands and Switzerland, actual data from the last inventory are used (Schelhaas et al 2014; Brändli 2010).

Figure 5.8. Distribution (Brus et al. 2013) and test locations of Fagus sylvatica

Towards the Sustainable Management of Forest Genetic Resources   FORGER FP7- 289119

Figure 5.9. Distribution (Brus et al. 2013) and test locations of Quercus robur

Figure 5.10. Distribution (Brus et al. 2013) and test locations of Picea abies

Towards the Sustainable Management of Forest Genetic Resources   FORGER FP7- 289119

Figure 5.11. Distribution (Brus et al. 2013) and test locations of Pinus sylvestris

Table 5.6. Characteristics of test locations

country	latitude	longitude	radiation	rain	average temperature	Fagus sylvatica	Quercus robur	Picea abies	Pinus sylvestris
			$MJ\ m^{-2}\ yr^{-1}$	$mm\ yr^{-1}$	C				
Czech Republic	50.25	17.25	3112	1135	5.6	x	x	x	
Hungary	46.75	16.75	3902	775	9.8	x	x		
Netherlands	52.25	5.25	3048	921	9.0	x	x	x	x
Romania	45.25	23.25	3850	852	7.4	x		x	
Spain	42.75	1.75	4505	1026	7.7	x			x
Sweden (South)	56.25	14.25	3183	688	6.7	x	x		
Switzerland	46.75	6.75	3648	1223	7.9	x			
Slovakia	48.75	19.75	3380	1143	4.7		x		
Germany (mid)	50.25	8.25	3148	779	8.5		x		
France	45.25	3.75	3991	878	8.7		x		x

Bulgaria	41.75	24.75	4491	564	7.9	x		x
Sweden (mid)	61.75	15.75	3166	570	1.9		x	x
Denmark	54.75	11.75	3203	594	8.2		x	
Germany (South)	47.75	8.25	3437	1270	8.0		x	
Austria	46.75	14.25	3739	1057	7.0		x	
Finland	63.25	24.25	2817	627	2.6		x	x
Poland	53.75	17.75	3129	656	7.2			x

5.3.2. Results

ForGEM was initialised on a well-drained soil with rather good water holding capacity, and there is no simulation (and thus limitation) of nitrogen or other nutrients. The simulated productivity should therefore be more or less in the range of the higher yield tables available for a country, and simulated differences are attributable to differences in climate and day length. Figure 5.12 compares the simulated productivity by ForGEM to the range between the lowest and highest yield table available for a country.

The growth and yield tables are from a broad range of years, the oldest used here dating back to the 1930s. Over the decades, increment of trees has clearly increased (Pretzsch et al. 2014), and some of the tables are outdated, especially the ones for Germany. Furthermore, the yield tables clearly differ in the productivity range they cover, with only 1 yield table for Quercus robur in France to a 10-fold difference for the same species in Czech Republic. It is therefore unclear how representative the presented ranges are for the real increment to be expected.

Fagus sylvatica

Quercus robur

Picea abies

Pinus sylvestris
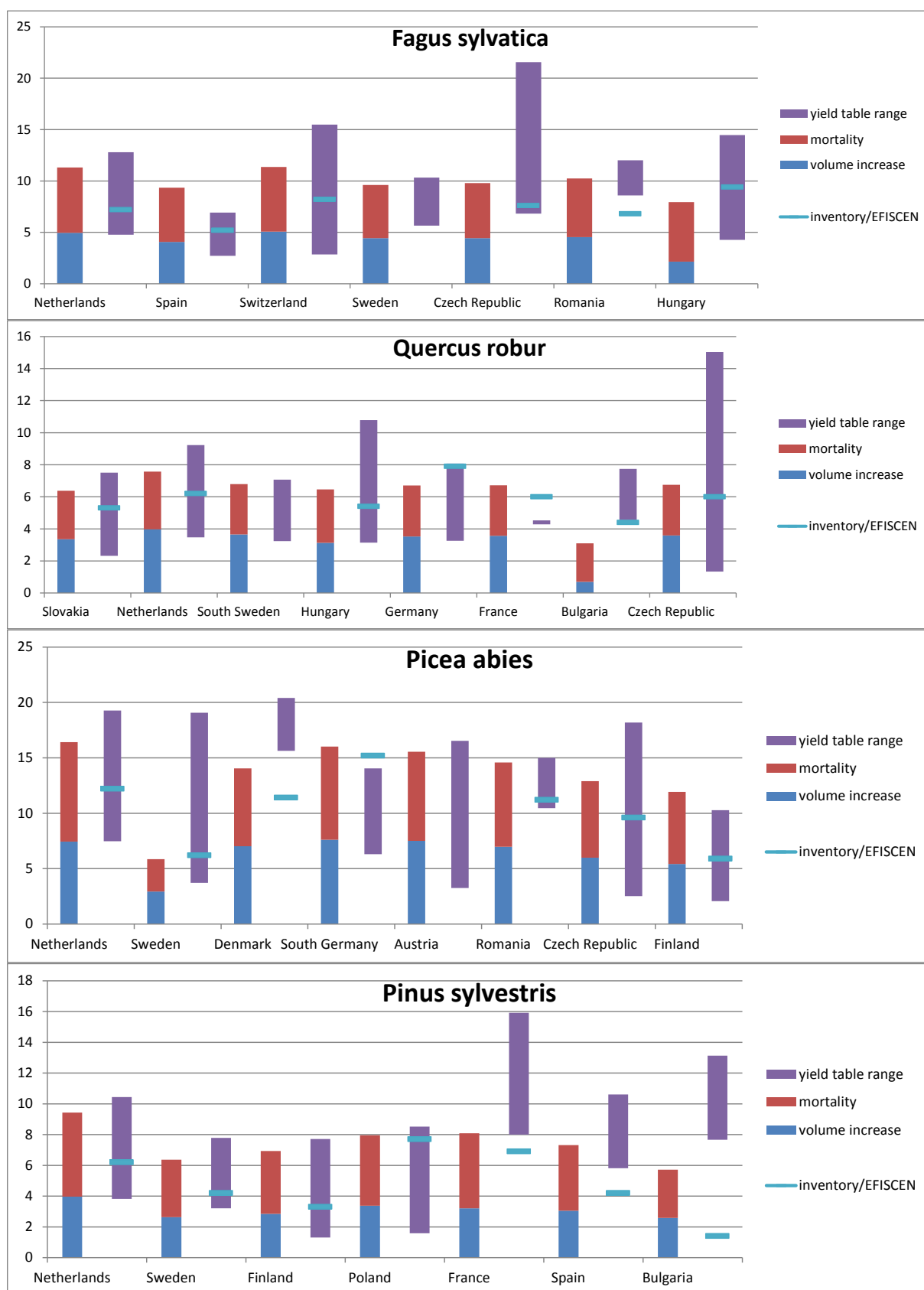
Figure 5.12. Simulated net annual productivity (m^3 ha^{-1} yr^{-1}) (5 replicates), separated in volume increase and mortality, compared to the range as given from the lowest and highest yield table available, and as derived from EFISCEN runs and inventories (Switzerland and Netherlands).

For Fagus sylvatica, the simulated productivity is mostly within the range as given by the yield tables, and higher as the national average. For Czech Republic, the simulated productivity is on the lower end of the yield table range, but the high end is much higher than in the other countries. For Romania, the simulated productivity is in the range of the 2 yield tables that were present for this country, while the national average is lower than this range. Hungary is at the dry end of the distribution range of beech, and this is the only site where ForGEM productivity is lower than the national average, but still within the range of the yield tables. The simulated productivity is probably very sensitive to the exact location within the country where the simulations take place.

Also for Quercus robur, simulated productivities are in the range of the yield tables, and generally somewhat higher than the national averages. For France, only 1 yield table was present. Simulated productivity in Bulgaria is too low, which might be caused by the selection of the exact simulation location. Also for Quercus robur, conditions in Bulgaria are at the dry and warm end of the distribution range. For Germany ForGEM is below EFISCEN, where it is clearly visible that the yield table range is low in comparison to the observations/EFISCEN simulations.

Most of the simulated productivities for Picea abies fall within the yield table range. Where they do not overlap, it seems likely that there are issues with the yield tables. For example, the range for Finland is much lower and smaller than for Sweden, while growing conditions are broadly similar. The EFISCEN increment for Denmark is lower than the lowest yield table, while for most countries it falls in the range of the yield tables. Germany shows the opposite pattern, likely caused by outdated yield tables. The match with EFISCEN increments is generally good, with ForGEM always being higher, which can be explained by the good site it should be simulating.

The simulated productivity for Pinus sylvestris is close to the highest yield tables, except for France, Spain and Bulgaria. However, the yield table ranges for those countries seem exceptionally high when compared to the EFISCEN increments. The match with EFISCEN increments is generally good, with EFISCEN usually having 40-60% of the increment of ForGEM, but for some countries (Poland, France) they are close to 100%.

In general, a higher productivity by ForGEM is expected than by EFISCEN (i.e. above the line in Figure 5.10). In this respect, the simulations perform rather well. Of the 3 observations below the line, 2 are broadleaves in dry conditions (Fagus in Hungary and Quercus in Bulgaria), indicating both the sensitivity of broadleaves to dry and warm conditions, and the need to carefully check the location and meteo data of the sites to simulate on the edges of the distribution range.
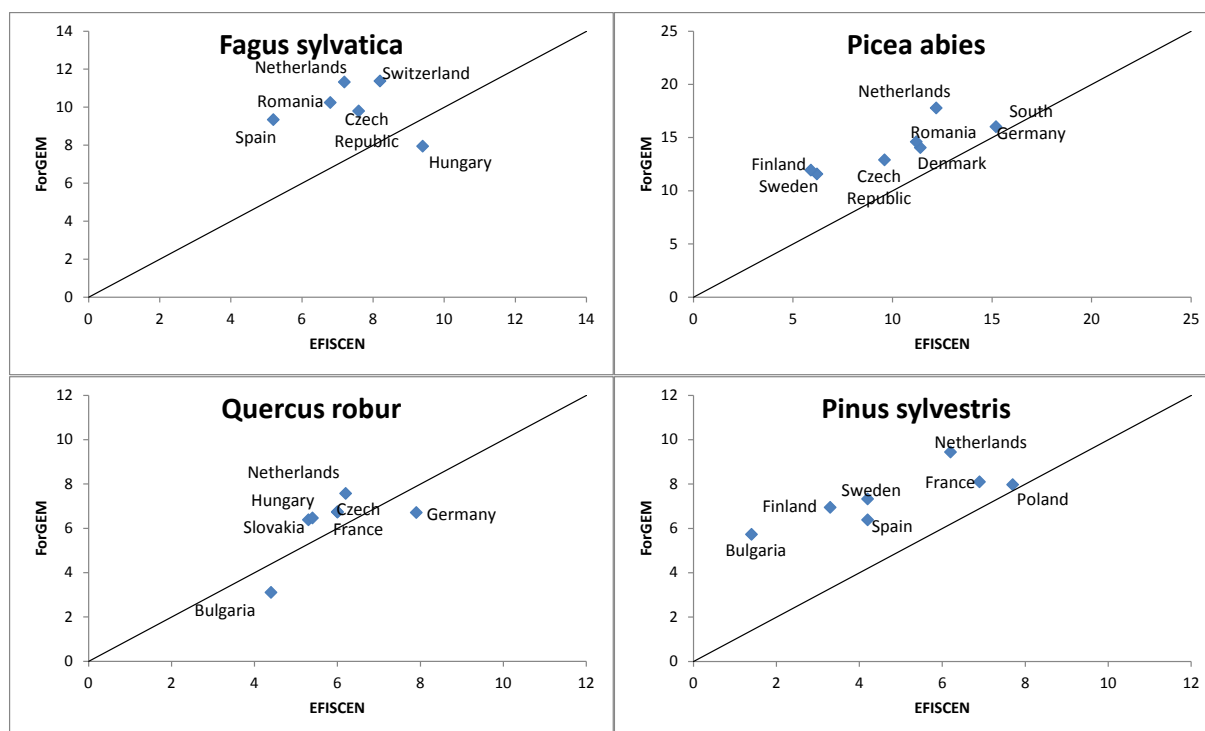
Figure 5.13. Simulated productivity by ForGEM versus productivity by EFISCEN for the 4 species.

5.3.3. Water use

For Fagus sylvatica, transpiration is very similar over all simulated sites (Figure 5.14). Soil evaporation is correlated with the average temperature of the sites: high temperatures (Spain, Hungary, Romania) lead to high evaporation and vice versa (Sweden). Leaching is basically the amount of water that is not used for other purposes, and is thus low where total precipitation is low (Sweden), and/or where water use by soil evaporation and plant transpiration is high (Hungary).

Quercus robur shows a similar pattern as Fagus, with rather little variation in plant transpiration. The absolute amount of transpiration is lower for Quercus, due to the lower LAI. Bulgaria has a much lower transpiration than the other sites. This is caused by relatively frequent mortality events, reducing plant cover drastically already early in the simulations, visible also in the low productivity of this site. Since no regeneration is allowed, parts of the site will not be covered by vegetation for longer periods of time. This enhances the soil evaporation. Most of the water in the Bulgarian site is used for plant transpiration and soil evaporation, so hardly any water is leaching. Soil evaporation in general is higher than for Fagus, due to the lower LAI, so more light is reaching the ground.

The same patterns are present for both Picea abies and Pinus sylvestris. The transpiration is rather stable over the sites, with higher transpiration for Picea due to its higher LAI. The high LAI of Picea also reduces the soil evaporation compared to Pinus. The soil evaporation of the conifers is lower than for the broadleaves due to the fact that they have leaves year-round. Leaching follows the same pattern as in the broadleaves, with the lowest value found for the warm and dry site of Bulgaria.
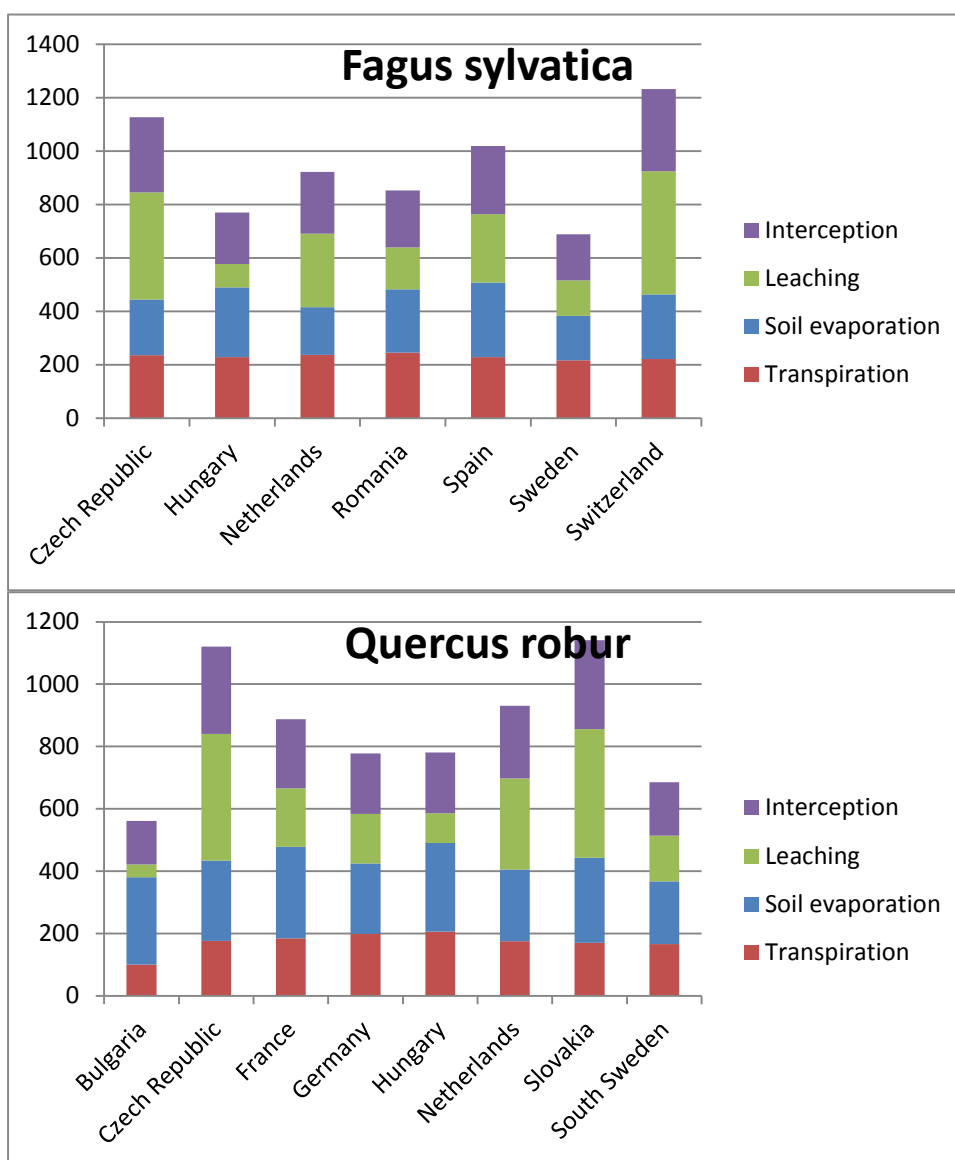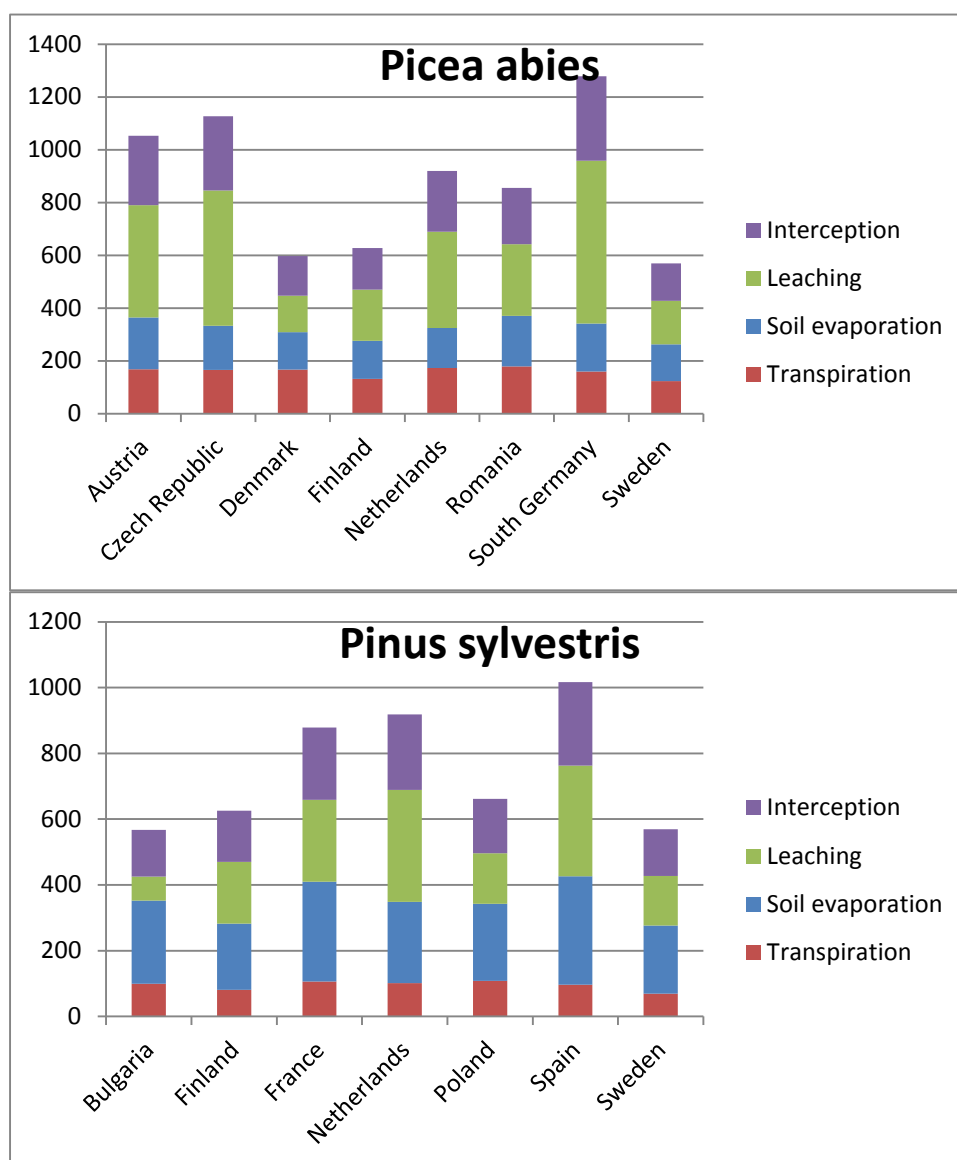
Figure 5.14. Simulated water fluxes (mm yr^{-1}) for 4 tree species at a range of European sites.

5.4. Sensitivity to N-content

5.4.1. Simulation setup

One of the aims of the modelling work within the project is to derive regionally specific parameters, adapted to the local climatic circumstances. For the model to be able to adapt to such circumstances, there should be a sensitivity to certain parameters, that can be used to optimise the performance of the trees. One of the parameters that could be optimised is the N-content in the foliage. Higher N-content leads to higher productivity, but also to increased maintenance respiration. The productivity increase is linear, while respiration is an exponential relationship. To test if the model really shows an optimum at a certain N-content, we tested a range of N-contents and the effect on total productivity.

Simulations were done for 2 species (Fagus sylvatica and Pinus sylvestris), at 3 different sites in Europe (Southern Sweden, Netherlands and Hungary), with 2 replicates and for a period of 100 years. N contents were varied by adapting the parameter cCarbonNitrogenRatioMinLF and cCarbonNitrogenRatioMinBB simultaneously according to Table 7. All other settings and climate variables were the same as in Chapter 4, i.e., the climate drivers included the climate change signal.

Table 5.7. Levels of foliage CN ratios used in the sensitivity analysis, and the resulting N content of the foliage.

CN ratio	N content
5.625	0.08
11.25	0.04
16.875	0.026667
22.5	0.02
28.125	0.016
33.75	0.013333
39.375	0.011429
45	0.01

50.625	0.008889
56.25	0.008
61.875	0.007273
67.5	0.006667

5.5. Results

Productivity increases with increased N-content for both species at low levels of N (below 3-4%) (Figure 5.15). At the dry and warm site in Hungary, productivity decreased at higher levels of N: sharply in Pinus and only slightly in Fagus. For the other sites, productivity seemed to level off, but with some strange behaviour in the Dutch site for Fagus at 4% N content. Also at some sites at low levels of N the results seem somewhat erratic, with total mortality in some replicates. This might be caused by certain dry years in the random weather series. More replicates seem useful here. In general, there seems to be an optimal N content at the warm sites, probably related to increased respiration at higher temperatures.

Transpiration follows the productivity pattern (Figure 5.16+5.17), where increased stem wood production translates only in slightly higher transpiration (Figure 5.18). This is probably a consequence of the allocation mechanism. Resources are first used to produce the optimal amount of foliage and reserves, and are only allocated to the stem if all other demands are satisfied. Higher production at higher N content will thus disproportionally benefit the stem growth.
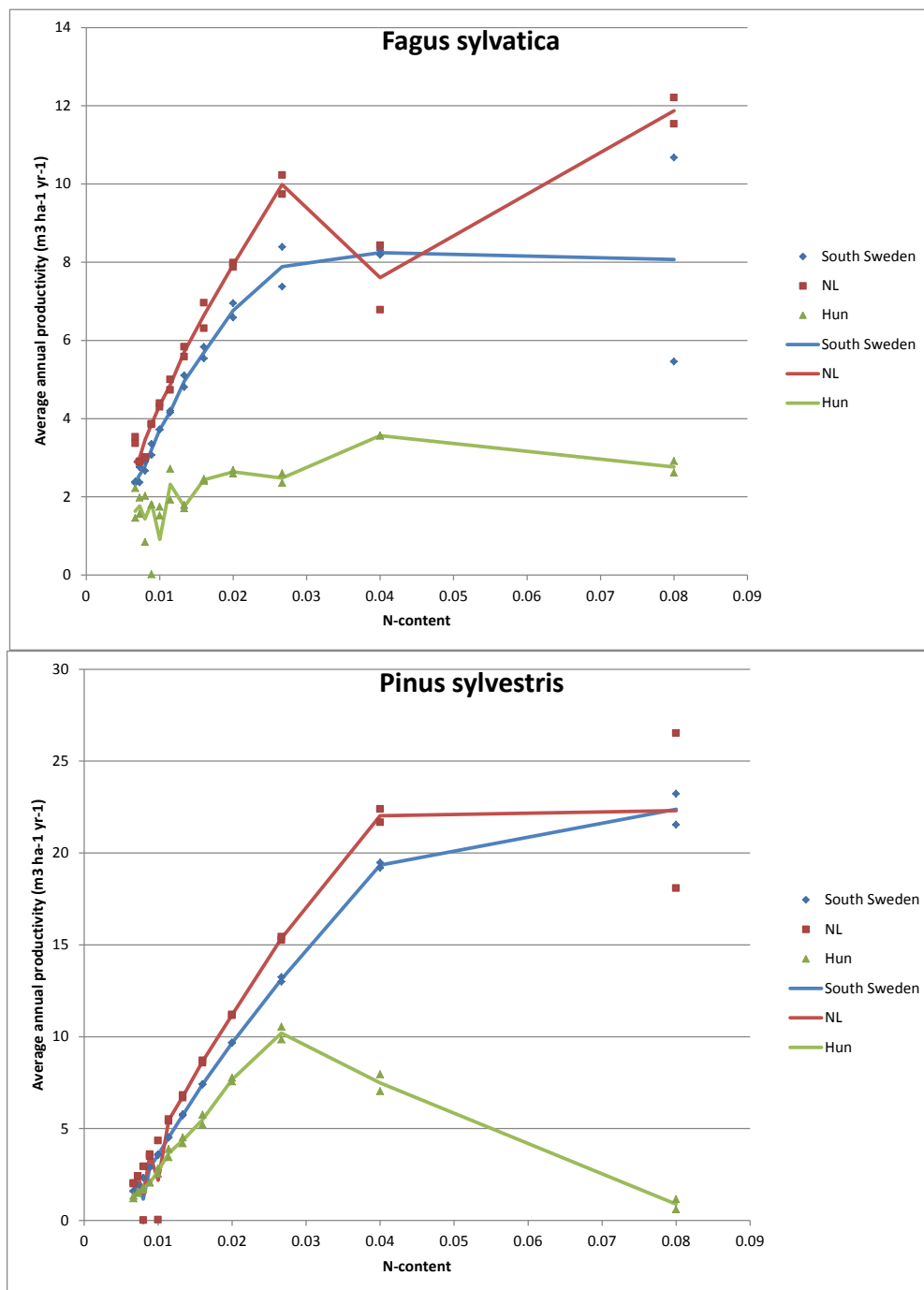
Figure 5.15. Productivity at 3 different sites (including climate change) as a function of N content of the foliage. Individual markers are individual replicates, the lines connect the average per simulated N- content.
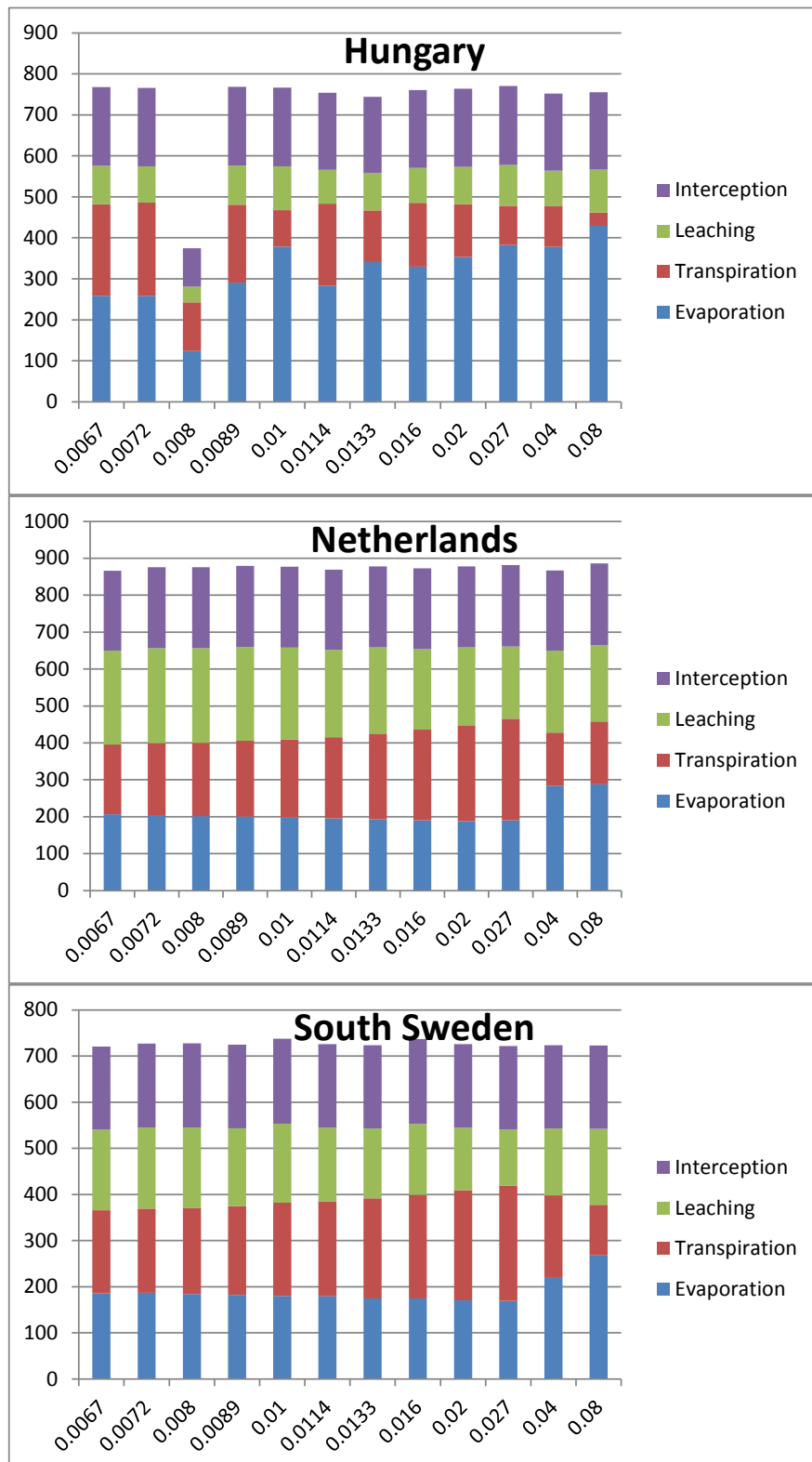
Figure 5.16. Simulated average water use (mm/year) by Fagus sylvatica in relation to N content in the foliage, 2 replicates.
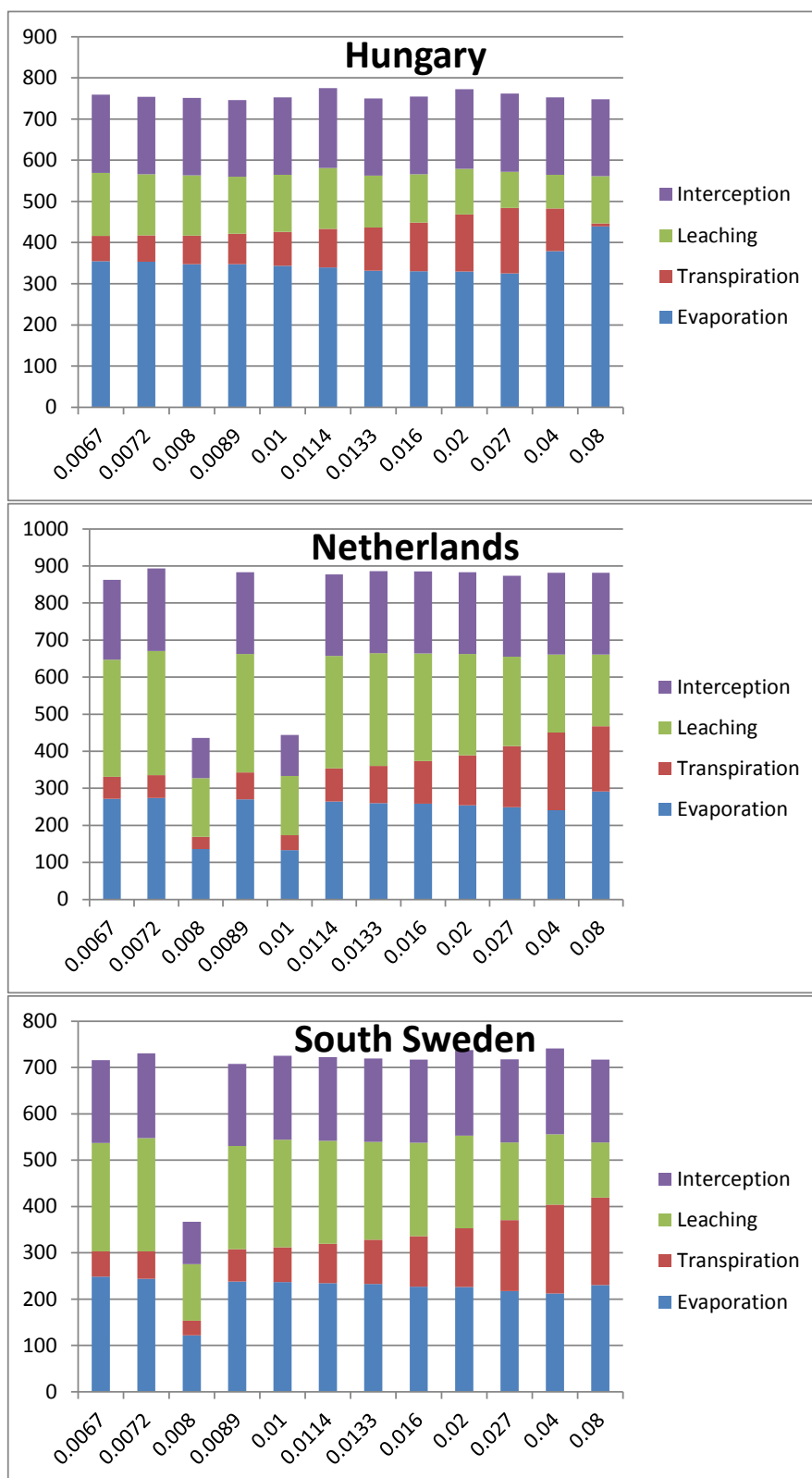
Figure 5.17. Simulated average water use (mm/year) by Pinus sylvestris in relation to N content in the foliage, 2 replicates.
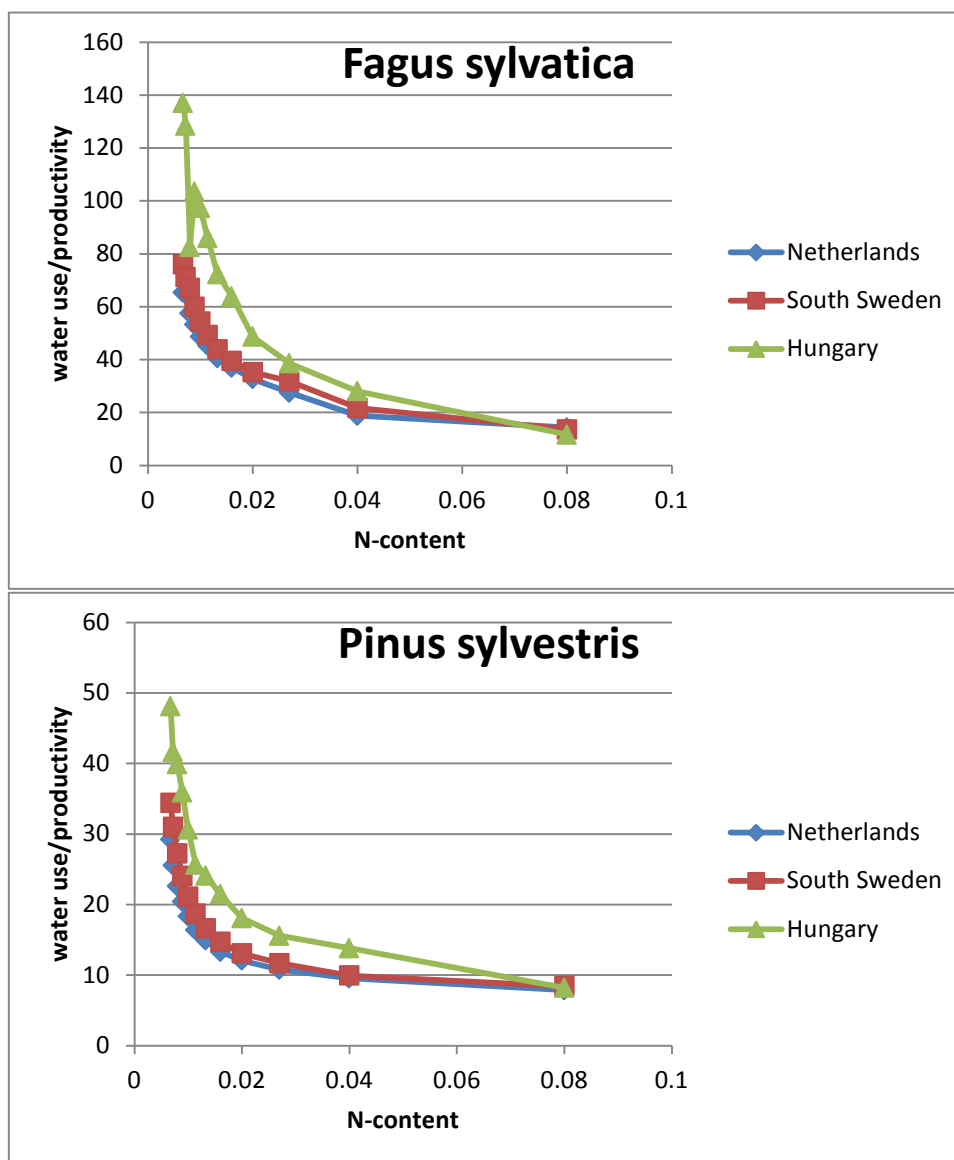
Figure 5.18. Water use per unit of productivity (mm/ m³ ha⁻¹) in relation to N-content of foliage.

5.6. Genetic analyses

The ForGEM model was eventually applied at 107 sites for each of the 4 tree species throughout Europe, in which the tree populations were allowed to adapt to local environmental conditions. The time horizon of the simulations was 500 years, i.e. 2-3 tree generations. These simulations proved to be very (computing) time intensive. The model

Towards the Sustainable Management of Forest Genetic Resources   FORGER FP7- 289119

runs take 3-4 month using 200 cores of High Performing Computer Cluster at the Dutch national computing facility for scientific research (SURFSARA - Academic Computing Centre Amsterdam), or over 500,000 CPU hours per species. Therefore, not all anticipated model runs appeared to be feasible.

Preliminary model runs on a smaller number of sites, indicated that adaptation to local conditions leads to higher productivity over the full temperature range, and the difference increases with water availability (Figure 5.19A). Thus, the least adaptive response was found under warm and dry conditions. Adaptation results in a loss of genetic diversity. The model results indicated that the loss of genetic diversity, relative to that available at the start of the simulations, was strongest under warm and dry conditions, and least under cool conditions. This selection pressure appeared to decline with increasing water availability (Figure 5.19B)
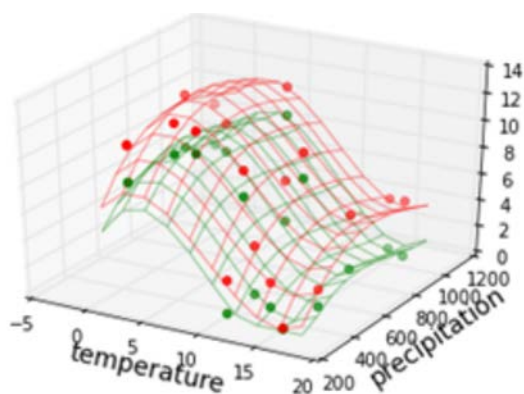
A. Productivity (m3/ha/yr) either with adaptation to local environmental conditions (green dots and response surface), or without adaptation to local environmental conditions (red dots and response surface)
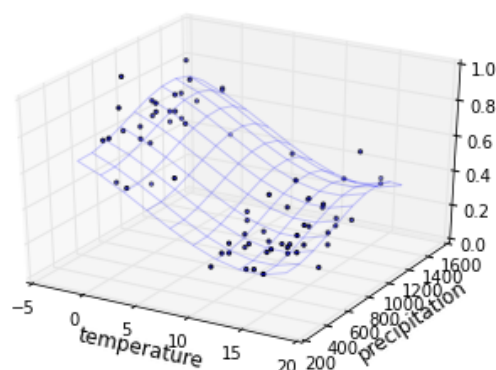
B. Genetic diversity of a trait related to water use efficiency (c1SoilWater), at the end of the simulation, relative to the genetic diversity at the start of the simulation

Figure 5.19. Model results for Fagus sylvatica on a limited number of sites to test the impact of genetic adaptation to local environmental conditions.

5.7. Discussion and Conclusions

The originally planned validation of the ForGEM model considered the following aspects:

- growth & yield: Testing model the output with existing growth and yield data over Europe, available at Alterra for the EFISCEN model
- reaction norms: model – data comparison of reaction norms of phenotypic traits (in particular phenology and drought) based on the results from Task 3.2
- vitality & survival: testing the model output with data on survival, based the results from Task 3.2

We were unable to test the model against observed reaction norms and vitality and survival data. The reasons for this were two-fold. Firstly, the availability of this data, and the analyses thereof, were more time consuming than originally planned, Secondly, and more importantly, the type of the data that was historically collected (outside the FORGER project) proved unsuitable for model validation. Much of the reaction norms are based on responses of tree height when planted in different environments. Height growth in the ForGEM model is, however, not based on a mechanistic understanding of height growth but based on height growth functions. Furthermore, the available vitality data are typically based on qualitative categories, whereas the model predicts individual-tree mortality probabilities, and are thus unsuitable for model validation.

Instead of the reaction norm and vitality & survival analyses, we did an extensive sensitivity analyses of the simulated productivity to environmental drivers, relevant for global change, and compared the reference runs (no change in environmental drivers) to observations on growth and yield data.

We conclude that the version of the ForGEM model presented here, based on the model description and parametrisation presented above is suitable to apply for climate change assessments at the European for *Fagus sylvatica*, *Quercus spp.*, *Picea abies* and *Pinus sylvestris*. A single set of parameter values was used per species. The current model is

suitable to allow model analyses on genetic adaptation to local conditions using the genetic module of the ForGEM model.

6. Process-model analyses

6.1. Introduction

The ForGEM model was used to analyse the following issues:

(i) *Response of species response to environmental change*. This was simulated by applying the model at 107 sites throughout Europe. These sites were selected such that they cover the full width of temperature and precipitation that forests face in Europe. The measure of performance evaluated is the annual increment in stem volume, expressed in m3 per hectare and year, and is averaged over a 100 year period. These results are presented as a response surface with temperature and precipitation the explanatory axes. Subsequently, the effect of a doubling of the ambient CO_2 concentration on this temperature x precipitation response surface was analysed. These analyses on elevated CO_2 were done for Fagus sylvatica and Picea abies only. Genetic adaptation to local environmental conditions was not taken into account in this analyses.

(ii) *Adaptation to local environmental conditions*. The ForGEM was subsequently applied on all these 107 sites such that the local populations adapted to local environmental conditions by genetic adaptation. The results at these sites was spatially interpolated to the entire geographic distribution of the species. This was done both for the values of selected model parameters and for their genetic diversity. Four model parameters were set-up as genetic parameters in the model (see Model description). Two of them related to uptake of water and thereby water use efficiency of the tree, and two of them related to tree phenology, and thereby to growing season light interception and thus carbon gain.

(iii) *Impact of management practices on adaptive traits and their genetic diversity*. The effect of different forest management systems on the locally adapted model parameters were analysed. This was done at 27 sites throughout the species' distribution area that cover the full range in temperature and precipitation.

(iv)   *Transfer of forest reproductive material*. The usage of forest reproductive materials
        pre-adaptive to future environmental conditions is a major issue for forest
        management as the climate is anticipated to change faster than the adaptation
        process can track. Thus assisted gene flow could be an option. The approach taken
        was that the locally adapted populations were transferred to test sites varying in
        temperature and precipitation, in fact the same sites as used in (ii). The difference in
        performance of the transferred provenance, relative to the locally adapted one, is
        presented.

6.2. Response of species response to environmental change

The ForGEM model was applied at 107 forest sites throughout Europe. The sites were
selected such that a wide range of temperature, precipitation and incoming radiation was
covered, i.e. with realistic climates where the species might be able to grow. Particular
attention was paid to gradients in these environmental drivers. Thus, gradients at the limits
of the potential distribution of tree species is more intensively sampled than the central
distribution of the species. The stand characteristic evaluated was the productivity,
expressed as annual increment in stem volume (m3/ha/yr), (See §5.2.1). Figure 6.1 present
the response surfaces of productivity of the 4 species to both temperature and precipitation.
The differences between in productivity between sites with similar temperature and
precipitation is due to differences in incoming radiation. Thus geographically at different
locations. Both Fagus and Quercus show a symmetric optimal response curve to
temperature, and an increase in productivity with increasing precipitation over the full
precipitation range. The response of Fagus to an increase in precipitation appears to be
stronger than that of Quercus. Picea shows an asymmetric optimal response curve to
temperature, with a much steeper response to the high-temperature end (roughly S-Europe)
compared to the low-temperature end (roughly N-Europe). The same change in temperature
thus has unequal effects in the productivity in Picea between N- and S-Europe. The response
surface of Pinus is not very smooth. Probably more sites should be evaluated in the high-end

of annual precipitation. The response of productivity to precipitation is much more flat in the coniferous species compared to the deciduous species. Only when the annual precipitation to very low amounts a reduction in productivity can be expected, whereas an increase in precipitation results in only a small productivity increase in the main part of the precipitation range (also see Figure 5.1).

Increasing ambient CO_2 was only applied to Fagus and Picea, as the response to CO2 appears to differ between the coniferous and deciduous species, but not so much within these functional groups (see Figure 5.1). This means that the effect of elevated CO2 is particularly strong in the centre of the distribution of these tree species, and much less at the edges of the distribution (Figure 6.2), thus the steepness of the response surfaces at the boundaries of the species' distribution increases. This means that in a higher CO2 world, the response in productivity to a change in either temperature and precipitation increases at the edges of the species' distribution.
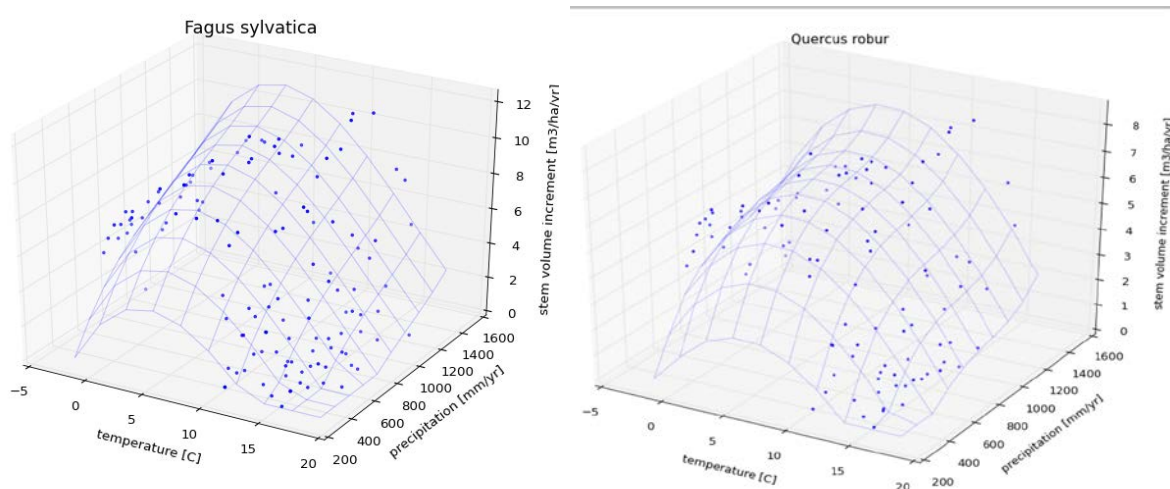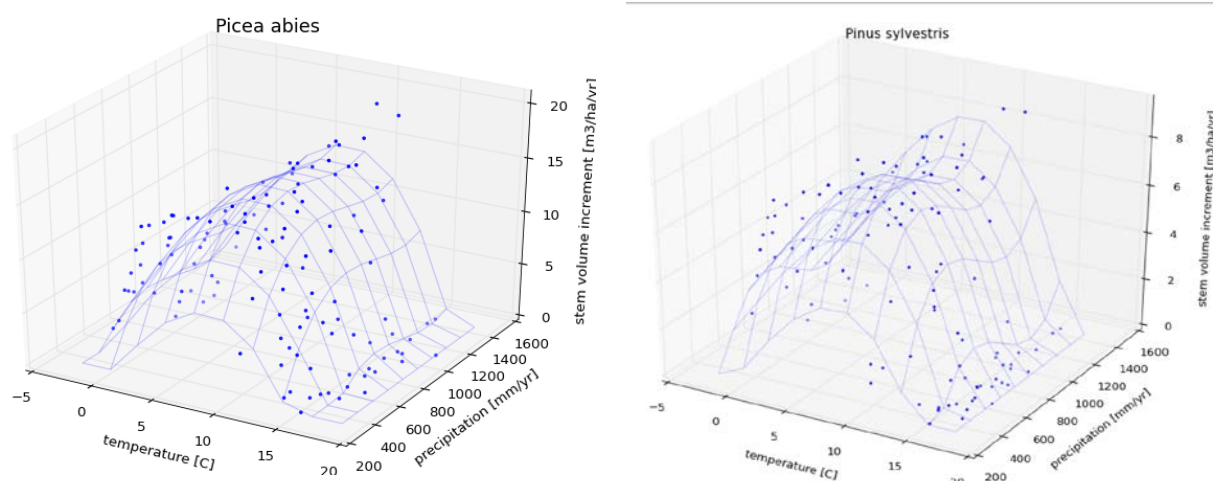
Figure 6.1. Response surfaces of productivity (stem volume increment m3/ha/yr) to temperature and precipitation of Fagus sylvatica, Quercus robur, Picea abies and Pinus sylvestris.
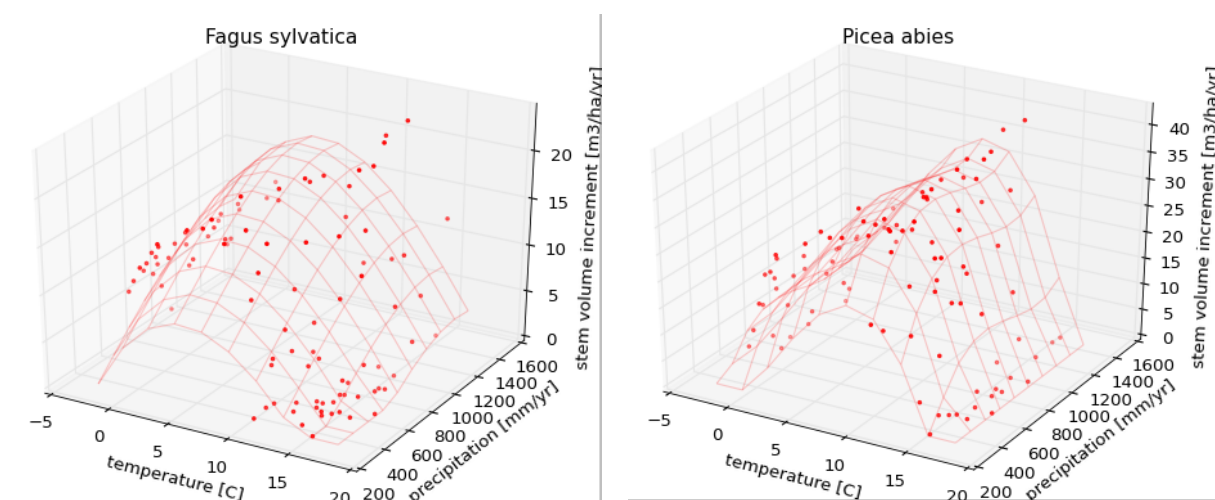

Figure 6.2. Response surfaces of productivity (stem volume increment m3/ha/yr) to temperature and precipitation of Fagus sylvatica and Picea abies to a doubling of ambient CO_2 concentration.

6.3. Adaptation to local environmental conditions

The plant eco-physiological processes that are allowed to genetically adapt during the model simulations were water use efficiency and bud burst phenology. These processes are characterized by a number of model parameters in the model. Changes in the parameters driven by selection pressure exerted by the environment thus result results in differential water use as well as in timing of the start of the growing season. These changes result in differences in productivity and survival of the trees. Below the results of genetic adaptation of two parameters related to water use efficiency (c1SoilWater2StomatalConductance and c2SoilWater2StomatalConductance (see Eqn. Photo 9) and two related to the onset of the growing season (sSo, sSr, see Table Pheno 2) are shown. Presented are the spatial interpolation of the values of the model parameters over Europe (Figure 6.3) and that of the genetic diversity of these parameter values (Figure 6.4). For c1SoilWater2StomatalConductance and sSr a clear selection pressure is exerted by the environment leading to clear patterns in the distribution of both the parameter values a the genetic diversity, whereas for c2SoilWater2StomatalConductance and sSo this is much less the case. Possibly either the number of sites evaluated or the duration of the model runs was insufficient for the spatial distribution of the latter parameters, given the relative low selection pressure the environment exerts on them.

c1SoilWater2StomatalConductance   c2SoilWater2StomatalConductance
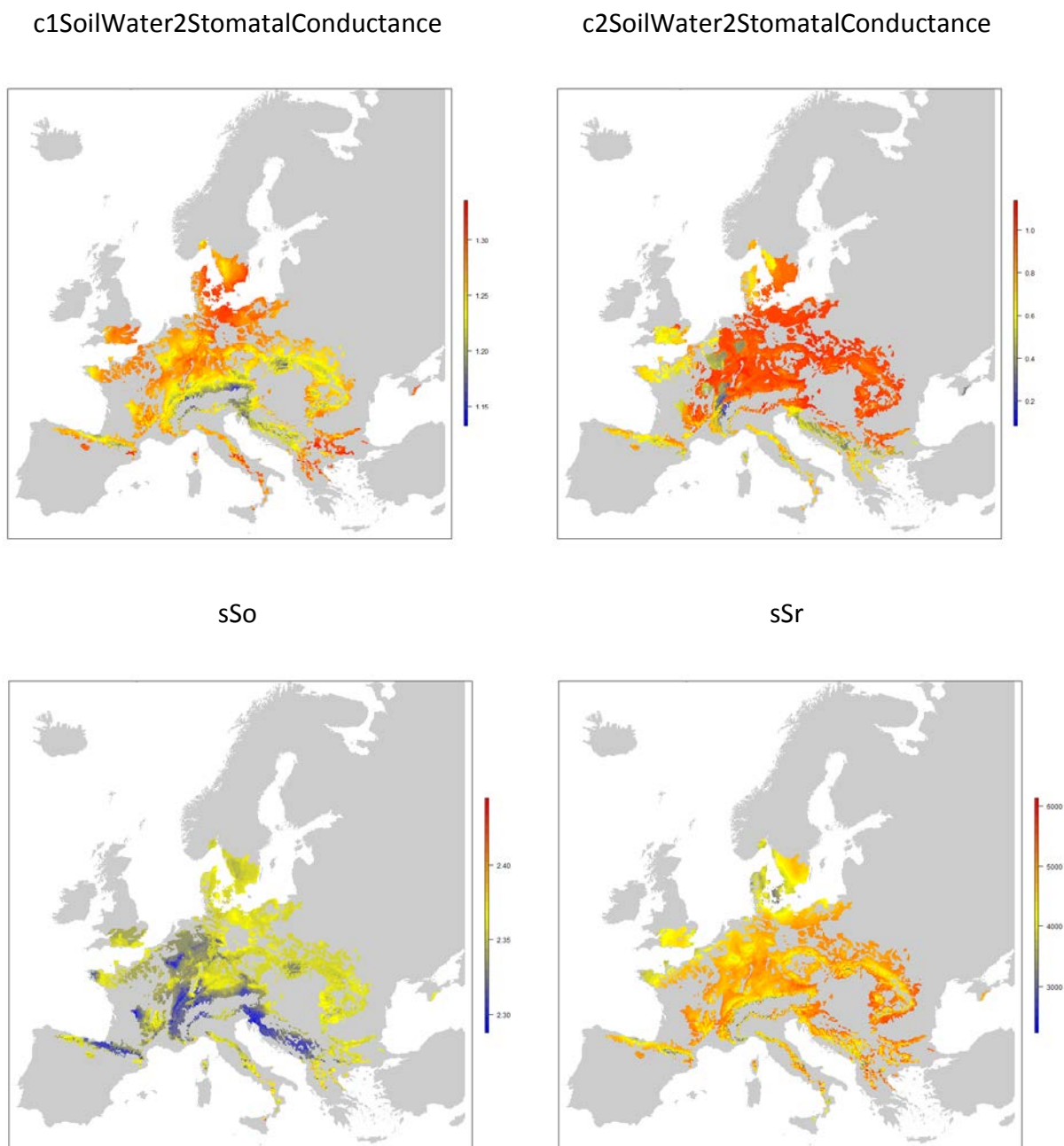

sSo   sSr

Figure 6.3. Distribution of the values of model parameters related to water use efficiency (c1Soilwater2StomatalConductance, c2SoilWater2StomatalConductance) and of the onset of the growing season (sSo, Ssr)
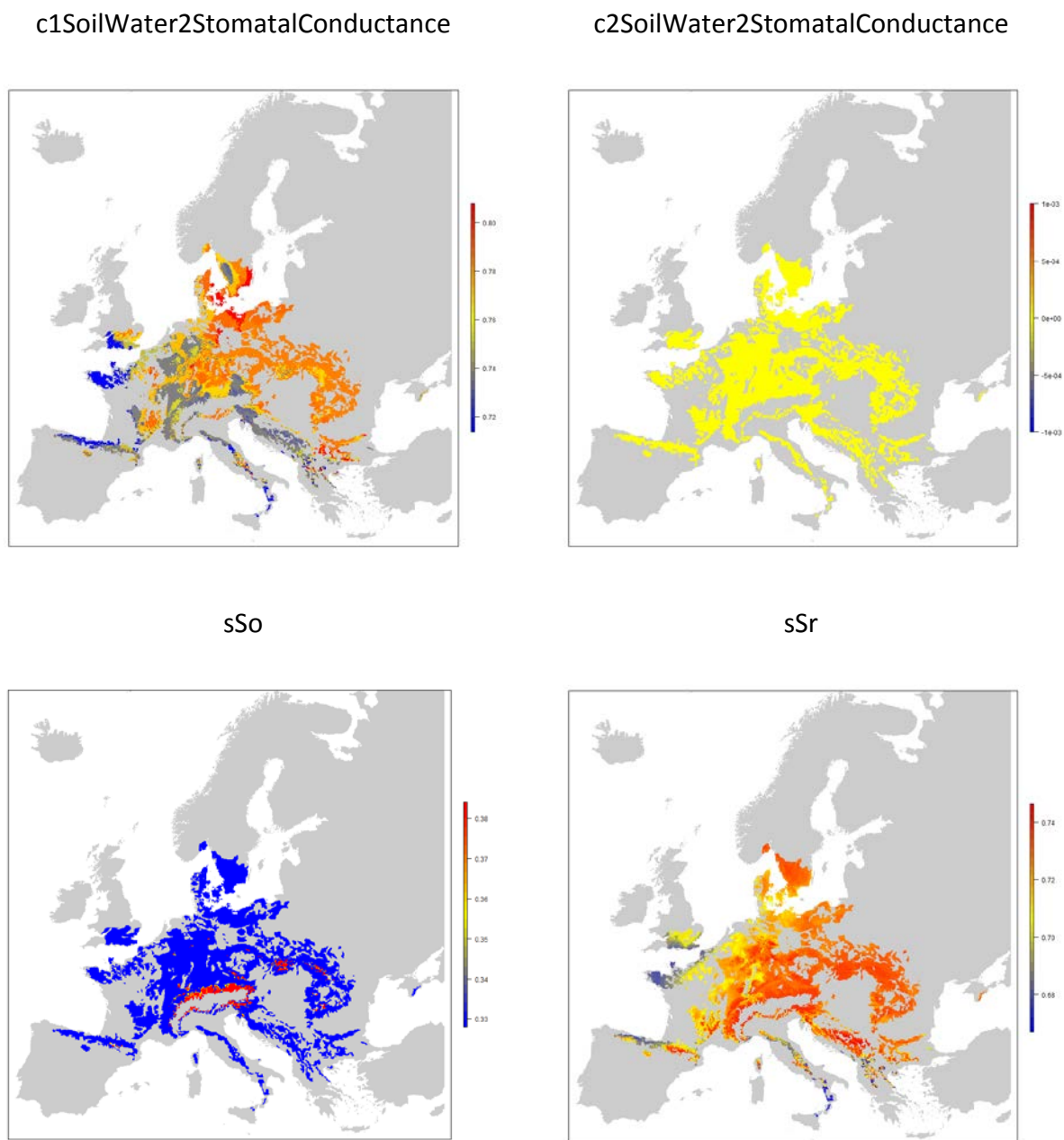
c1SoilWater2StomatalConductance   c2SoilWater2StomatalConductance

sSo   sSr

Figure 6.4. Distribution of the genetic diversity of model parameters related to water use efficiency (c1Soilwater2StomatalConductance, c2SoilWater2StomatalConductance) and of the onset of the growing season (sSo, Ssr)

The effect of selection pressure exerted on these parameters on the response surface of annual growth to temperature and precipitation is that the responsiveness to precipitation increases, in particular at the high end of the temperature range (Figure 6.5). Possibly the low responsiveness of the single genotype (i.e. without adaptation) to precipitation is to low when tested over the full temperature and precipitation range.
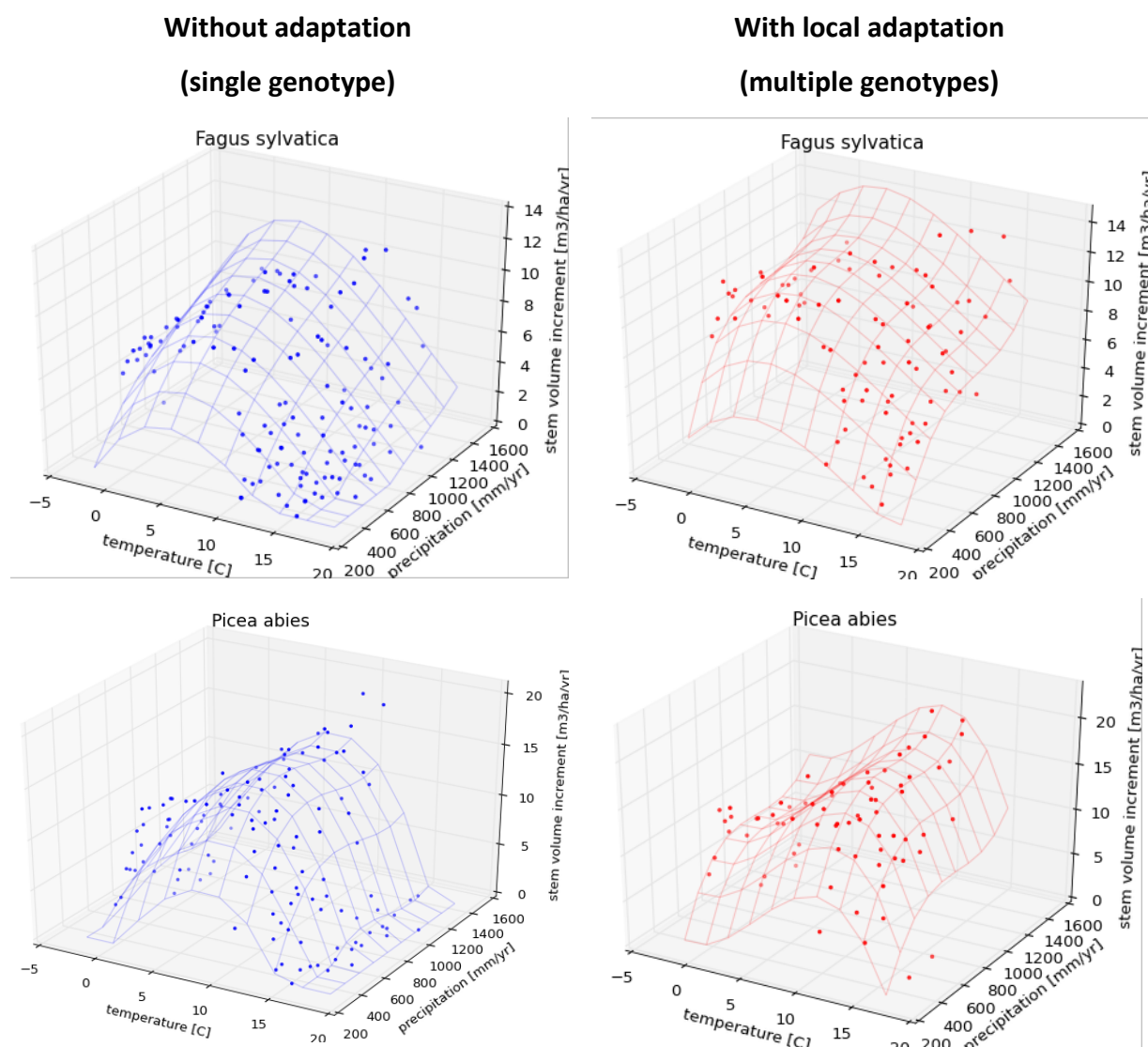
Without adaptation

(single genotype)

With local adaptation

(multiple genotypes)

Figure 6.5. Response surfaces of productivity (stem volume increment m3/ha/yr) to temperature and precipitation of with and without adaptation for Fagus sylvatica and Picea abies. (NB the response surfaces without adaptation are the same as presented in Figure 6.1).

6.4. Impact of management practices on adaptive traits and their genetic diversity

In earlier studies the interactions between climate change and forest management was extensively studied (Kramer et al. 2010, Kramer et al. 2008b). The overall finding was that the rate of adaptation to climate change is enhanced by forest management by shortening the interval between regeneration events, thus allowing more selection to take place. This, however, at the expense of adaptive capacity of the stand which then needs to be replenished either by natural or artificial means (natural or assisted gene flow). Due to limitations in processor time, these analyses were not repeated at the full European scale.

As new analyses, we assessed the impact of different forest management approaches on the distribution of the key-adaptive traits we evaluated, related to bud burst phenology and water use. These analyses were performed for both Fagus sylvatica and Picea abies. For Fagus the forest management systems applied were a shelter cut (FMA4, Table 4.1), and 2 variants of a group cut system (FMA3, table 4.1), one with scarification after the group cut and one without. Soil scarification is used in forestry to remove vegetation and thereby providing a suitable seedbed for seed germination. However, any seedlings and saplings of the species are also removed (see (Kramer et al. 2008b) for details on these forest management systems). These management systems were applied on 27 forest stand distributed throughout Europe.

Figure 6.6 shows the overall response of a parameter affecting water use efficiency of Fagus under these 3 forest management systems, averaged over 26 sites, as on one site Fagus did not survive. The adaptive response of this parameter is highest under the shelter wood system, and the system with gap making and soil scarification yields the lowest adaptive response (Figure 6.6A). Figure 6.3B presents the effects of these management systems of genetic diversity of this particular model parameter. Overall, over a 100 year period the differences between the effects of management both on the trait values and the genetic diversity thereof is minor. Figure 6.7 presents the differences between management systems on the adaptive response of the same model parameter but then for each site

where the ForGEM model was run (cf. Figure 6.6B). Between locations, the same forest management system thus may have different impact on the rate of adaptive response.
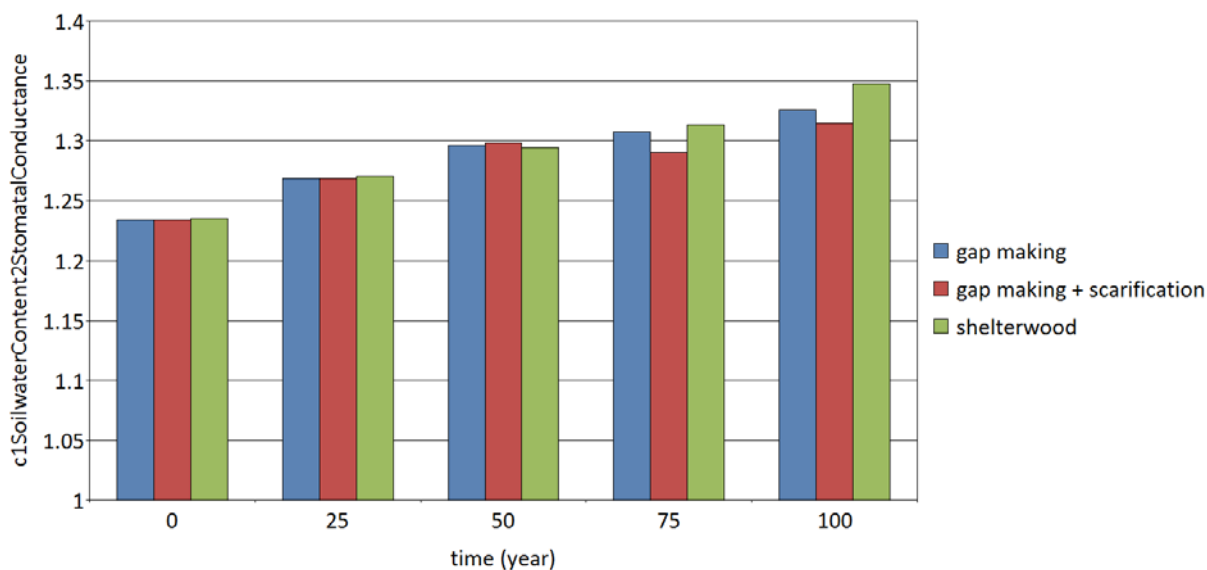
A. Effect of forest management on adaptive response
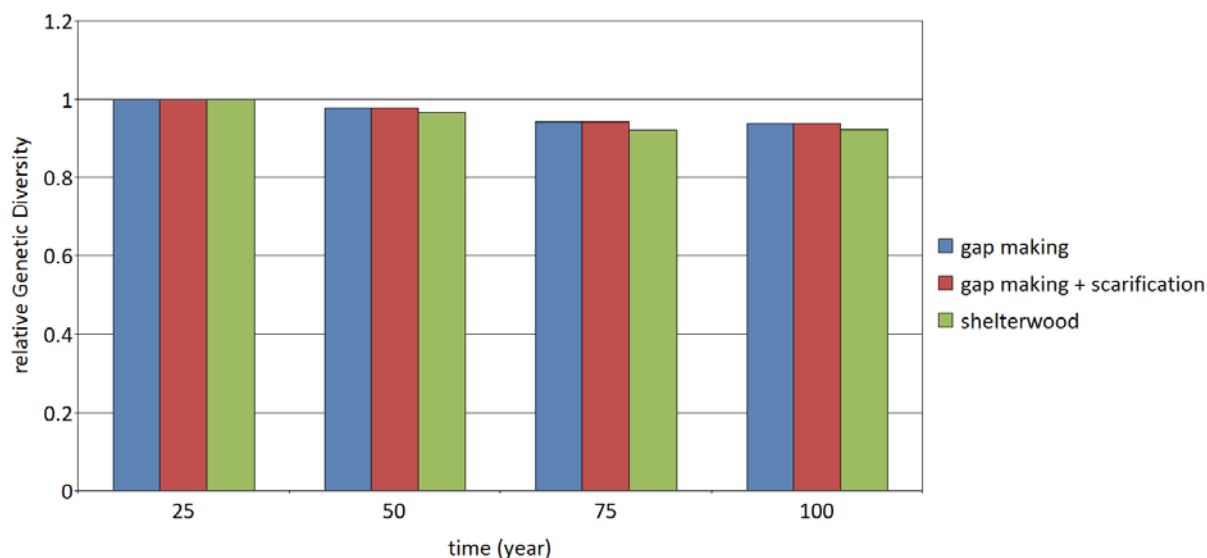
B. Effect of forest management on genetic diversity, relative to the genetic diversity at the start of the simulation

Figure 6.6. Effect of 3 forest management systems on the adaptive response of a model parameters associated with water use efficiency of Fagus. Averaged over 26 forest stands distributed over Europe.
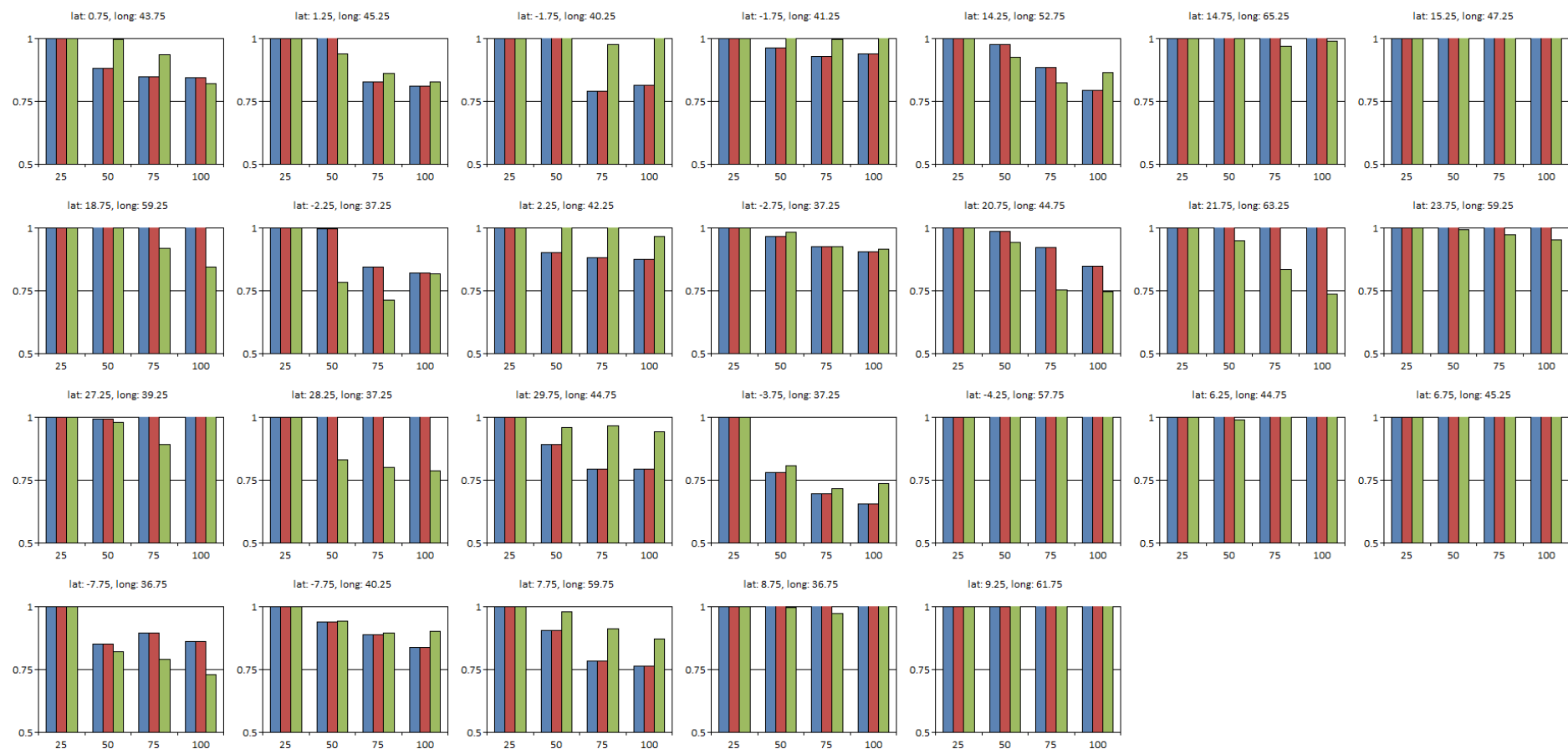
Figure 6.7. Effect of 3 forest management systems on genetic diversity relative to the start of the simulation, for a trait associated with water use efficiency of Fagus sylvatica (cf. Figure 62B). lat and lon indicate the latitude and longitude of the forest stand, respectively. Same legend as for Figure 6.6.

6.5. Transfer of forest reproductive material

A key question in the forest management is which provenance to use to anticipate on climate change. From the model runs, that where populations were allowed to adapt to local environmental conditions (§6.3), 27 sites were selected being widely spread along both temperature and precipitation gradients. These 27 provenances were subsequently planted and grown, *in silico*, at each of the 27 sites, including the site to which the provenance was adapted. Thus leading to a provenance trial 27 x 27 provenances and trial sites. Evaluated was the difference in stem volume increment of the tested provenance relative to that of the provenance adapted to the site. Thus, the testing of a provenance at the site it was adapted to leads to a difference of stem volume increment of zero.
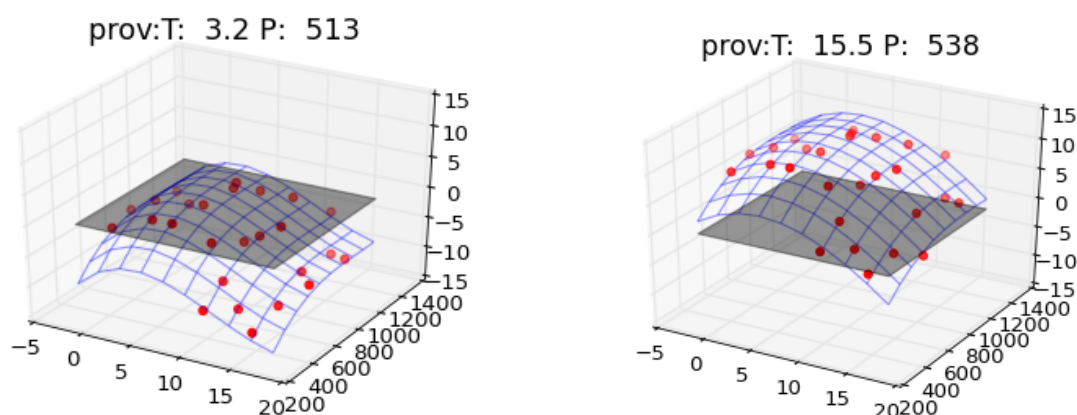

Figure 6.7 Example of a trial of 2 provenances of Fagus sylvatica. One provenance obtained from a climate with annual mean temperature of 3.2C and an annual precipitation of 513 mm (N-Europe); and a second provenance from a climate with annual mean temperature of 15.5C and an annual precipitation of 538mm (S-Europe). Both provenances were tested at 27 sites, though did not survive at all sites. Y-axes indicates the difference in stem volume increment (m3/ha/yr) between the tested provenance and locally adapted provenance.

The grey rectangle indicates the zero-plane: below the plane the provenance tested performs worse than the locally adapted provenance; above the plane the provenance tested performs better than the local provenance.

Figure 6.7 shows that a provenance obtained from the north of Europe performs worse than the local provenance in particular under much warmer and dryer conditions (See prov: T: 3.2 P: 513). Whereas a provenance obtained from the south of Europe, adapted to much warmer conditions and effectively much dryer because of the higher evapotranspiration, generally performs better than provenances adapted to local climate. The latter is because the provenance of south Europe experiences a stronger selection pressure on water use. That increased water use is also favourable under cooler and moister conditions where the provenance experiences less selection pressure.

The finding that provenances from north Europe perform generally worse compared to the local provenance throughout the environmental range of Fagus, and provenances from the south of Europe perform better was generally found (Figure 6.8.). For Picea abies the same transfer analyses were done also for the same sites (Figure 6.9). Here the pattern is less clear as for beech, because the responses of Picea to precipitation are rather weak compared to those of Fagus (see Figure 5.1). Thus the selection pressure operating on Picea by droughts will be less that the selection pressure exerted on Fagus.

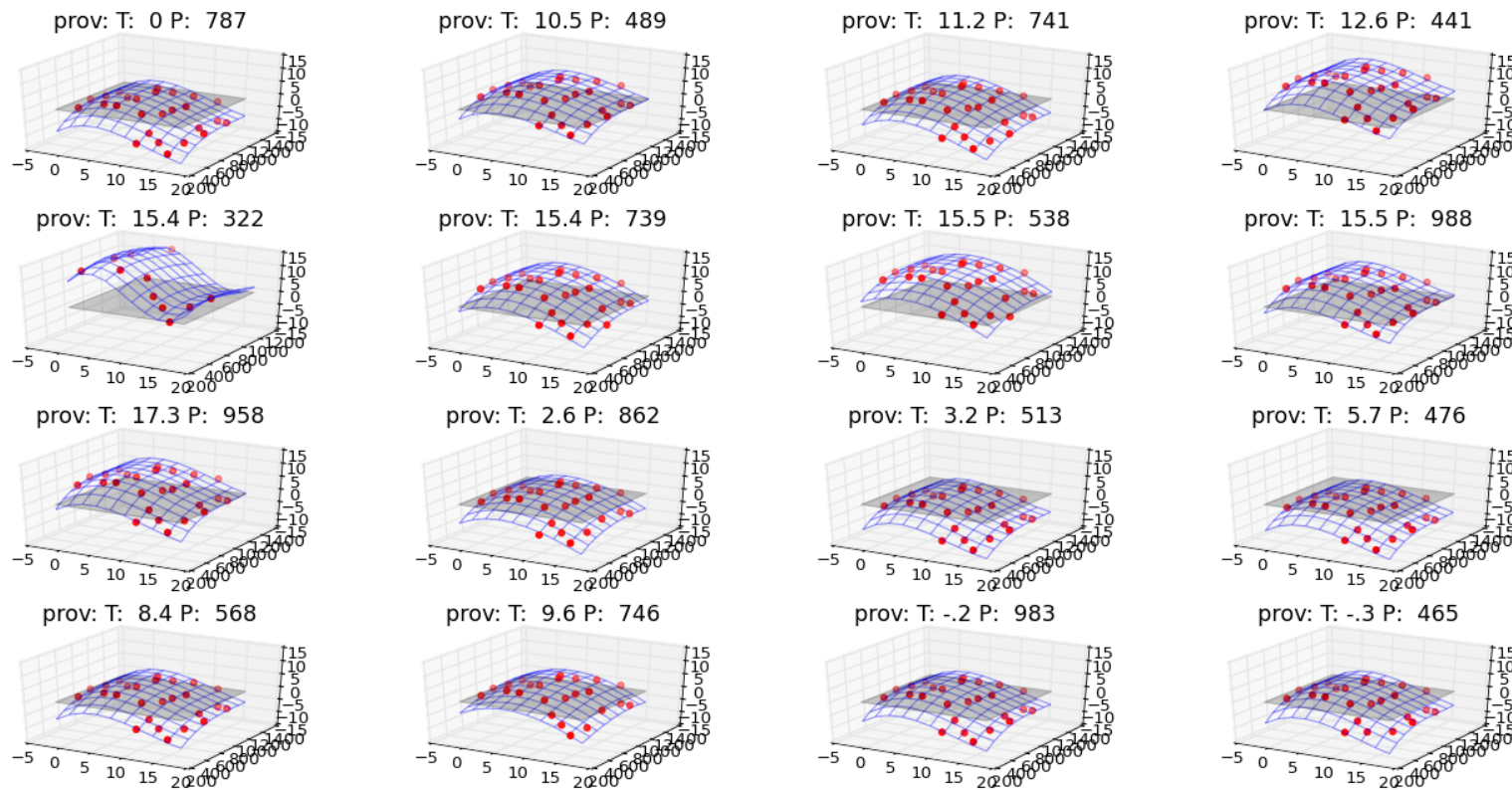difference in stem volume increment compared to local provenance

Figure 6.8. Overview of provenance trial of 16 provenances of Fagus sylvatica tested in 16 test sites. The header of each figure indicates the climate from which the provenance is obtained. See legend of Figure 6.7.

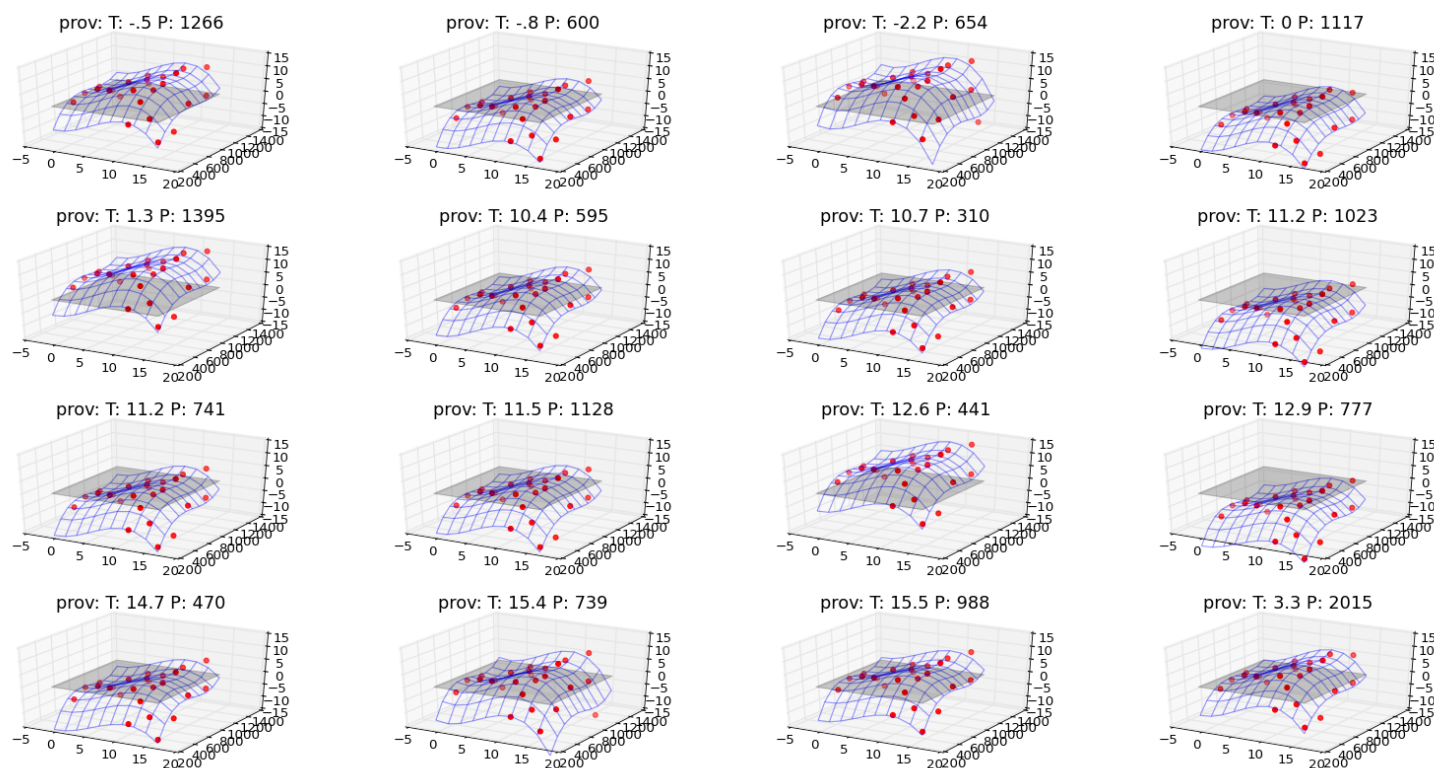difference in stem volume increment compared to local provenance

Figure 6.9. Overview of provenance trial of 16 provenances of Piea abies tested in 16 test sites. The header of each figure indicates the climate from which the provenance is obtained. See legend of Figure 6.7.

6.6. Conclusions

As stated in the Introduction, the model ForGEM was used to predict the impacts of: (i) environmental change, (ii) management practices and (iii) transfer of forest reproductive materials, on genetic diversity and the rate of adaptive response of functional traits. These analyses were performed to meet the overall objectives of Work package 3: *To analyse historic, current and future management and use of forest genetic resources.* The tasks necessary to meet that objective were:

- 3.4.1. Selection of sites and scenarios

- 3.4.2. Process-model parametrization

- 3.4.3. Process-model initialization

- 3.4.4. Process-model validation

- 3.4.5. Process-model analyses

The results and conclusions on Tasks 3.4.1 to 3.4.4 in the previous chapters. Here the conclusions on task 3.4.5 are formulated.

- *Environmental change*. The model results indicated that the deciduous tree species and coniferous tree species differed in their response to precipitation, temperature and, to a lesser extend ambient CO_2 concentration. Within these plant functional groups the responses to these environmental drivers was similar.

- *Management practise.* Overall, and on a time horizon of 100 year, there were minor differences between the management systems on their effect on the rate of adaptive response of the traits, and thereby on the loss of genetic diversity by selection. However, between sites, distributed throughout the species range, there were clear differences on the importance of the role of management on the adaptive response and genetic diversity of these adaptive traits.

- *Transfer of forest reproductive material*. The *in silico* provenance trials showed the general pattern that provenances obtained from the north of Europe, and tested throughout the distribution range, performed worse compared the locally adapted

populations for most of the test sites. Whereas provenances obtained from the south of Europe, generally performed better compared to the provenances adapted to the conditions of the test site.

6.7. Overall conclusions

Overall we conclude that the ForGEM model is a suitable tool to make future assessment on impact of climate change, the effect of management on genetic diversity and rate of adaptation, and to evaluate a large number of provenance trials at many environmental conditions.

The genetic model analyses proved to be very expensive in terms of computing power required to make the abovementioned assessments. In total we spend around 1.3. million computing processor unit (CPU) hours, which was not enough to calculate adaptation to local environmental conditions of all 4 tree species. Currently, the model and all necessary auxiliary data and database structures are uploaded at the national academic supercomputing centre in the Netherlands, and is available for use by others.

7. References

Bakker, M. (1980) *Enkele waarnemingen aan zaadverspreiding en kiemingskans bij Betula pubescens Ehrh*, Amsterdam: Stichting Noordhollandsch Landschap.

Bossema, J. (1979) 'Jays and Oaks: An Eco_Ethological Study of a Symbiosis', *Behaviour,* 70, 1-117.

Bouman, F. (2000) *Verspreiding van zaden,* Utrecht: KNNV Uitgeverij.

Brendel, O., Le Thiec, D., Scotti-Saintagne, C., Bodenes, C., Kremer, A. and Guehl, J. M. (2008) 'Quantitative trait loci controlling water use efficiency and related traits in Quercus robur L.', *Tree Genetics & Genomes,* 4(2), 263-278.

Brus, D. J., Hengeveld, G. M., Walvoort, D. J. J., Goedhart, P. W., Heidema, A. H., Nabuurs, G. J. and Gunia, K. (2012) 'Statistical mapping of tree species over Europe', *European Journal of Forest Research,* 131(1), 145-157.

Degen, B., Gregorius, H.-R., & Scholz, F., (1996) 'ECO-GENE, a model for simulation studies on the spatial and temporal dynamics of genetic structures of tree populations', *Silvae Genetica,* 45, 323-329.

Duncker, P. S., Barreiro, S. M., Hengeveld, G. M., Lind, T., Mason, W. L., Ambrozy, S. and Spiecker, H. (2012) 'Classification of Forest Management Approaches: A New Conceptual Framework and Its Applicability to European Forestry', *Ecology and Society,* 17(4).

Estrada, A. and Fleming, T. H. (1986) *Frugivores and seed dispersal,* Dordrecht: Junk.

Evans, J. R. (1989) 'Photosynthesis and nitrogen relationships in leaves of C3 plants', *Oecologia,* 78, 9-19.

Falconer, D. S., & Mackay, T.F.C. (1996) *Introduction to Quantitative Genetics,* Edinbrough: Addison Wesley Longman Ldt.

Falconer , D. S. and Mackay, T. F. C. (1996) *Introduction to Quantitative Genetics, 4th ed.,* Adison Wesley Longman Group Ltd.

Fenner, M. (1985) *Seed ecology,* London: Chapman and Hall.

Fenner, M. (1992) *Seeds: the ecology of regeneration in plant communities,* Wallingford: C.A.B. International.

Fleming, T. H. and Estrada, A. (1993) *Frugivory and seed dispersal : ecological and evolutionary aspects.,* Dordrecht: Kluwer.

Gregorius, H.-R. (1978) 'The concept of genetic diversity and its formal relationship to heterozygozity and genetic distance', *Math. Biosc.,* 41(41), 253-271.

Gregorius, H. R. (1977) 'The genotype*environment-to-phenotype relationship', *Theoretical and Applied Genetics,* 49, 165-176.

Gregorius, H. R. (1986) 'Measurements of genetical differentiation amoung subpopulations', *Theoretical and Applied Genetics,* 71, 826-834.

Gregorius, H. R. (1987) 'The relationship between the concepts of genetic diversity and differentiation', *Theoretical and Applied Genetics,* 74, 397-401.

Gregorius, H. R. (1988) 'The meaning of genetic variation within and between subpopulations', *Theoretical and Applied Genetics,* 76, 947-951.

Grote, R. (1998) 'Integrating dynamic morphological properties into forest growth modelling: II Allocation and mortality', *Forest Ecology and Management,* 111(2-3), 193-210.

Hänninen, H. and Kramer, K. (2007) 'A framework for modelling the annual cycle of trees in boreal and temperate regions', *Silva Fennica,* 41(1), 167-205.

Hanssen, A. (2000) *Untersuchungen zur genetische Variation der Buch in Hessen*, Hannover, Muenden: Hessisches Ministerium Fuer Umwelt, Landwirtschaft und Forsten.

Hartl, D. L. and Clark, A. G. (1997) *Principles of Population Genetics,* 3rd ed.*,* Sunderland, Massachusetts: Sinauer Associates, Inc.

Hattemer, H. H. (1991) 'Measuring genetic variation' in Muller-Starck, G. Z., M., ed. *Genetic Variation in European Populations of Forest Trees*, Frankfurt am Main: J.D. Sauerlander's Verlag, 2-20.

Hengeveld, G. H. M., Schelhaas, M.-J., Heidema, N. (in prep.) 'Synthetic European Forest Structure Database'.

Hengeveld, G. M., Nabuurs, G. J., Didion, M., van den Wyngaert, I., Clerkx, A. P. P. M. and Schelhaas, M. J. (2012) 'A Forest management map of European forests', *Ecology and Society,* 17(4).

Jansen, J. J., Sevenster, J. and Faber, P. J. (1996) 'Opbrengsttabellen voor belangrijke boomsoorten in Nederland', *IBN-rapport-221 / Hinkeloord Report No 17*, 202 pp.

Jansen, P. A. (2003) *Scatterhoarding and tree regeneration: ecology of nut dispersal in a Neotropical rainforest*.

Karlsson, M. (2001) *Natural regeneration of broadleaved tree species in Southern Sweden : effects of silvicultural treatments and seed dispersal from surrounding stands*, Alnarp: Swedish University of Agricultural Sciences.

Kattge, J. and Knorr, W. (2007) 'Temperature acclimation in a biochemical model of photosynthesis: a reanalysis of data from 36 species', *Plant Cell Environ,* 30(9), 1176-90.

Kramer, K. (1994) 'A modelling analysis of the effects of climatic warming on the probability of spring frost damage to tree species in The Netherlands and Germany.', *Plant, Cell & Environment,* 17, 367-377.

Kramer, K. (2007) 'Resilience of European forests: towards a non-equilibrium view for the management of diversity' in Koskela, J. B., A.;Cros, T. du, ed. *Climate Change and Forest Genetic Diversity: implications for sustainable forest management in Europe*, 43-52.

Kramer, K., Buiteveld, J., Forstreuter, M., Geburek, T., Leonardi, S., Menozzi, P., Povillon, F., Schelhaas, M., du Cros, E. T., Vendramin, G. G. and van der Werf, D. C. (2008a) 'Bridging the gap between ecophysiological and genetic knowledge to assess the adaptive potential of European beech', *Ecological Modelling,* 216(3-4), 333-353.

Kramer, K., Buiteveld, J., Forstreuter, M., Geburek, T., Leonardi, S., Menozzi, P., Povillon, F., Schelhaas, M. J., Teissier du Cros, E. and Vendramin, G. G. (2008b) 'Bridging the gap between ecophysiological and genetic knowledge to assess the adaptive potential of European beech', *Ecological Modelling,* 216(3), 333-353.

Kramer, K., Degen, B., Buschbom, J., Hickler, T., Thuiller, W., Sykes, M. T. and Winter, W. d. (2010) 'Modelling exploration of the future of European beech (Fagus sylvatica L.) under climate change--Range, abundance, genetic diversity and adaptive response', *Forest Ecology and Management,* 259, 2213-2222.

Kramer, K., Groot Bruinderink, G. W. T. A. and Prins, H. H. T. (2006a) 'Spatial interactions between ungulate herbivory and forest management', *Forest Ecology and Management,* 226(1-3), 238-247.

Kramer, K., Groot Bruinderink, G. W. T. A. and Prins, H. H. T. (2006b) 'Spatial interactions between ungulate herbivory and forest management', *Forest Ecology and Management,* 226(1), 238-247.

Kramer, K., H. Baveco, R.J. Bijlsma, A.P.P.M. Clerkx, J. Dam, T.A. Groen, G.W.T.A. Groot Bruinderink, I.T.M. Jorritsma, J. Kalkhoven, A.T. Kuiters, D. Lammertsma, H.H.T. Prins, M. Sanders, R. Wegman, S.E. van Wieren, S. Wijdeven & R. van der Wijngaart . (2001) *Landscape forming processes and diversity of forested landscapes - description and application of te model FORSPACE.*, Wageningen: Alterra-report 216.

Kramer, K. and Hänninen, H. (2009) 'The annual cycle of development of trees and process-based modelling of growth to scale up from the tree to the stand' in Noormets, A., ed. *Phenology of Ecosystem Processes. Applications in Global Change Research*, Springer Verlag, 201-228.

Kramer, K., van der Werf, B. and Schelhaas, M.-J. (2015) 'Bring in the genes: genetic-ecophysiological modeling of the adaptive response of trees to environmental change. With application to the annual cycle', *Frontiers in Plant Science,* 5.

Kramer K.; van der Werf, D. (2010) 'Equilibrium and non-equilibrium concepts in forest genetic modelling: population-and individually-based approaches', *Forest Systems,* 3(4), 100-112.

LaBastide, J. G. A. C. and Van Vredenburch, H. (1970) *Influence of weather conditions on the seed production of some forest trees in the Netherlands.*, Wageningen: Wageningen UR.

Larsen, A. B. (1996) 'Genetic structure of populations of beech (Fagus sylvatica L.) in Denmark', *Scandinavian Journal of Forest Research,* 11(3), 220-232.

Leinonen, I. (1996) 'Dependence of dormancy release on temperature in different origins of pinus sylvestris and betula pendula seedlings', *Scandinavian Journal of Forest Research,* 11(2), 122-128.

Leinonen, I., Repo, T., Hänninen, H. and Burr, K. (1995) 'A second-order dynamics model for the frost hardiness of trees', *Annals of Botany,* 76, 89-95.

Mäkelä, A. and Hari, P. (1986) 'Stand growth models based on carbon uptake and allocation in individual trees', *Ecological Modelling,* 33, 205-229.

McGaughey, R. J. (1997) *Visualizing forest stand dynamics using the stand visualization system,* translated by 248-257.

Metzger, M. J., Brus, D. J., Bunce, R. G. H., Carey, P. D., Gonçalves, J., Honrado, J. P., Jongman, R. H. G., Trabucco, A. and Zomer, R. (2013) 'Environmental stratifications as the basis for national, European and global ecological monitoring', *Ecological Indicators,* 33(0), 26-35.

Towards the Sustainable Management of Forest Genetic Resources FORGER FP7- 289119

Metzger, M. J., Brus, D.J. , Bunce, R.G.H. , Carey, P.D. , Goncalves,J. , Honrado, J.P. , Jongman,R.H.G. , Trabucco, A. , Zomer, R. (in press) 'Environmental stratifications as the basis for national, European and global ecological monitoring', *Ecological Indicators*.

Metzger, M. J., Bunce, R. G. H., Jongman, R. H. G., Mucher, C. A. and Watkins, J. W. (2005) 'A climatic stratification of the environment of Europe', *Global Ecology and Biogeography,* 14(6), 549-563.

Murray, D. R. (1986) *Seed dispersal,* Sydney: Academic Press.

Nei, M. (1987) *Molecular evolutionary genetics.,* New York: Columbia Univ. Press.

Pelkonen, P. and Hari, P. (1980) 'The independence of the springtime recovery of CO2 uptake in Scots pine on temperature and internal factors', *Flora,* 169, 398-404.

Penning de Vries, F. W., Brunsting, A. H. and van Laar, H. H. (1974) 'Products, requirements and efficiency of biosynthesis: a quantitative approach.', *Journal of Theoretical Biology,* 45(2), 339-377.

Penning de Vries, F. W. T. (1975) 'Use of assimilates in higher plants' in *Photosynthesis and productivity in different environments. J. Cooper (ed.), International Biological Programme 3, Cambridge University Press, Cambridge, pp.459-481.*

Pienaar, L. V. and Turnbull, K. J. (1972) 'The chapman-Richards generalization of Von Bertalanffy's growth model for basal area growth and yield in even-aged stands', *Forest Science,* (19), 2-22.

Repo, T., Mäkelä, A. and Hänninen, H. (1990) 'Modelling frost resistance of trees', *Silva Carelica,* 15, 61-74.

Schelhaas, M., Weideven, S. (2005) *Zelfregulerende bossen*, Alterra-Report 1270.

Schelhaas, M. J. (2008) 'The wind stability of different silvicultural systems for Douglas-fir in the Netherlands: a model-based approach', *Forestry,* 81(3), 399-414.

Schelhaas, M. J., Kramer, K., Peltola, H., van der Werf, D. C. and Wijdeven, S. M. J. (2007) 'Introducing tree interactions in wind damage simulation', *Ecological Modelling,* 207(2-4), 197-209.

Schopmeyer, C. S. (1974) *Seeds of woody plants in the United States,* Washington: Usda.

Siegl, T. A. V. S. (1990) *Fruktifikation der Fichte (Picea abies (L.) Karsten) : eine Interpretation des Fruktifikationsgeschehens anhand des geernteten Saatgutes aus dem*

Towards the Sustainable Management of Forest Genetic Resources FORGER FP7- 289119

Einzugsgebiet der Bayerischen Staatlichen Samenklenge Laufen von 1957 bis 1988 und der Meldungen zu Bluetenansatz und Zapfenbehang von 1954 bis 1988., Muenchen.: Ludwig-Maximilians-Universitaet.

Valentine, H. T. (1988) 'A carbon-balance model of stand growth: a derivation employing pipe-model theory and the self-thinning rule'.

Van Hees, A. F. M. (1997) 'Growth and morphology of pedunculate oak (Quercus robur L.) and beech (Fagus sylvatica L.) seedlings in relation to shading and drought', *Annales des Sciences Forestieres,* 54(1), 9-18.

Van Hees, A. F. M. and Clerkx, A. P. P. M. (2003) 'Shading and root-shoot relations in saplings of silver birch, pedunculate oak and beech', *Forest Ecology and Management,* 176(1-3), 439-448.

Van Hees, A. F. M., Kuiters, A. T. and Slim, P. A. (1996) 'Growth and development of silver birch, pedunculate oak and beech as affected by deer browsing', *Forest Ecology and Management,* 88(1-2), 55-63.

Willson, M. F. (1983) *Plant reproductive ecology,* New York: Wiley,.

Wösten, J. H. M., Lilly, A., Nemes, A. and Le Bas, C. (1999) 'Development and use of a database of hydraulic properties of European soils', *Geoderma,* 90(3-4), 169-185.

Wösten, J. H. M., Pachepsky, Y. A. and Rawls, W. J. (2001) 'Pedotransfer functions: bridging the gap between available basic soil data and missing soil hydraulic characteristics', *Journal of Hydrology,* 251(3-4), 123-150.

Young, J. A. and Young, C. G. (1992) *Seeds of woody plants in North America,* Portland, OR: Dioscorides Press.

Youngblood, A. and Max, T. A. (1992) *Dispersal of white spruce seed on Willow Island in interior Alaska*, Portland: Pacific Northwest Research Station.

Zasada, J. C., M.J. Foote & F.J. Deneke . (1978) *Case history of an excellent white spruce cone and seed crop in Interior Alaska : cone and seed production, germination, and seedling survival.,* Portland.: Usda.

Zeide, B. (1987) 'Analysis of the 3/2 Power Law of Self-Thinning', *Forest Science,* 33(2), 517-537.